

STRUCTURAL MANIPULATION OF CONJUGATED POLYMERS

A Thesis
Presented to
The Academic Faculty

by

Selma Bakbak

In Partial Fulfillment
of the Requirements for the Degree
Doctor of Philosophy in the
School of Chemistry and Biochemistry

Georgia Institute of Technology
May 2006

STRUCTURAL MANIPULATION OF CONJUGATED POLYMERS

Approved by:

Dr. Dr. Uwe H. F. Bunz Advisor
School of Chemistry and Biochemistry
Georgia Institute of Technology

Dr. Laren M. Tolbert
School of Chemistry and Biochemistry
Georgia Institute of Technology

Dr. Joseph Perry
School of Chemistry and Biochemistry
Georgia Institute of Technology

Dr. David M. Collard
School of Chemistry and Biochemistry
Georgia Institute of Technology

Dr. Anselm C. Griffin
The School of Polymer, Textile and
Fiber Engineering
Georgia Institute of Technology

Date Approved: January 05, 2006

**To My Husband, Kagan Kuyu
And My Daughter, Kayla Ela Kuyu**

ACKNOWLEDGEMENTS

First, I would like to thank to my husband Kagan Kuyu, for his love and support. He was next to me holding my hand and without him; this dissertation could not have been done. I would like to thank to my daughter Kayla for coming into our lives, she is the biggest joy and made me smile everyday.

I am very grateful to my mother Sevim Bakbak and my sisters Sevda, Derya, and Hulya, even though they are so far away from me they were with me with their love and encouragement during my school years. My in-laws Asuman and Altan Kuyu believed in me and showed me great support by taking care of our daughter for the last couple of months.

It is my privilege to thank to my advisor Dr. Uwe H. F. Bunz for giving me the opportunity to work in exciting projects and not only helping me as my supervisor but also encouraging and challenging me throughout my academic program.

I sincerely thank to my committee members Dr. Laren M. Tolbert, Dr. Joseph Perry, Dr. David M. Collard, Dr. Anselm C. Griffin for their helpful advice and their precious time.

I would like to thank to all past and present Bunz group members. I learned so much from you and enjoyed my time with you. From all some deserve special thanks. Belma you are a great friend and role model to me. I would like to thank Sandra, Carlito, and Brian, for not only being great lab mates but also life long friends. I am very grateful to know you all.

I would like to thank to my collaborators and all my friends for their support.

TABLE OF CONTENTS

	Page
ACKNOWLEDGEMENTS	iv
LIST OF TABLES	vii
LIST OF FIGURES	viii
LIST OF SCHEMES	x
LIST SYMBOLS AND ABBREVIATIONS	xii
SUMMARY	xiii
<u>CHAPTER</u>	
1 Conjugated Polymers	1
1.1 Background	1
1.2 Conclusion	8
1.3 References	9
2 Multitopic Third Generation Tris(Pyrazolyl)Methane Ligands Build on Alkyne Structural Scaffolding: First Example of Mixed Tris(Pyrazolyl)Methane/Tris(Pyrazolyl)Borate Ligand	11
2.1 Introduction	11
2.2 Result and Discussion	13
2.3 Conclusion	23
2.4 Experimental	25
2.5 References	39
3 Selective Click Chemistry via Microwave As an Approach To New Small Molecules	41
3.1 Introduction	41
3.2 Result and Discussion	44

3.3 Conclusion	52
3.4 Experimental	53
3.5 References	69
4 Click-Chemistry As a Powerful Tool For The Construction of Functionalized Poly(P-Phenyleneethynylene)s: Comparison Of Pre- and Postfunctionalization Schemes.	71
4.1 Introduction	71
4.2 Result and Discussion	72
4.3 Conclusion	84
4.4 Experimental	85
4.5 References	93
5 1,3-Dipolar Cycloaddition For Poly(Arylenetriazole)s and Nanostructured Semiconductors By Heated Probe Tips	95
5.1 Introduction	95
5.2 Result and Discussion	97
5.3 Conclusion	106
5.4 Experimental	108
5.5 References	114
6 Solid State Polymerize Thiophenes and Thio-Derivatives	117
6.1 Introduction	117
6.2 Result and Discussion	118
6.3 Conclusion	125
6.4 Experimental	126
6.5 References	130
7 Conclusion	131
APPENDIX A: Crystallographic Data	134

LIST OF TABLES

	Page
Table 2.1: Summary of intermolecular non covalent interactions for 2.7	21
Table 3.1: Library of triazoles obtained under thermal conditions in a CEM discovery microwave system.	46
Table 4.1: Optical Properties, Yields, Degree of Polymerization and Degree Functionalization of 4.3, 4.4 and 4.6	81
Table 5.1: Substituent key, optical and analytical data for polymers 5.3-5.6, 5.8 -5.9.	99
Table A.1: Crystallographic Data for 2.2, 2.4, 7 and 2.10.	135

LIST OF FIGURES

	Page
Figure 1.1: Structure of conjugated polymers.	2
Figure 1.2: AFM image of nanoribbons of polyfluorene–poly(ethyleneoxide) block copolymer. Adapted from Ref. ¹⁴	3
Figure 1.3: Fluorescence Spectra of glucose–PPE with [Hg(tfa) ₂] in DMF. The inset is the Stern–Volmer plot. Adapted from Ref. ¹⁹	4
Figure 1.4: Schematic representation of the quenching of glucose PPE by mercury trifluoroacetate. Two or more sugar substituents involve in the complexation of a single ion (sphere). Adapted from Ref. ¹⁹	5
Figure 1.5: Schematic representation of K ion-induced aggregation. Adapted from Ref. ²⁰	6
Figure 1.6: Thiophene polymers reflect red (left), green (middle) and blue (right) colors. Adapted from Ref. ²²	7
Figure 1.7: Color changes upon addition of toxins. From left to right: Sialic acid-PT and Sialic and influenza virus A, Sialic PT and influenza virus B, mannose-PT and mannose-PT and <i>E. coli</i> . Adapted from Ref. ²³	8
Figure 2.1: Molecular structures of alkynyl-containing tris(pyrazolyl)methane ligands.	16
Figure 2.2: Three dimensional supramolecular structure of HC ₂ CCH ₂ OCH ₂ C(pz) ₃ 2.2	17
Figure 2.3: Two dimensional sheet structure of IC ₆ H ₄ [CH ₂ OCH ₂ C(pz) ₃] ₂ (2.4)	18
Figure 2.4: Supramolecular structure of 3,3',5,5'-[(pz) ₃ CCH ₂ OCH ₂] ₄ (C ₆ H ₃ C ₂ C ₆ H ₃)	19
Figure 2.5: Molecular structure and atom labelling Scheme of Fe{[κ ³ (B)(pz) ₃ CCH ₂ OCH ₂ C ₂ C ₆ H ₄]B(pz) ₃] ₂ (2.10).	22
Figure 3.1: ORTEP plots of compounds 3.18 , 3.23 , 3.24 , 3.25 , 3.37 , and 3.38	47
Figure 3.2: Single crystal X-ray analysis of 3.51 reveals that the triazole rings are slightly twisted with respect to the central benzene ring.	49
Figure 3.3: Optical data of polymer 3.57	52
Figure 4.1: Post and prepolymerization functionalization strategies.	73
Figure 4.2: UV-vis and emission spectra of polymer 4.3 (left) and polymer 4.4 (right)	75

Figure 4.3: UV-vis and emission spectra of polymer 4.6a conventional and polymer 4.10 in chloroform and in the solid state.	82
Figure 5.1: Synthesis of o poly(arylenetriazolyene)(PArT) by click chemistry	96
Figure 5.2: Absorption and emission spectra of 5.7-5.13 in chloroform	100
Figure 5.3: Emission spectra of 5.9 in chloroform, upon addition of methanol and acid	100
Figure 5.4: Emission spectra of 5.8 in chloroform and hydrochloric acid additions to a solution.	101
Figure 5.5: DSC data for mixture of 5.4 and 5.5 .	102
Figure 5.6: Heated cantilever writing (230 °C) on an 80 nm thin film of a mixture of the diyne 5.6 and diazide 5.3 on a cover slip.	103
Figure 5.7: HOMO (left) and the LUMO (right) of the 1,3-dipolar cycloadduct 5 (phenylacetylene and phenyl azide).	104
Figure 5.8: HOMO (-4.97 eV, top) and the LUMO (-2.01 eV; Gap = 2.96 eV, bottom) of the 1,3-dipolar cycloadduct 1 ((dimethylamino)phenylacetylene and 2,5-pyrazinediazide).	105
Figure 6.1: Pictures of monomer 9 (left), polymer 11 (middle) and 12 (right).	120
Figure 6.2: Crystal structure of monomer 1 .	122
Figure 6.3: XRD data of monomer 1 and polymer 3 .	123
Figure 6.4: IR data of monomer 1 (top), polymer 3 (middle) and 5 (bottom).	123
Figure 6.5: Solid state ¹³ C NMR data of doped polymer 3 , 4 , 11 and 12 .	124
Figure 6.6: Solid state ¹³ C NMR data of natural polymer 5 , 6 , 13 and 14 .	125

LIST OF SCHEMES

	Page
Scheme 2.1: Preparation of alkynyl-containing tris(pyrazolyl)methane ligands.	15
Scheme 2.2: Preparation of mixed tris(pyrazolyl)methane-tris(pyrazolyl)borate ligands.	22
Scheme 2.3: Iron-containing products obtained from attempted Sonogashira coupling reactions between $\text{Fe}[\text{IC}_6\text{H}_4\text{B}(\text{pz})_3]_2$ and $\text{HC}_2\text{C}_6\text{H}_4\text{-terpy}$	23
Scheme 3.1: Thermal 1,4 and 1,5 triazoles formation.	42
Scheme 3.2: Copper catalyzed synthesis of 1,4-triazoles.	43
Scheme 3.3: Synthesis of 3.7 obtained under thermal conditions in a CEM discovery microwave system.	44
Scheme 3.4: Synthesis of iodine substituted 1,4-triazoles from the corresponding silanes.	48
Scheme 3.5: Use of iodine substituted triazole 3.51 to yield conjugated molecules.	49
Scheme 3.6: Synthesis of iodinated triazole.	50
Scheme 3.7: Synthesis of polyphenylenetriazoline.	51
Scheme 4.1: Synthesis of the polymer 4.4 .	74
Scheme 4.2: In situ generation of 4.4 and its reaction with azides 4.5a-c yielding 4.6a-c and prefunctionalization approach towards 4.6a-c .	76
Scheme 4.3: Synthesis of polymer 4.3a via a prefunctionalized strategy starting from monomer 4.3 .	78
Scheme 5.1: Synthesis of a conjugated polymer by a 1,3-dipolar cycloaddition	96
Scheme 5.2: Synthesis of didodecyl diazide fluorene monomer	97
Scheme 5.3: Copper catalyzed synthesis of 5.7-5.10 and 5.12 and 5.13 .	98
Scheme 5.4: Protonation of triazole ring.	101
Scheme 6.1: Synthesis of solid state doped polymers 3-4 and natural 5-6 .	118
Scheme 6.2: Synthesis of Polymer 13 and 14 .	119

LIST SYMBOLS AND OF ABBREVIATIONS

Φ	Fluorescence Quantum Yield
DMF	N,N-dimethyl formamide
DMSO	Dimethyl sulfoxide
GPC	Gas Permeation Chromotography
HOMO	Highest Occupied Molecular Orbital
HSCH	Heck-Cassar-Sonogashira-Hagihara
IR	Infrared
LED	Light Emitting Diodes
LUMO	Lowest Unoccupied Molecular Orbital
MP	Melting Point
MS	Mass Spectrometry
NMR	Nuclear Magnetic Resonance
PAE	Poly(aryleneethynylene)
PPE	Poly(phenyleneethynylene)
PT	Polythiophene
TFA	Trifluoroacetic Acid
THF	Tetrahydrofuran
TIPS	Triisopropylsilyl
TMS	Trimethylsilyl
UV-Vis	Ultraviolet-Visible
XRD	X-ray Diffraction

SUMMARY

The syntheses of new classes of conjugated polymers are presented. The synthesis of novel alkyne bridged trispyrazolylmethane ligands, their coordination behavior and their crystallographic properties are studied. A series of functionalized poly(paraphenyleneethynylene)s, PPEs, are produced by click chemistry with post and pre-polymerization. Unpredictable solid-state polymerizations of defect free conjugated polythiophenes are investigated. Finally, by click chemistry aromatic diazides and aromatic diynes are coupled to produce a library of 1,2,3-triazoles and new conjugated polymers, poly(arylenetriazoline)s.

CHAPTER 1

CONJUGATED POLYMERS

1.1 Background

Polymers are long chain molecules which are utilized everyday in plastics such as polystyrene and polyethylene. In general, polymers are considered good insulators. However, conjugated polymers are not insulators, but are classified as organic semiconductors.¹ Conjugated polymers contain a back bone consisting of alternating single and double bonds between carbon-carbon or carbon-nitrogen atoms. Even though conjugated polymers are known as linear or rigid rods, they are not completely straight and flat, but twisted along their back bones.² Polymer chains consist of sp^2 -hybridized carbons and p-electrons. These p-electrons form a delocalized pi-system, which gives rise to the polymer's semi-conducting properties. Conjugated polymers are currently very important materials and are used widely in industry for the development of devices such as light-emitting diodes, thin film transistors, photovoltaic cells, sensors, plastic lasers, and nonlinear optical systems.³⁻⁵

In 1990, an electroluminescence device was developed utilizing conjugated polymers by Friend and coworkers at the University of Cambridge.^{5a} After the development of the first polymer light emitting diode (PLED), development has proceeded extremely fast in the area of electroluminescence for technological advance of

screens and displays. In early 1990s, the first photodiodes were prepared utilizing conjugated polymers in the same way as the PLEDs.⁶ A researcher in Shirakawa's group in Japan accidentally used too much catalyst for the synthesis of non-conductive polyacetylene, which formed a thin, silvery film. Shirakawa, along with Alan MacDiarmid from the University of Pennsylvania, discovered that the conductivity of polyacetylene could be increased by a factor of ten million by bromine doping. In 2000, the work of Alan Heeger, Alan MacDiarmid, and Hideki Shirakawa won the Nobel Prize for Chemistry for their work in the discovery and development of electrically conductive polymers.⁷

Many conjugated polymers are highly fluorescent and can exhibit molecular wire properties.⁸ Polymers have many binding sites and therefore if even one analyte binds with the polymer, a change in fluorescence can be observed due to the conjugation of the polymer. This property is very important for sensing applications of polymers.

The simplest example of a conjugated polymer is polyacetylene⁹ $(CH)_n$. However conjugated polymers exist in a variety of structures such as poly(*p*-phenylene)¹⁰ (PA), polythiophene¹¹ (PT), poly(*p*-phenylenevinylene)^{1a,10a} (PPV), and poly(*p*-phenyleneethynylene)^{1a,12} (PPE) as shown in Figure 1.1.

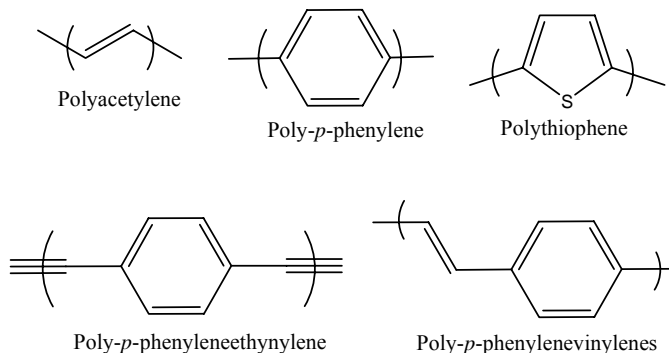


Figure 1.1. Structure of conjugated polymers.

Since the discovery of LEDs, conjugated polymers have been among the most studied polymers in the last decade. I will briefly point out these groups of conjugated polymers and show recent developments for each group.

Poly(*p*-phenylenes)s:

Poly(*p*-phenylenes) can be synthesised directly from benzene or benzene derivatives in the presence of aluminium chloride and cupric chloride as an oxidizing agent.^{2b} They have a more rod-like structure and therefore most of them are insoluble in most organic solvents. They are often combined with other polymers, such as polystyrene, which have a higher solubility in organic solvents which allows for their interesting properties to be studied.¹³

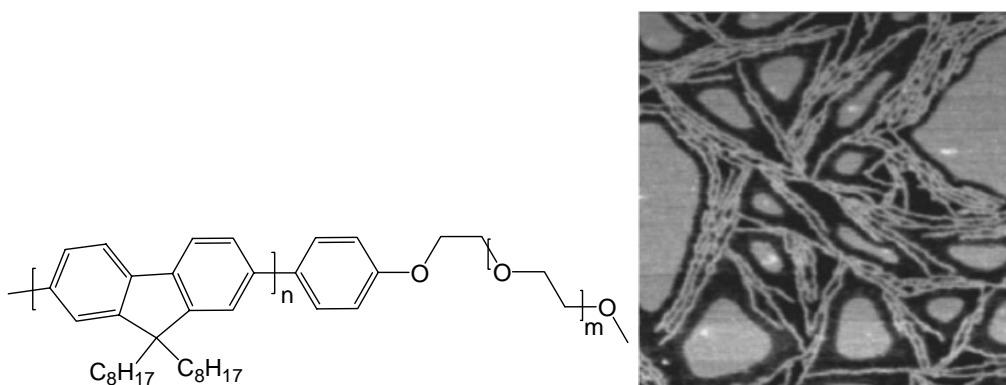


Figure 1.2. AFM image of nanoribbons of polyfluorene–poly(ethyleneoxide) block copolymer. Adapted from Ref.¹⁴

Conjugated polymers form nano-sized optoelectronic devices by self-assembly.¹⁴ Using copolymers of polyfluorene and low molecular weight poly(ethylene oxide) (PEO) forms nanoribbons in THF as seen in Figure 1.2.¹⁵ The nanoribbons which are formed on

mica have an 11 nm width and 1 nm height. The π - π interactions between the conjugated regions play a role in this ribbon formation. When toluene was used as a solvent, more organized ribbons were formed.

Poly(*p*-phenyleneethynylene)s:

PPEs form from the reaction between aromatic dihalides and aromatic diynes by utilizing the Heck-Cassar-Sonogashira-Hagihara coupling.¹⁶ This coupling method can be used for almost any functional groups. In this coupling, Pd is used as the catalytic species. One of the disadvantages of using Pd is that it often yields a low molecular weight or a low degree of polymerization. PPEs can also be synthesized by an ADIMET reaction however the reaction is sensitive to functional groups and needs high reaction temperatures.¹⁷

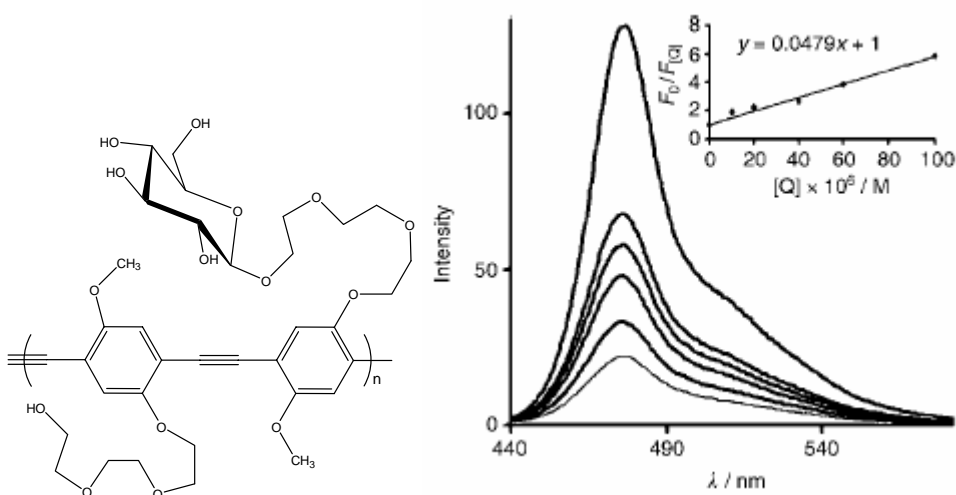


Figure 1.3. Fluorescence Spectra of glucose–PPE with $[\text{Hg}(\text{tfa})_2]$ in DMF. The inset is the Stern–Volmer plot. Adapted from Ref.¹⁹

The Bunz group has designed sugar substituted PPEs for biosensor applications, however they did not find specific response to sugar binding proteins.¹⁸ Here Bunz and

coworkers used PPEs for heavy metal sensing.¹⁹ The interaction of a sugar coated PPE with mercury and lead ions was significant (Figure 1.3). When HgCl_2 was added to a solution of polymer, quenching was observed. The quenching effect was increased when the sugar unit contained a triethylene glycol linker. In the case of lead ions, dramatic enhancements of the quenching were observed. This enhancement can be explained by the fact that two glucose units are involved in the complexation of a single metal ion in the backbone as shown in Figure 1.4. It is important to investigate detection sensitivity of sugar-substituted polymers with mercury and lead salts.

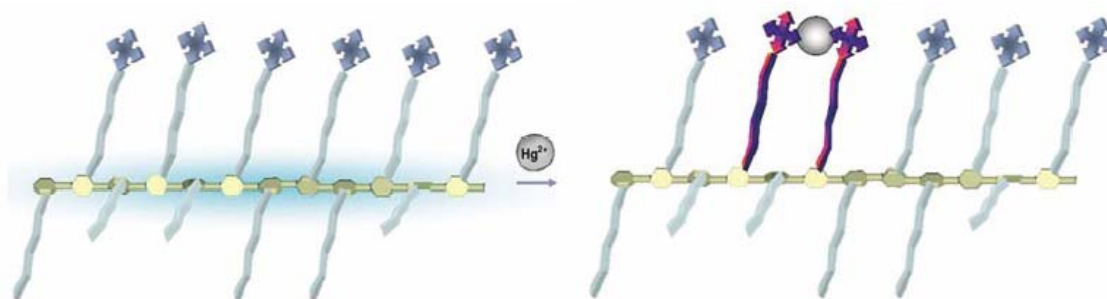


Figure 1.4. Schematic representation of the quenching of glucose PPE by mercury trifluoroacetate. Two or more sugar substituents involve in the complexation of a single ion (sphere). Adapted from Ref.¹⁹

Swager demonstrated sensing by utilizing the aggregation behavior of conjugated polymers.^{12b,20} 15-crown-5-substituted PPE showed aggregation by addition of potassium ions. However, no change was seen in the absorbance and emission spectra of the polymer with addition of Na and Li ions. Li and Na ion make 1:1 complexes with crown ether PPEs, but K ions forms a 2:1 complex with the same polymer. K ions complex between two crown ethers on different polymer chains (Figure 1.5).

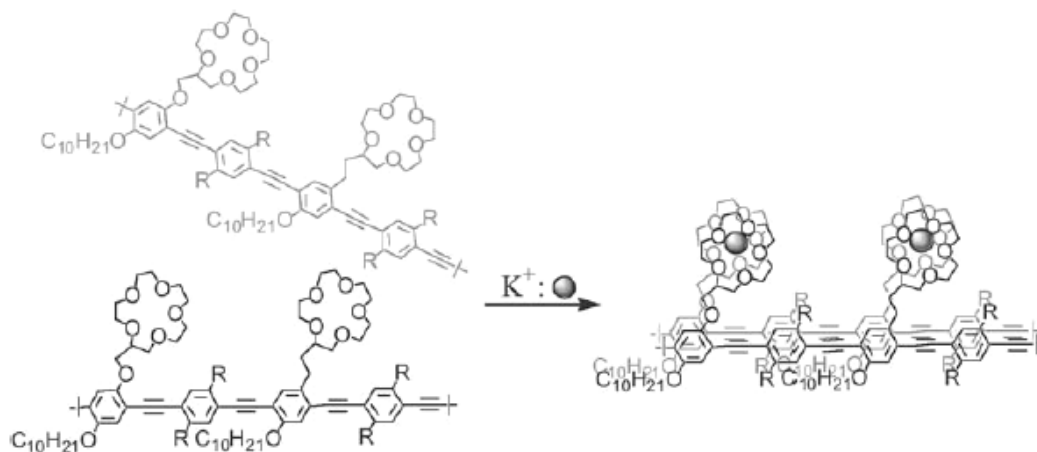


Figure 1.5. Schematic representation of K ion-induced aggregation. Adapted from Ref.²⁰

Polythiophenes:

Thiophene polymers have less linearity and rigidity in its system. The bond between the second and the third carbon and the bonds connecting the thionyl rings have more single bond character. Conjugated polythiophenes have been extensively studied and used as electrodes because of their good conductivity. They have a wide range of applications in batteries, electronics and non linear optical devices.¹¹ The novel conducting polymer, poly(3,4-ethylenedioxythiophene) (PEDOT), is the most studied conducting polymer.²¹ Its low oxidation potential, moderate band gap, and high conductivity makes it very attractive for many applications including hole injection layers in OLED, anti-static coating and solar cells.²¹

Recently, Sonmez and coworkers discovered a green colored conjugated polythiophene.^{21b,22} It was difficult to obtain a polymer which absorbed in the green region. Red and blue conducting polymers have been used widely in electronic device formation for last decade. With these three primary color polythiophenes, they can be

mixed in various proportions to obtain many different colors as seen in Figure 1.6. These polymers can be mixed either in their neutral or oxidized state. This new discovery will have a big impact in the area of electronic device fabrication with conjugated polymers.

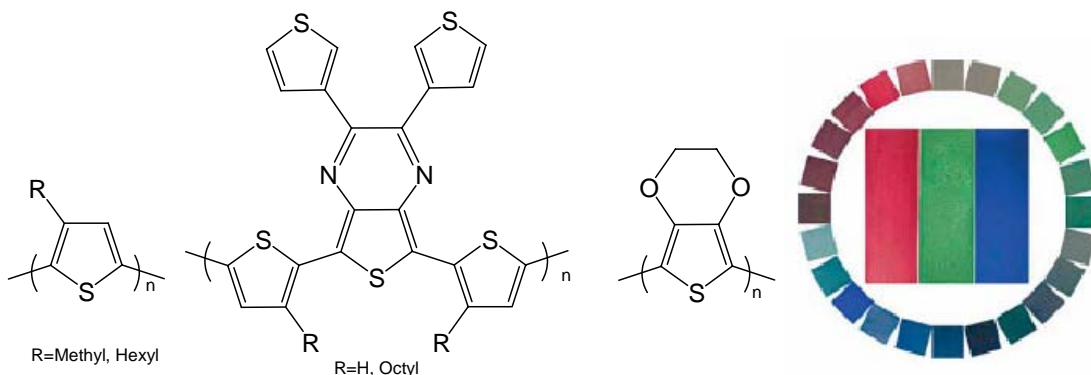


Figure 1.6. Thiophene polymers reflect red (left), green (middle) and blue (right) colors. Adapted from Ref.²²

Sugar coated polydiacetylene and polythiophenes were used for sensing applications. Baek and Charch prepared glycothiophenes with sialic acid and mannose ligands as side chains.²³ The binding ability of the polymers with other biological agents such as lectins, viruses, and bacteria were studied. As a result, the binding of the polymers with the biological agents caused a color change in the polymer solutions as seen in Figure 1.7. As seen in figure, addition of toxins form red colors in polymer solutions.



Figure 1.7 Color changes upon addition of toxins. From left to right: Sialic acid-PT, Sialic acid-PT and influenza virus A, Sialic PT and influenza virus B, mannose-PT and mannose-PT and *E. coli*. Adapted from Ref.²³

1.2 Conclusion:

Conjugated polymers are very desirable for many different applications as outlined above. Their synthetic adaptability to a broad range of functional groups inspires us to make new classes of conjugates and conjugated polymers. The synthesis of various interesting conjugated polymer and their optical properties will be explained along with the research goals for future applications in device fabrication and metal sensing.

1. Synthesis of a series of novel alkyne bridged trispyrazolylmethane ligands and their crystallographic properties.
2. Synthesis of 1,2,3-triazole from aromatic diazides with aromatic diynes to form a library of triazoles for a new of conjugated polymer synthesis.
3. Post and pre modification of PPEs by click chemistry
4. Using Click chemistry to functionalize and structure surfaces by organic semiconductors.
5. Making defect free polythiophenes which form from the crystalline state.

1.3 References:

1. a) Bunz, U. H. F. *Chem. Rev.*, **2000**, *100*, 1905-1644. b) Giesa, R. *J. M. S.-Rev. Macromol. Chem. Phys.*, **1996**, *36*, 631. c)
2. a) *Handbook of Conducting Polymers, 2nd edn.*, ed. T. A. Skotheim, R. L. Elsenbaumer and J. R. Reynolds, Marcel Dekker, New York, 1998. b) Bredas J. L.; Silbey, R., *Conjugated Polymers*, Kluwer academic Publishers 1991.
3. a) Dore, K.; Dubus, S.; Ho, H. -A.; Levesque, I.; Brunette, M.; Corbeil, G.; Boissinot, M.; Boivin, G.; Bergeron, M. G.; Boudreau, D.; Leclerc M. *J. Am. Chem. Soc.*, **2004**, *126*, 4240. b) Virji, S.; Huang, J.; Kaner, R. B.; Weiller, B. H. *Nano. Lett.*, **2004**, *4*, 591. c) Huang, J.; Kaner, R. B., *J. Am. Chem. Soc.*, **2004**, *126*, 851.
4. Gaylord, B. S.; Heeger, A. J.; Bazan, G. C. *J. Am. Chem. Soc.*, **2003**, *125*, 896.
5. a) Burroughes, J. H.; Bradley, D. D. C.; Brown, A. R.; Marks, R. N.; Mackay, K. D.; Friend, R. H.; Burn, P. L.; Holmes, A. B. *Nature*, **1990**, *347*, 539. (b) Friend, R. H.; Gymer, R. W.; Holmes, A. B.; Burroughes, J. H.; Marks, R. N.; Taliani, C.; Bradley, D. D. C.; Dos Santos, D. A.; Bredas, J. L.; Loglund, M.; Salaneck, W. R. *Nature*, **1999**, *397*, 121. (c) Sirringhaus, H.; Tessler, N.; Friend, R. H. *Science*, **1998**, *280*, 1741.
6. N. P. Fox, *Metrologia* **1991**, *28*, 197-202.
7. a) Heeger, A. J. *Synthetic Metals* **2001**, *125*, 23-42. b) MacDiarmid, A. G. *Reviews of Modern Physics* **2001**, *73*, 701-712. c) Shirakawa, H. *Angewandte Chemie, International Edition* **2001**, *40*, 2575-2580.
8. a) Yang, J. -S.; Swager, T. M. *J. Am. Chem. Soc.*, **1998**, *120*, 5321. (b) Yang, J. -S.; Swager, T. M. *J. Am. Chem. Soc.*, **1998**, *120*, 11864.
9. Enkelmann, V. *Adv. Polym. Sci.* **1984**, *63*, 91.
10. a) Scherf, U. *Top. Curr. Chem.* **1999**, *201*, 163. b) Schluter, A. D.; Wegner, G. *Acta Polym.* **1993**, *44*, 59.
11. a) Yamamoto, T. *Bull. Chem. Soc. Jpn.* **1999**, *72*, 621. b) Yamamoto, T.; Takagi, M.; Kizu, K.; Maruyama, T.; Kubota, K.; Kanbara, H.; Kurihara, T.; Kaino, T. *J. Chem. Soc., Chem. Commun.* **1993**, 797.
12. a) Bunz, U., H., F., *Adv Polym Sci*, **2005**, *177*, 1-52. b) Zhen, J.; Swager, T. M., *Adv Polym Sci*, **2005**, *177*, 151-179.
13. Cianga, I.; Yagci, Y., *Prog. Polym Sci*, **2004**, *29*, 387-399.

14. Schenning, A. P. H. J.; Meijer, E. W. *Chem. Commun.*, **2005**, 3245–3258
15. Luo, Y. H.; Liu, H. W.; Xi F.; Li, L.; Jin, X. G.; Han, C. C.; Chan, C. M., *J. Am. Chem. Soc.*, **2003**, *125*, 6447.
16. a) Sonogashira, K.; Tohda, Y.; Hagihara, N. *Tetrahedron Lett.*, **1975**, *16*, 4467. b) Dieck, H. A.; Heck, R. F. *J. Organomet. Chem.*, **1975**, *93*, 259. (c) Cassar, I. *J. Organomet. Chem.*, **1975**, *93*, 253.
17. Kloppenburg, L.; Song, D.; Bunz, U. H. F. *J. Am. Chem. Soc.* **1998**, *120*, 7973.
18. Erdogan, B.; Wilson, J. N.; Bunz, U. H. F. *Macromolecules*, **2002**, *35*, 7863.
19. Kim, I.-K.;Erdogan, B.; Wilson, J. N.; Bunz, U. H. F. *Chem. Eur. J.* **2004**, *10*, 6247 – 6254.
20. Zheng, J.; Swager, T. M., *Adv Polym Sci*, **2005**, *177*, 151–179.
21. a) Groenendaal, L. B.; Jonas, F.; Freitag, D.; Pielartzik, H.; Reynolds, J. R., *Advanced Materials* **2000**, *12*, 481-494. b) Barbarella, G.; Melucci, M.; Sotgiu, G. *Journal of Materials Chemistry* **2005**, *17*, 1581-1593. c) Kirchmeyer, S.; Reuter, K., *Journal of Materials Chemistry* **2005**, *15*, 2077-2088.
22. Sonmez, G.; Sonmez, H. B.; Shen, C. K. F.; Wudl, F. *Advanced Materials* **2004**, *16*, 1905-1908.
23. Baek, M. G.; Stevens, R. C.; Charych, D. H. *Bioconjugate Chem.* **2000**, *11*, 777.

CHAPTER 2

MULTITOPIC THIRD GENERATION

TRIS(PYRAZOLYL)METHANE LIGANDS BUILD ON ALKYNE STRUCTURAL SCAFFOLDING: FIRST EXAMPLE OF MIXED TRIS(PYRAZOLYL)METHANE/TRIS(PYRAZOLYL)BORATE LIGAND*

2.1 Introduction

The design of solids with specific architectures is a current topic of research that has potential applications in diverse areas from catalysis to separations to gas storage. One approach to developing such materials is to take advantage of the coordination chemistry of metals with carefully designed multitopic ligands. The construction of robust and fairly predictable architectures can be achieved by synthetically tailoring the length between and geometric disposition of the ligating units in rigidly linked organic frameworks.¹ Studies using more flexible ligand architectures are less numerous but are potentially more attractive in the sense that one can envision shape-adaptable

* Thanks to my collaborator Dr. James R. Gardinier and Dr. Radu F. Semeniuc for their help.

architectures whose final structure could be environmentally dependent, similar to proteins, for example.²

Molecular recognition in biological system explains with induced-fit mechanism, which specific substrates induce the organization of the recognition site. Dr. Ogura's group showed an impressive demonstration of metal-directed assembly of molecular recognition.^{2c} A construction of three-dimensional cagelike Pd(II) complex forms only in the presence of specific guests. If a molecular guest isn't present, oligomeric products form. These oligomers disappear and cagelike complex form when the host molecule is added.

Dr. Reger's group has been developing the chemistry of semi-rigid, multitopic tris(pyrazolyl)methane ligands of the type $C_6H_{6-n}[CH_2OCH_2C(pz)_3]_n$ ($n = 2, 3, 4, 6$; pz = pyrazolyl ring).³ These ligands, when bound to metals, are structurally adaptive in that their final molecular and supramolecular structures, depending on the nature of the metal, the anion, and included solvent, among other factors.^{3a} The multiple coordination modes of the $C(pz)_3$ unit and the inherent functionalities such as the π -systems, the acidic hydrogens of the arene on the pyrazolyl groups and on the ethereal arms have resulted in a variety of structurally magnificent compounds organized by noncovalent interactions. In order to develop more sophisticated architectures based on intermolecular interactions it is necessary to introduce new functionalities into the ligand backbones. Alkynes are attractive functional groups to build into these types of ligands because they have a fixed, linear geometry, they can become involved in π -stacking interactions, and they are good ligands for a variety of metals.

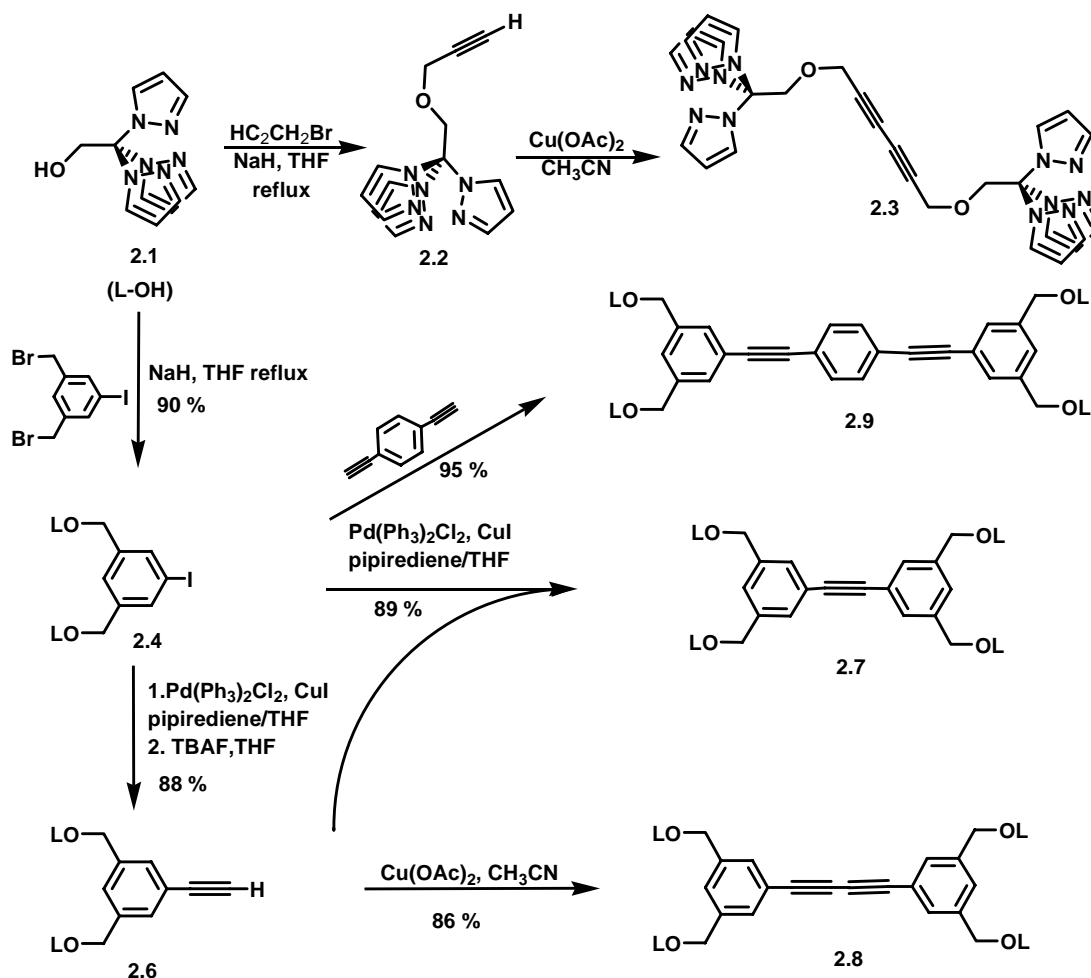
In this chapter we explore the synthesis of a new family of semi-rigid linked tris(pyrazolyl)methane ligands that take advantage of Sonogashira coupling reactions⁴ to give phenylalkynyl based systems. These compounds represent a new class of “third generation” poly(pyrazolyl)borate and poly(pyrazolyl)methane ligands,⁵ specifically functionalized at the non-coordinating “back” position. In poly(pyrazolyl)methane chemistry, the derivatization of the central carbon in HC(pz)₃ to the alcohol HOCH₂C(pz)₃^{3j} and then to the linked ligands of the type C₆H_{6-n}[CH₂OCH₂C(pz)₃]_n was the first development of “third generation” tris(pyrazolyl)methane compounds.³ The use of Sonogashira coupling reactions with Fe[(*p*-IC₂C₆H₄)B(3-Mepz)₃]₂ to produce compounds of the formula Fe[(*p*-RC₂C₆H₄)B(3-Mepz)₃]₂, (R = H, Me₃Si, Ph) was our first foray of “third generation” poly(pyrazolyl)borate ligands.⁵ By utilizing this alkyne coupling methodology, we report here the preparation of the compounds containing both a tris(pyrazolyl)methane and a tris(pyrazolyl)borate ligating unit that can be considered “third generation” at each site.

2.2 Result and Discussion

A series of new multitopic ligands with rigid linear geometry are formed by joining tris(pyrazolyl)methane and tris(pyrazolyl)borate units with alkynyl linkers using Sonogashira and related coupling reactions. These ligands are new examples of “third generation” poly(pyrazolyl)borate and poly(pyrazolyl)methane ligands, ligands functionalized at the non-coordinating “back” positions of either the boron or central carbon atoms.

Syntheses of tris(pyrazolyl)methane ligands.

A summary of the routes to the new alkynyl-containing tris(pyrazolyl)methane ligands is given in Scheme 2.1. The reaction between the sodium alkoxide, Na[OCH₂C(pz)₃] [prepared in situ from NaH and the parent alcohol HOCH₂C(pz)₃ (**2.1**)], and either propargyl bromide or di(bromomethyl)-iodobenzene afforded the monotopic terminal alkyne **2.2** and ditopic iodophenyl derivative **2.4**, respectively, in high yields. The iodophenyl derivative **2.4**, was converted to the terminal alkynyl derivative **2.6**, by standard protocol (Sonogashira coupling with trimethylsilylacetylene followed by deprotection with tetrabutylammonium fluoride). Both terminal alkynes were subject to a number of coupling reactions. Thus, **2.2** and **2.6** were homocoupled with an excess of copper(II) acetate to give the ditopic derivative **2.3** and the tetratopic derivative **2.8**. Sonogashira coupling of **2.4** with **2.6** provided the tetratopic diphenylethynylene derivative **2.7**. The bright blue luminescent tetratopic derivative **2.9** was prepared in quantitative yield by coupling **2.6** with diiodobenzene or in modest yield by coupling **2.4** with diethynylbenzene. The identity of compounds **2.2-2.9** was established by a combination of elemental analyses, NMR spectroscopic methods, IR, mass spectral data, and in the case of **2.2**, **2.4**, and **2.7** by single crystal X-ray diffraction.



Scheme 2.1. Preparation of alkynyl-containing tris(pyrazolyl)methane ligands.

Structures of tris(pyrazolyl)methane ligands.

ORTEP diagrams of **2.2**, **2.4**, and **2.7** are shown in Figure 2.1. While the intramolecular bond lengths and angles are rather unexceptional in these three compounds, the ability of the alkynyl and pyrazolyl groups to participate in noncovalent interactions is evident on their supramolecular structures.

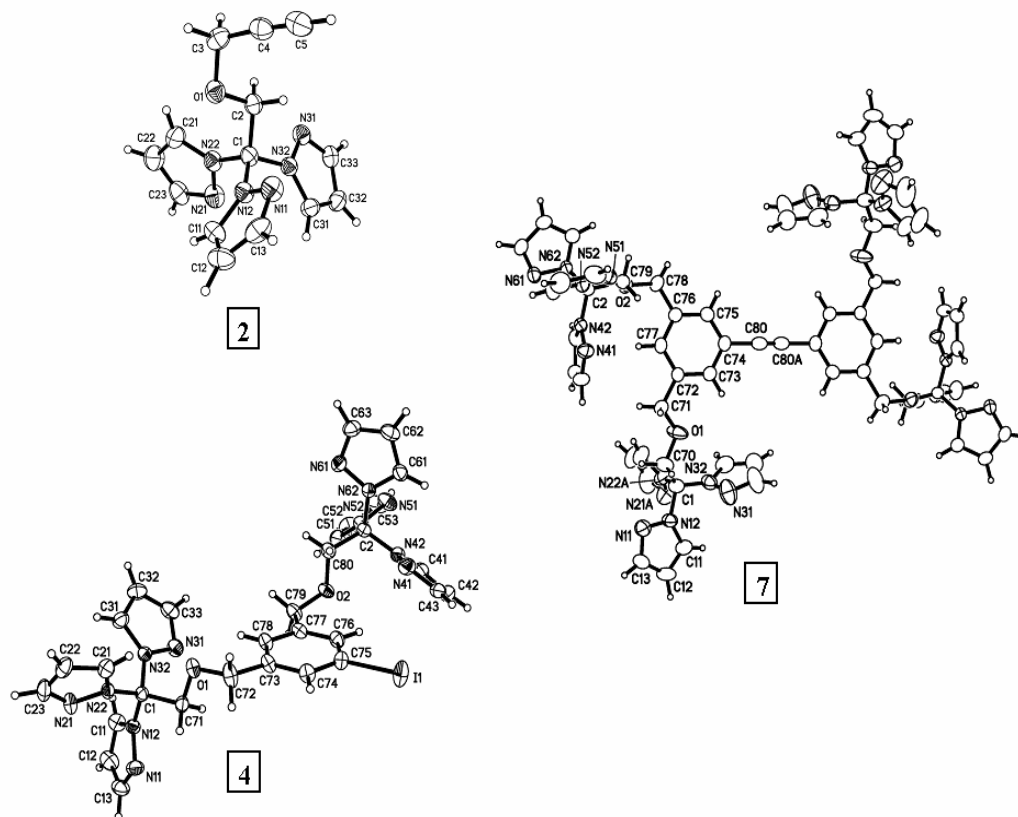


Figure 2.1 Molecular structures of alkynyl-containing tris(pyrazolyl)methane ligands.

In the case of **2.2**, the three dimensional supramolecular structure is comprised of two sets of CH- π interactions. As shown by red lines on the left side Figure 2.2, CH- π interactions between a pyrazolyl hydrogen donor [H(21)] and the π -cloud of the pyrazolyl ring containing N(12) organize the molecules of **2.2** into chains that run along the *c* axis. The geometry of the interaction, CH(21)-Ct[N(12)] 2.93 Å, 137.8° (Ct = ring centroid), is within expected values.^{13,14} These chains are shown rotated 90° into the *a*, *b* plane in the center of Figure 2.2. The right side of the Figure, also in the *a*, *b* plane, shows that the chains are organized into a three dimensional structure by CH- π interactions (green lines) with the alkynyl hydrogens [H(5)] interacting with the pyrazolyl groups that contain

N(31). The geometry of this type of interaction {CH(5)-Ct[N(31)] 3.12 Å, 166.8°} is also within accepted values.¹⁵

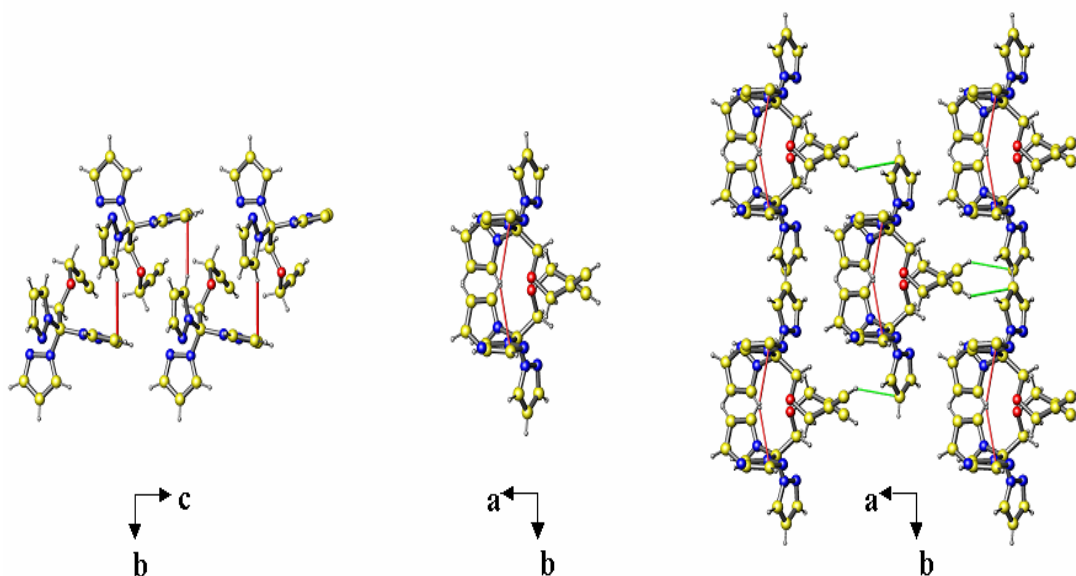


Figure 2.2 Three dimensional supramolecular structure of $\text{HC}_2\text{CCH}_2\text{OCH}_2\text{C}(\text{pz})_3$ **2.2** held together via pyrazolyl CH- π (pyrazolyl) interactions (red lines) and alkynyl CH- π (pyrazolyl) interactions (green lines).

The supramolecular structure of **2.4** (Figure 2.3) is that of sheets organized by CH- π and CH \cdots I interactions in the crystal. A set of prototypical CH- π interactions (red lines, Figure 2.3) between H(33) on a pyrazolyl ring and the π -cloud of the pyrazolyl ring containing N(61) {CH(33)-Ct[N(61)] 2.93 Å, 165.2°} organizes neighboring molecules of **2.4** into dimers (Figure 2.3, left). These dimers are further organized into chains that run along the crystallographic [111] direction by another set of CH- π interactions (pink lines, Figure 2.3, middle) that occur between H(71a) from a methylene group and the π -cloud of the pyrazolyl ring containing N(21), CH(71a)-Ct[N(21)] 3.09 Å, 148.1°. These chains are organized into sheets by a set of CH \cdots I interactions (green lines, Figure 2.3, right) along the c axis involving the acidic hydrogen at the 3-position of a pyrazolyl ring,

H(23). The geometry of the interaction $[\text{CH}(23)\cdots\text{I}, 3.08 \text{ \AA}, 162.9^\circ]$ is similar to that seen in other systems.¹⁶

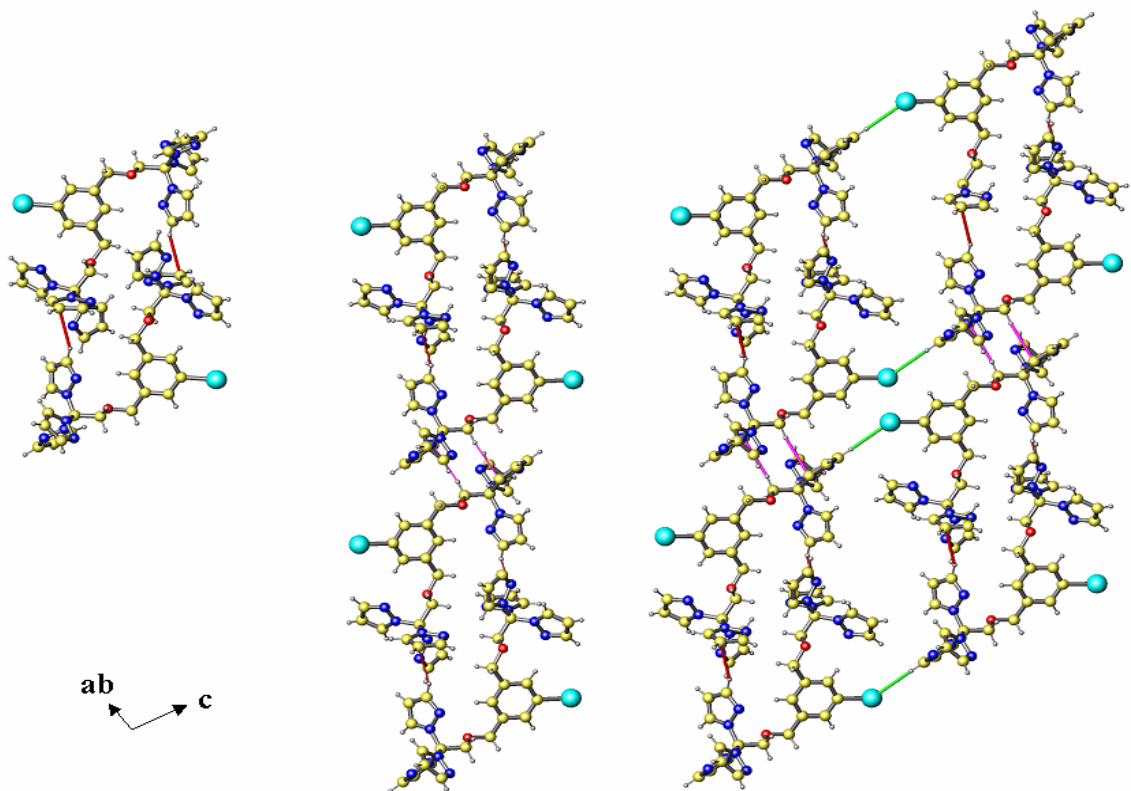


Figure 2.3 Two dimensional sheet structure of $\text{IC}_6\text{H}_4[\text{CH}_2\text{OCH}_2\text{C}(\text{pz})_3]_2$ (**2.4**) comprised of $\text{CH}-\pi$ interactions (red and pink lines) and $\text{CH}\cdots\text{I}$ interactions (green lines).

Interestingly, it has not yet been possible to crystallize the related complex 1,3- $\text{C}_6\text{H}_4[\text{CH}_2\text{OCH}_2\text{C}(\text{pz})_3]_2$ (where a hydrogen replaces the iodine) which exists as an oil.^{3d} This fact underscores the importance of introducing groups that can participate in noncovalent interactions (as in the case of the iodine group and allowing $\text{CH}\cdots\text{I}$ interactions) for the ultimate purpose of learning to control the crystal packing behavior of molecular solids. Another intriguing feature in the current system and its phenyl analogue, in terms of the future of ‘crystal engineering’ is that it remains unclear what role the orientation of the ethereal arms have on the crystal packing behavior or vice

versa. Thus, **2.4** has the ether sidearms located above and below the plane of the central arene ring but the arms in the metal complex $\{1,3\text{-C}_6\text{H}_4[\text{CH}_2\text{OCH}_2\text{C}(\text{pz})_3]_2(\text{Mn}(\text{CO})_3)_2\}(\text{BF}_4)_2^{3\text{d,f}}$ have the opposite orientation with both on the same side of the arene ring.

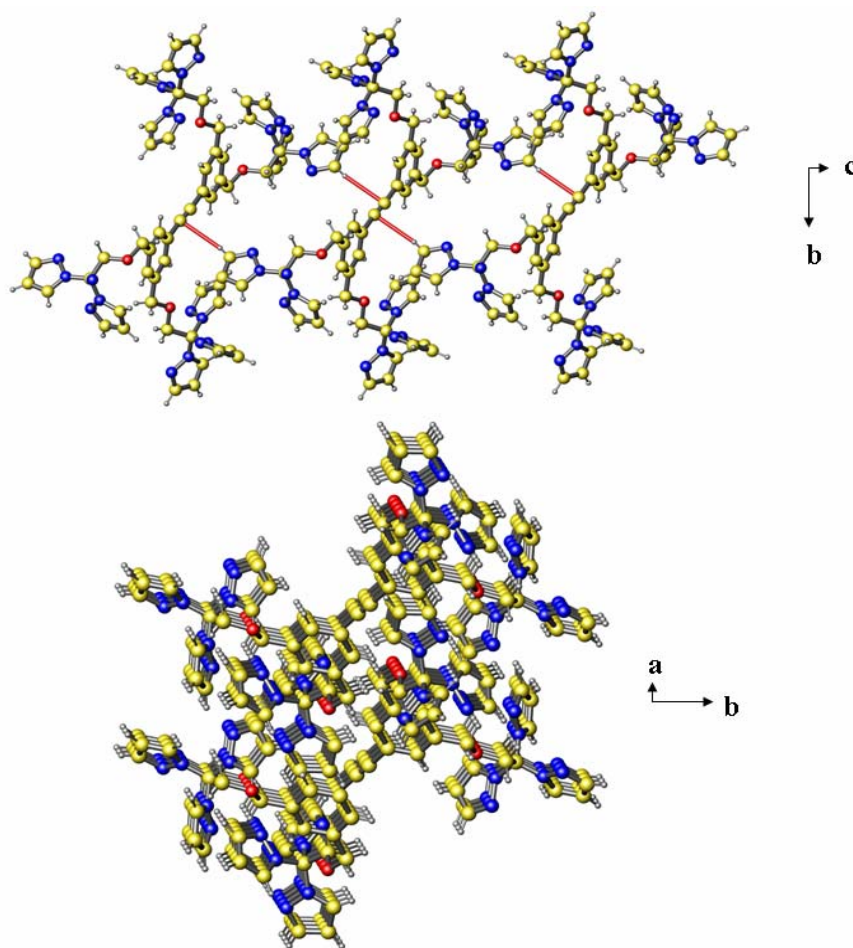


Figure 2.4 Supramolecular structure of 3,3',5,5'-[(pz)₃CCH₂OCH₂]₄ (C₆H₃C₂C₆H₃) (**2.7**). Top: View emphasizing one chain created by CH(pz)- π (alkyne) interactions (red lines). Bottom: 3D network of **2.7**.

The supramolecular structure of **2.7** (Figure 2.4) is three-dimensional, mainly as a result of CH- π interactions (Table 2.1), including some that involve the central alkynyl spacer as originally intended at the outset of this research. The building blocks are held into chains by CH- π interactions, which occurs between the acidic hydrogen H(53) at the

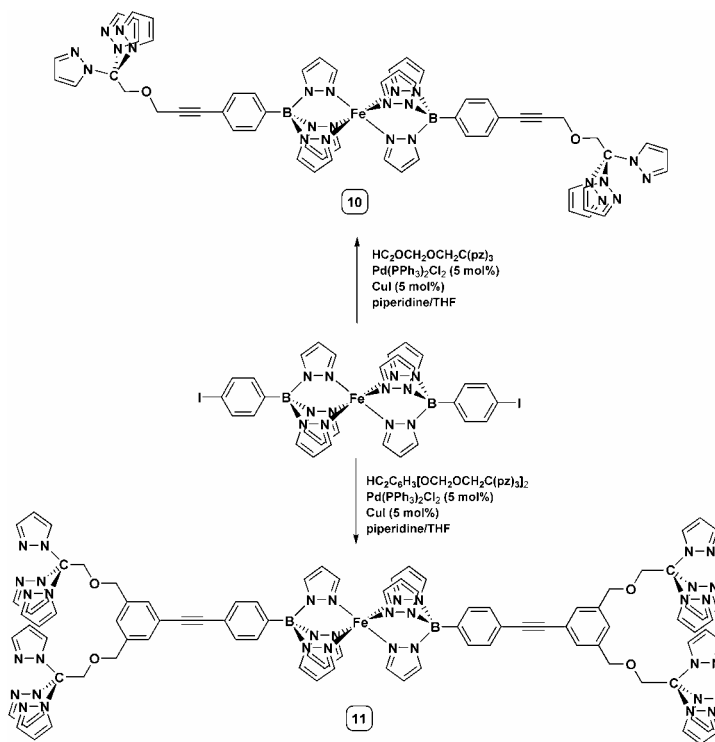
three position of a pyrazolyl ring and the π -cloud of the alkyne fragment. The geometrical parameters for this interaction [CH(53)-C(80) distance of 2.74 Å, C-H-C angle of 149.9°] are in line with other CH- π alkyne interactions.¹⁵ Given the fact that the molecule is centrosymmetric, this interaction links the molecular building blocks into chains positioned in the *bc* plane and running along *c* axis of the unit cell. One chain, build up from three molecules, is shown at the top of Figure 2.4, where the red lines represent the CH- π (alkyne) interactions. These chains are connected into a 3D network as a result of two sets of CH- π interactions (bottom of Figure 2.4). In contrast to the previous CH- π interaction where the acceptor π cloud was located on the alkyne moiety, here in both cases the hydrogen atom acceptors are pyrazolyl rings. For the first set of interaction the hydrogen donor is the pyrazolyl ring containing the C(12) ring {C-H(12)-Ct[N(41)] distance=2.80 Å and C-H-Ct angle=158.0°}. For the second set, the hydrogen donor involves an ethereal methylene group located on one of the side arms of the compound {CH(78a)-Ct[N(51)], 3.07 Å, 145.4°}. It is worth mentioning that this arrangement is supported by CH-N interactions that occur between H(21b) of the rotationally disordered pyrazolyl ring and N(11) of a neighboring well-behaved pyrazolyl ring. The combination of these interactions build up the 3D network of **2.7**.

Table 2.1. Summary of intermolecular non covalent interactions for **2.7**

Donor(D)-H...Acceptor (Å)	D-H...A (Å)	D-H...A (°)
Chain formation		
<i>C(53)-H(53)...</i> <i>C(80)</i>	2.74	149.9
3D network		
C(12)-H(12)...Ct[N(41)]	2.80	158.0
C(78)-H(78a)...Ct[N(51)]	3.07	145.4
C(21b)-H(21b)...N(11)	2.56	161.1

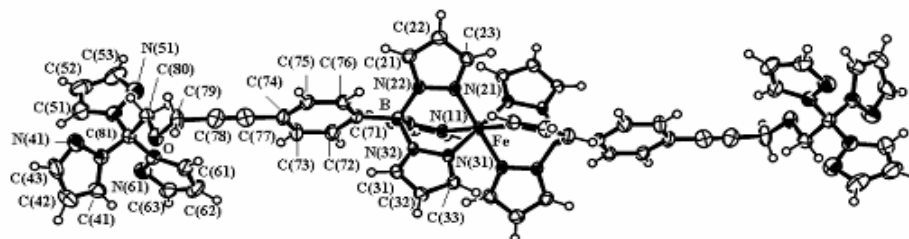
Mixed tris(pyrazolyl)borate/tris(pyrazolyl)methane metallo-ligands.

The chemistry used to build organic ligands in Scheme 2.1 can be extended to properly functionalized metal complexes. Reger has previously reported the syntheses of $\text{Fe}[(p\text{-IC}_6\text{H}_4)\text{B}(3\text{-Rpz})_3]_2$ ($\text{R} = \text{H}, \text{Me}$) compounds with interesting spin-crossover properties (for $\text{R} = \text{Me}$).⁸ The compound $\text{Fe}[(p\text{-IC}_6\text{H}_4)\text{B}(\text{pz})_3]_2$ was smoothly converted to the dialkynlated bitopic $\text{Fe}[\kappa^3(\text{B})\text{-(pz)}_3\text{CCH}_2\text{OCH}_2\text{-C}_2\text{-C}_6\text{H}_4\text{B}(\text{pz})_3]_2$ (**2.10**) by reaction with **2.2** and a similar reaction with **2.6** yields the tetratopic metalloligand $\text{Fe}[\kappa^3(\text{B})\text{-}\{3,5\text{-}[(\text{pz})_3\text{CCH}_2\text{OCH}_2]_2\text{C}_6\text{H}_3\text{C}_2\}\text{C}_6\text{H}_4\text{B}(\text{pz})_3]_2$ (**2.11**) (Scheme 2.2) by using Sonogashira coupling reactions. These iron-containing unsubstituted pyrazolyl derivatives are purple, low spin diamagnetic species at room temperature, and the NMR spectra showed the expected resonances with chemical shifts in typical ranges 1 to 10 ppm.

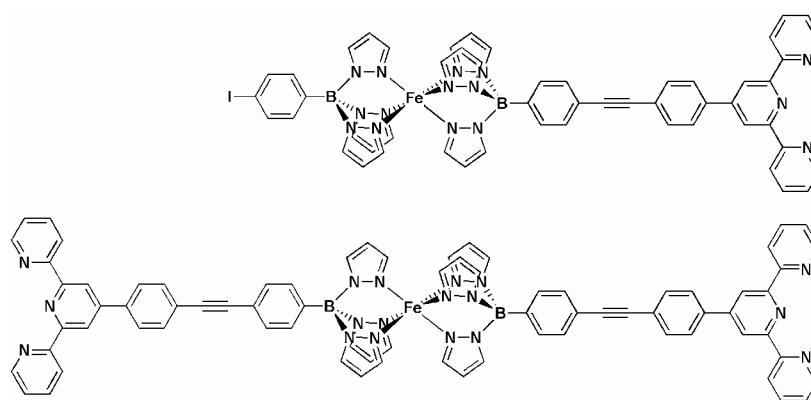


Scheme 2.2 Preparation of mixed tris(pyrazolyl)methane-tris(pyrazolyl)borate ligands.

The solid state structure of **2.10** has been determined crystallographically, Figure 2.5. While disorder problems precluded a high accuracy structure, the Fe-N average bond distance of 1.96 is typical of low spin iron(II), as expected from the color and NMR spectra. Disorder problems in the structure prevent further analysis of the crystal packing.



It was found that a similar Sonogashira coupling reaction between $\text{HC}_2\text{C}_6\text{H}_4\text{-terpy}$ and $\text{Fe}[(p\text{-IC}_6\text{H}_4)\text{B}(\text{pz})_3]_2$ afforded a highly insoluble solid mixture that showed signals in the ESI(+) mass spectra that could be attributed to the mono- and dialkynyl coupled products (Scheme 2.3). Considering the ease of the previous reactions, it is evident that the low solubility of the mono and disubstituted (alkynylphenyl)terpy derivatives in every solvent hampered the completion of the reaction in addition to inhibiting the potential for product separation and characterization.



Scheme 2.3 Iron-containing products obtained from attempted Sonogashira coupling reactions between $\text{Fe}[\text{IC}_6\text{H}_4\text{B}(\text{pz})_3]_2$ and $\text{HC}_2\text{C}_6\text{H}_4\text{-terpy}$

2.3. CONCLUSION

We have prepared a new family of semi-rigid, multitopic ligands based on linking tris(pyrazolyl)methane units via central alkynyl spacers. Sonogashira coupling reactions were used to prepare phenylalkynyl based compounds while oxidative Glaser homocoupling reactions have been used to prepare butadiynyl based compounds. The main architectural feature of the new linked ligands is their overall rigid linear geometry, but with semi-rigid ending groups. The flexibility of these ending groups is important to future chemistry as they provide solubility and structural adaptivity to metal complexes.

In addition, we have shown that these compounds exhibit rich supramolecular (structural) chemistry that is a function of the added substituents along the ligand periphery - the addition of iodide allows for CH \cdots I interactions whereas the addition of alkynyl moieties allows for extended structures based on CH- π interactions involving this electron rich group. While we have centered our chemistry on symmetrical multitopic ligands based on tris(pyrazolyl)methane units, the chemistry outlined here is applicable for other ligand systems.

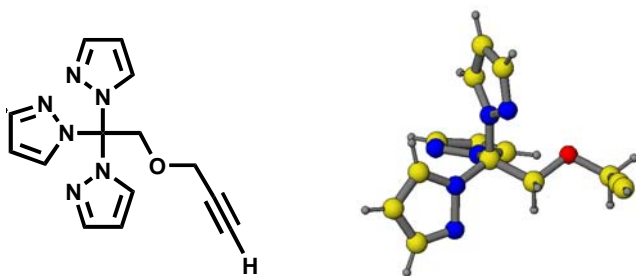
Importantly, we were able to use this chemistry to prepare new examples of “third generation” poly(pyrazolyl)borate and poly(pyrazolyl)methane ligands. First generation poly(pyrazolyl)borate ligands, initially introduced by Trofimenko,¹⁷ are the simple [HB(Rpz)₃][−] type ligands with non-bulky substituents at the 3-position. Second generation ligands, also introduced by Trofimenko,¹⁸ are those with bulky substituents at the 3-position. Third generation ligands are designed to be those specifically functionalized at the non-coordinating, “back” position of the ligands, either at boron or carbon and a number of examples have been reported previously.^{3,14,19} In this chemistry we have prepared the first third generation compound containing both the tris(pyrazolyl)methane and tris(pyrazolyl)borate ligating units where the borate end was bound to iron(II). This chemistry opens up the door for the further exploration into incorporating methyl-substituted pyrazolyls (which undergo spin transitions in iron(II) chemistry) or even other metal systems with the purpose of putting electro- and/or photoactive centers into highly organized coordination network solids.

2.4 EXPERIMENTAL

General Considerations

All operations were carried out under a nitrogen atmosphere by using either standard Schlenk techniques or in a Vacuum Atmospheres HE-493 inert atmosphere dry box, unless otherwise specified. Solvents for synthetic procedures and spectroscopic studies were dried by conventional methods and distilled under N₂ atmosphere immediately prior to use. The compounds HOCH₂C(pz)₃ (1),^{3j} 3,5-di(bromomethyl) iodobenzene,⁶ 4-ethynylphenyl-terpyridine,⁷ and Fe[(IC₆H₄)B(pz)₃]₂,⁸ were prepared by literature procedures. Melting point determinations were made on samples contained in glass capillaries by using an Electrothermal 9100 apparatus and are uncorrected. Mass spectrometric measurements recorded in ESI(+/-) mode were obtained on a Micromass Q-ToF spectrometer whereas those performed by using direct probe analyses were made on a VG 70S instrument. NMR spectra were recorded by using either a Varian Gemini 300 or a Varian Mercury 400 instrument, as noted within the text. Chemical shifts were referenced to solvent resonances at δ_{H} 7.25 and δ_{C} 77.0 for CDCl₃; and δ_{H} 2.05 and δ_{C} 29.15 for acetone-d₆.

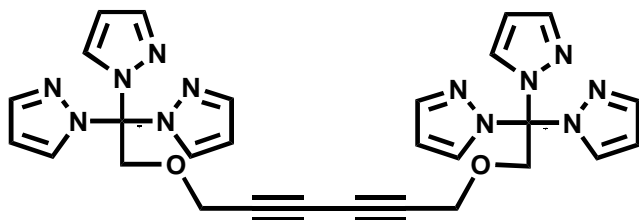
I would like to thank James R. Gardinier and Radu F. Semeniuc for their help specially on synthesis of **2.10** and **2.11**.



HC₂CH₂OCH₂C(pz)₃ **2.1**

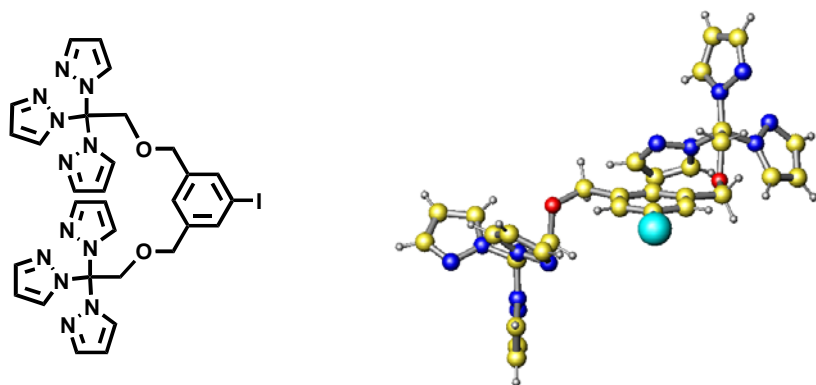
Tris-2,2,2-(1-pyrazolyl) ethanol, HOCH₂C(pz)₃ (5.67 g, 23.2 mmol) was dissolved in 150 mL dry THF and was added dropwise over 30 min via cannula to a suspension of 0.930 g NaH (23.1 mmol) in 50 mL dry THF. The mixture was stirred and heated at reflux 2 h, then propargyl bromide, HCCCH₂Br (2.76 g, 23.2 mmol), was injected via syringe. After the mixture was heated at reflux for 24 h, 100 mL H₂O was carefully added. The organic and aqueous portions were separated, the aqueous portion was extracted with two 100 mL portions of CH₂Cl₂, then the combined organic extracts were washed with 100 mL saturated NaHCO₃ solution and water (3x100 mL). After separation, the organics were dried over anhydrous MgSO₄, filtered, and the solvent was removed by rotary evaporation to give a brown solid residue. After chromatography on silica gel with hexane: ethyl acetate (1:1) as an eluent 3.35 g (52%) of **2.2** was obtained as a colorless solid. ¹H NMR (300 MHz, CDCl₃): δ 7.67 (d, J = 1 Hz, 3H, H₃-pz), 7.42 (d, J = 2 Hz, 3H, H₅-pz), 6.38 (d of d, 3H, J = 2,1 Hz, H₄-pz), 5.00 (s, 2H, OCH₂C (pz)₃), 4.20 (d, 2H, J = 2.5 Hz, OCH₂CC), 2.43 (m, 1H, CCH); ¹³C NMR (75.4 MHz, CDCl₃): δ 141.6 (C₃-pz), 131.0 (C₅-pz), 106.8 (C₄-pz), 89.5 (C_α), 78.7, 76.0 (C≡C), 73.0 (CH₂), 59.4 (CH₂); ¹H NMR (300 MHz, acetone-d₆): δ 7.61 (d, J = 1 Hz, 3H, H₃-pz), 7.47 (d, J = 2 Hz, 3H, H₅-pz), 6.36 (d of d, 3H, J = 2,1 Hz, H₄-pz), 5.17 (s, 2H, OCH₂C(pz)₃), 4.23 (d, 2H, J = 2.4 Hz, OCH₂CC), 3.10 (m, 1H, CCH); ¹³C NMR (75.4 MHz, acetone-d₆): δ 141.2 (C₃-

pz), 131.3 (C₅-pz), 106.6 (C₄-pz), 90.0 (C_a), 79.3, 76.8 (C≡C), 72.9 (CH₂), 59.0 (CH₂); IR: ν 3261, 3128, 2927, 2111, 1793, 1749, 1710, 1606, 1516, 1321, 1204, 1041, 947; High Res ESI(+) MS Calculated for [M+Na], [C₁₄H₁₄N₆ONa], 305.1127, found 305.1134; Anal. Calcd (Obs) for C₁₄H₁₄N₆O: C, 48.00 (48.32); H, 4.03 (3.89); N, 23.99 (24.26); Mp, 75-76 °C.



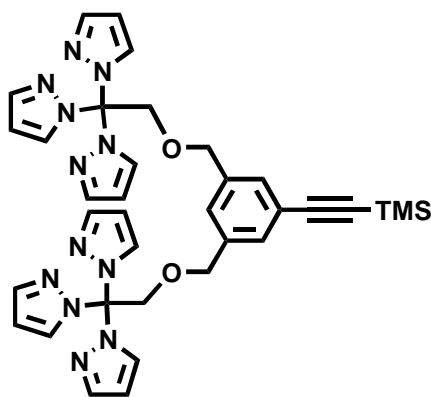
[-C₂CH₂OCH₂C(pz)₃]₂ (2.3). A mixture of 0.600 g (2.13 mmol) HC₂CH₂OCH₂C(pz)₃ (**2.2**) and 3.86 g (21.0 mmol) anhydrous Cu(OAc)₂ in 30 mL acetonitrile was stirred at 70°C for 6 h. The mixture was then partitioned between 150 mL each of CH₂Cl₂ and water, the organic fraction was collected and the aqueous fraction was extracted with three 50 mL portions of CH₂Cl₂. The combined organics were dried over MgSO₄, filtered and solvent was removed under vacuum to leave 0.540 g (90 %) crude **2.3** as a pale yellow solid. Purification of the crude yellow solid by column chromatography on silica gel with Et₂O as the eluent (R_f = 0.6) afforded 0.502 g (84%) pure **2.3** as a colorless solid. ¹H NMR (300 MHz, CDCl₃): δ 7.67 (d, J = 1.6 Hz, 6H, H₃-pz), 7.39 (d, J = 2.5 Hz, 6H, H₅-pz), 6.35 (dd, 6H, J = 2,1 Hz, H₄-pz), 5.19 (s, 4H, OCH₂C(pz)₃), 4.24 (s, 4H, OCH₂CC); ¹³C NMR (75.4 MHz, CDCl₃): δ 141.4 (C₃-pz), 130.7 (C₅-pz), 106.6 (C₄-pz), 89.5 (C_a), 74.9, 73.4 (C≡C), 71.4 (CH₂), 60.0 (CH₂); IR: ν 3147, 3123, 2959, 2936, 2878, 2627, 2569, 2432, 2181, 2137, 1765, 1614, 1518, 1427, 1389, 1325, 1261, 1198,

1042, 947, 916, 862, 791, 756; Accurate ESI(+) MS Calculated for [M+H], [C₂₈H₂₇N₁₂O₂], 563.2380, found 563.2387, Anal. Calcd (Obs) for C₂₈H₂₆N₁₂O₂: C, 59.78 (59.39); H, 4.66 (4.89); N, 29.88 (29.53); Mp, 143-145°C.



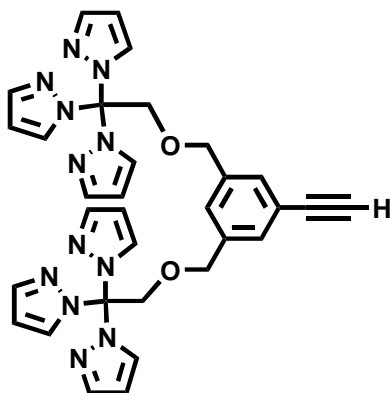
3,5-[(pz)₃CCH₂OCH₂]₂C₆H₃I (2.4). A solution of 0.463 g (1.19 mmol) 3,5-(BrCH₂)₂C₆H₃I in 20 mL THF was added via cannula to a 40 mL THF solution containing 2.38 mmol NaOCH₂C(pz)₃ [generated in-situ from 0.580 g (2.38 mmol) HOCH₂C(pz)₃ (**2.1**) and an excess of NaH (0.067 g, 2.79 mmol)]. The resulting mixture was stirred and heated at reflux for 12h. Water was carefully added, followed by 100 mL of methylene chloride. The aqueous and organic fractions were separated; the aqueous fraction was extracted with three 100 mL portions of CH₂Cl₂. The combined organic portions were washed with 100 mL, 6 wt% NaHCO₃ [to remove any unreacted HOCH₂C(pz)₃], then with 100 mL H₂O. The organics were dried over MgSO₄, filtered and solvent was removed by rotary evaporation to leave a pale yellow oil. The oil was adsorbed onto a pad of silica and loaded on a short pad of fresh silica. The plug was first flushed with CH₂Cl₂ to remove an unidentified impurity (TLC R_f = 0.75), and then with Et₂O to elute the desired product (TLC R_f = 0.75). Removing diethyl ether by rotary evaporation left a colorless oil that was triturated with 5 mL hexanes to give a colorless

solid. The hexane solution was decanted, and the remaining solid was dried under vacuum to give 0.768 g (90 %) of pure **4** as a colorless solid. Suitable crystals for X-ray diffraction were grown by dissolving a portion in Et₂O and adding an equal volume of hexanes and allowing the solution to evaporate slowly. ¹H NMR (300 MHz, CDCl₃): δ 7.67 (d, J = 1 Hz, 6H, H₃-pz), 7.41 (d, J = 3 Hz, 6H, H₅-pz), 7.38 (m, 2H, C₆H₃I), 6.92 (s, 1H, C₆H₃I), 6.36 (dd, 6H, J = 3,1 Hz, H₄-pz), 5.11 (s, 4H, OCH₂C(pz)₃), 4.43 (s, 4H, OCH₂CC); ¹³C NMR (75.4 MHz, CDCl₃): δ 141.6 (C₃-pz), 139.7 (aryl), 136.2 (aryl), 131.1 (C₅-pz), 126.1 (C₄-aryl), 106.8 (C₄-pz), 94.7 (C_i-I), 89.7 (C_a), 73.9 (CH₂), 73.3 (CH₂); IR: ν 3375, 3167, 3080, 2936, 2918, 2866, 2388, 1732, 1601, 1566, 1516, 1423, 1391, 1329, 1280, 1250, 1225, 1200, 1153, 1113, 1096, 1068, 1045, 995, 968, 947, 930, 916, 903, 864, 847, 794, 750, 689, 677; Accurate ESI(+) MS Calculated for [M+H], [C₃₀H₃₀N₁₂O₂I] 717.1659, found 717.1653; Anal. Calcd. (Obs.) for C₃₀H₂₉N₁₂O₂I: C, 50.29 (50.34); H, 4.08 (4.26); N 23.46 (23.28); Mp, 124 – 127 °C.

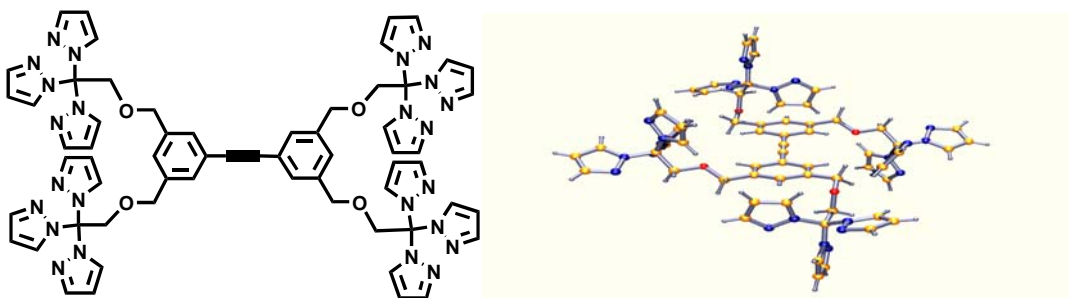


3,5-[(pz)₃CCH₂OCH₂]₂C₆H₃(C₂SiMe₃) (2.5**).** A Schlenk tube containing 1.83 g (2.55 mmol) of 3,5- [(pz)₃CCH₂OCH₂]₂C₆H₃I (**2.4**), 90 mg (0.13 mmol, 6 mol%) Pd(PPh₃)₂Cl₂, and 24 mg (0.13 mmol, 6 mol%) CuI was evacuated and backfilled with nitrogen three

times. Dry THF (10 mL) and piperidine (5 mL) were added by syringe through a septum secured by copper-wire, the resulting mixture was frozen (-196°C), evacuated, and backfilled with N_2 . Next, 1.0 mL (7.2 mmol HC_2SiMe_3) was added to the frozen mixture under a N_2 blanket by syringe. The mixture was placed in an external 40°C water bath (the stopcock was momentarily opened to the nitrogen line bubbler to relieve excess pressure) and was stirred at 40°C overnight. The mixture was poured into 100 mL H_2O and the aqueous phase was extracted with three 100 mL portions of CH_2Cl_2 followed by one 100 mL portion of Et_2O . The combined organics were dried over MgSO_4 , filtered and solvent was removed to give a brown oil. The oil was subject to chromatography on SiO_2 , the column was first eluted with methylene chloride to remove fast-moving impurities then with Et_2O where the desired product elutes near the solvent front. A second chromatographic separation on basic Al_2O_3 with CH_2Cl_2 as the eluent (R_f 0.8) affords the desired compound as a colorless semi-solid (1.4 g 82%). ^1H NMR (CDCl_3): δ 7.67 (d, J = 1 Hz, 6H, $\text{H}_3\text{-pz}$), 7.42 (d, J = 2 Hz, 6H, $\text{H}_5\text{-pz}$), 7.17 (br s, 2H, $\text{C}_6\text{H}_3\text{I}$), 6.92 (s, 1H, $\text{C}_6\text{H}_3\text{I}$), 6.34 (dd, 6H, J = 2, 1 Hz, $\text{H}_4\text{-pz}$), 5.11 (s, 4H, $\text{OCH}_2\text{C}(\text{pz})_3$), 4.44 (s, 4H, OCH_2CC), 0.27 (s, 9H, SiCH_3); ^{13}C NMR (75.4 MHz, CDCl_3): δ 141.6 ($\text{C}_3\text{-pz}$), 137.7 (aryl), 131.1 ($\text{C}_5\text{-pz}$), 130.9 (aryl), 127.1 ($\text{C}_4\text{-aryl}$), 123.7 ($\text{C}_i\text{-Si}$), 106.8 ($\text{C}_4\text{-pz}$), 104.7, 94.9 ($\text{C}\equiv\text{C}$), 90.0 (C_α), 73.8 (CH_2), 73.7 (CH_2), 0.15 (SiCH_3); Accurate ESI(+) MS Calculated for $[\text{M}+\text{H}]$, $[\text{C}_{35}\text{H}_{39}\text{N}_{12}\text{O}_2\text{Si}]$, 687.3088, found 687.3080; Anal. Calcd. (Obs.) for $\text{C}_{35}\text{H}_{38}\text{N}_{12}\text{O}_2\text{Si}$: C, 61.20 (60.71); H, 5.58 (5.84).

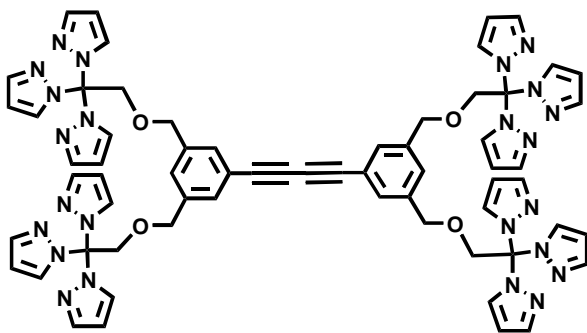


3,5-[(pz)₃CCH₂OCH₂]₂C₆H₃(C₂H) (2.6). A 4.4 mL (4.4 mmol) aliquot of a 1.0 *M* NBu₄F solution in THF was added to a solution of **2.5** (3.00 g, 4.40 mmol) in 5 mL THF. After the mixture had stirred for 30 min, it was partitioned between 50 mL CH₂Cl₂ and 100 mL H₂O. The organic and aqueous phases were separated and the aqueous phase was extracted with three 50 mL portions CH₂Cl₂. The combined organics were dried over MgSO₄, filtered and solvent was removed by rotary evaporation to leave 2.65 g (88%) **2.6** as a nearly colorless, pale yellow solid. ¹H NMR (300 MHz, CDCl₃): δ 7.67 (d, *J* = 1 Hz, 6H, H₃-pz), 7.43 (d, *J* = 2 Hz, 6H, H₅-pz), 7.20 (br s, 2H, C₆H₃), 6.95 (br s, 1H, C₆H₃), 6.35 (dd, 6H, *J* = 2, 1 Hz, 6H, 4-*H* pz), 5.13 (s, 4H, OCH₂C(pz)₃), 4.46 (s, 4H, OCH₂CC), 3.08 (s, 1H, CCH); ¹³C NMR (CDCl₃): δ 141.6 (C₃-pz), 137.9 (aryl), 131.1 (C₅-pz), 130.9 (aryl), 127.4 (aryl), 122.6 (aryl), 106.8 (C₄-pz), 90.0 (C_α), 83.3 (C≡C), 77.7 (C≡C), 73.8 (CH₂), 73.6 (CH₂); IR(solution in CH₂Cl₂): ν 3300, 3049, 2987, 2925, 2852, 2684, 2518, 2411, 2346, 2301, 2150, 2122, 2057, 2027, 1926, 1423, 1268, 1150, 1091, 1040, 896, 737; Accurate ESI(+) MS: Calcd. for [M+H], [C₃₂H₃₁N₁₂O₂], 615.2693, found 615.2684; Anal. Calcd. (Obs.) for C₃₂H₃₀N₁₂O₂: C, 62.53 (62.22); H, 4.92 (4.91); N, 27.34 (27.27); Mp, 102-103°C.



{3,3',5,5'-[(pz)₃CCH₂OCH₂]₄(1,1'-C₆H₃C₂C₆H₃)} (**2.7**). A mixture of 5.00 g (7.00 mmol) **2.4** and 4.30 g (7.0 mmol) **2.6** was dissolved in THF (5 mL) and purged with N₂. Under a nitrogen blanket Pd(PPh₃)₂Cl₂ (100 mg, 2 mol %), CuI (67 mg, 5 mol %), and piperidine (5 mL) were each added to the mixture. The flask was flushed for 15 min with a slow stream of nitrogen then an additional 5 mL of THF was added. The mixture was stirred overnight in a 60°C water bath, then 100 mL methylene chloride was added. After aqueous work up (washing with H₂O and brine), crude **2.7** was obtained as a light yellow solid (8.85 g 74%). Purification was achieved by adsorbing crude **2.7** onto a pad of silica, loading the silica onto a pad of fresh silica, eluting with Et₂O to remove any impurities, then with THF to give the desired product that moves with the solvent front. Removing solvent by rotary evaporation, triturating with Et₂O, filtering, and drying the colorless Et₂O insoluble solid under vacuum afforded **7·H₂O**. ¹H NMR (300 MHz, CDCl₃): δ 7.67 (d, J = 1 Hz, 12H, H₃-pz), 7.43 (d, J = 2 Hz, 12H, H₅-pz), 7.25 (s, 4H, C₆H₃), 6.96 (s, 2H, C₆H₃), 6.35 (dd, J = 2, 1 Hz, 12H, H₄-pz), 5.14 [s, 8H, OCH₂C(pz)₃], 4.48 (s, 8H, OCH₂CC), 1.62 (br s, 2H, H₂O); ¹³C NMR (75.4 MHz, CDCl₃): δ 141.6 (C₃-pz), 138.0 (aryl), 131.1 (C₅-pz), 130.5 (aryl), 127.1 (aryl), 123.6 (aryl), 106.8 (C₄-pz), 90.0 (C_α), 89.4 (C≡C), 73.84 (CH₂), 73.79 (CH₂); IR (solution in CH₂Cl₂): ν 3056, 2990, 2825, 2680, 2518, 2412, 2346, 2301, 2053, 1419, 1388, 1323, 1268, 1199, 1161, 1123, 1106, 1088, 947, 896, 737, 703; Accurate ESI(+) MS Calculated for [7+H],

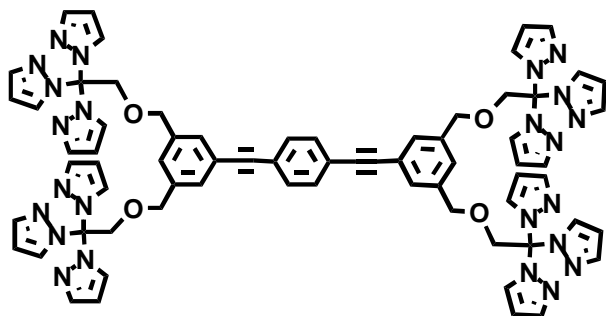
[C₆₂H₅₉N₂₄O₄], 1203.5151, found 1203.5127; Anal. Calcd (Obs) for C₆₂H₆₀N₂₄O₅: C, 60.97 (60.51); H, 4.86 (4.75); N, 27.52 (27.13); Mp, 207 – 209 °C w/ dec.



{3,5-[(pz)₃CCH₂OCH₂]₂C₆H₃C₂-}₂ (**2.8**). A 2.47 g (12.4 mmol) Cu(OAc)₂·H₂O was added to a solution of 0.760 g (1.24 mmol) **2.6** in 50 mL CH₃CN. The resulting heterogeneous mixture was stirred at 70 °C for 5 hours, then was added to 150 mL H₂O. The aqueous phase was extracted with three 100 mL portions CH₂Cl₂. The combined organics were dried over MgSO₄, filtered, and solvent was removed to leave a yellow oil. The yellow oil was adsorbed onto silica and then was added to a plug of fresh silica. The plug was first eluted with Et₂O to remove unidentified impurity, and then with THF to give the desired compound that moved with the solvent front. Solvent was removed by rotary evaporation and the residue was triturated with 10-20 mL Et₂O to precipitate the product that was collected by filtration. The Et₂O insoluble solid was washed with 5 mL hexanes, and dried under vacuum to leave 0.650 g (86%) of pure **2.8** as a colorless solid.

¹H NMR (300 MHz, CDCl₃): δ 7.68 (d, *J* = 1 Hz, 12H, H₃-pz), 7.43 (d, *J* = 3 Hz, 12H, H₅-pz), 7.23 (s, 4H, C₆H₃), 6.97 (s, 2H, C₆H₃), 6.36 (dd, *J* = 3, 1 Hz, 12H, 4-*H* pz), 5.13 (s, 8H, OCH₂C(pz)₃), 4.47 (s, 8H, OCH₂CC); ¹³C NMR (75.4 MHz, CDCl₃): δ 141.6 (C₃-pz), 138.1 (aryl), 131.2 (aryl), 131.1 (C₅-pz), 127.8 (C_{*i*}-aryl), 122.3 (C_{*i*}-aryl), 106.8

(C₄-pz), 90.0 (C_a), 81.4, 74.3 (C≡C), 73.9 (CH₂), 73.6 (CH₂); IR: ν 3056, 2990, 2832, 2680, 2522, 2408, 2346, 2305, 2156, 2122, 2053, 1602, 1426, 1264, 1202, 1150, 1109, 1092, 982, 899, 744, 703; ESI(+) MS Calculated for [M+H], [C₆₄H₃₉N₂₄O₄], 1227.5151, found 1227.5150; Anal. Calcd (Obs) for C₆₄H₅₈N₂₄O₄: C, 62.63 (62.38); H, 4.76 (4.69); N, 27.39 (27.15); Mp, 180-182 °C.



3,3',5,5'-[(pz)₃CCH₂OCH₂]₄[p-(1,1'-C₆H₃C₂)₂C₆H₄] (2.9). Method A. A mixture of 0.555 g (0.903 mmol) 3,5-[(pz)₃CCH₂OCH₂]₂C₆H₃(C₂H) (**6**), 0.136 g (0.412 mmol) *p*-I₂C₆H₄, 0.023 g (0.033 mmol) Pd(PPh₃)₂Cl₂, 20 mL THF, and 10 mL piperidine was subject to two freeze, pump, thaw cycles and was frozen once more. Then, 2 mg (0.01 mmol) CuI was added under a nitrogen blanket, the vessel (sealed with a copper wire reinforced septum) was evacuated and the mixture was subject to two more freeze pump thaw cycles, then the flask was back filled with nitrogen. The mixture was heated to 60°C with an external water bath, the stopcock was momentarily opened to the nitrogen line to relieve excess pressure, and the mixture was allowed to heat at 60°C 12h with stirring. The resulting yellow solution was added to 10 g of silica gel and solvents were removed by rotary evaporation. The dry silica gel was loaded onto a fresh pad of silica and eluted first with hexanes then Et₂O to remove any unwanted impurities. Flushing the

plug with with 2:1 (v:v) THF:hexanes elutes the desired compound in a pale yellow band (TLC R_f = 0.8; bright blue luminescence when irradiated with either 254 nm or 365 nm light). Evaporation of solvent, triturating the residue with hexanes, filtering and drying under vacuum afforded 0.529 g (95%) **9·2H₂O** as a hygroscopic and solvophilic pale yellow solid. ¹H NMR (300 MHz, CDCl₃): δ 7.68 (d, J = 1 Hz, 12H, H₃-pz), 7.53 (s, 4H, C₆H₄), 7.44 (d, J = 3 Hz, 12H, H₅-pz), 7.26 (s, 4H, C₆H₃), 6.96 (s, 2H, C₆H₃), 6.36 (dd, J = 3, 1 Hz, 12H, 4-*H* pz), 5.15 (s, 8H, OCH₂C(pz)₃), 4.49 (s, 8H, OCH₂CC), 1.66 (br s, 4H, H₂O); ¹³C NMR (75.4 MHz, CDCl₃): δ 141.6 (C₃-pz), 138.0 (C₆H₃), 131.8 (C₆H₃), 131.1 (C₅-pz), 130.5 (C_{2,3,5,6}-C₆H₄), 127.1 (C_i-C₆H₄), 123.6 (C_{4/i}-C₆H₃), 123.3 (C_{4/i}-C₆H₃), 106.8 (C₄-pz), 91.1 (C≡C), 90.0 (C_α), 89.6 (C≡C), 73.8 (CH₂), 73.7 (CH₂); IR: ν 3151, 3130, 3040, 2934, 2868, 2716, 2557, 2432, 2210, 1915, 1865, 1770, 1730, 1599, 1514, 1454, 1423, 1391, 1325, 1254, 1200, 1161, 1126, 1109, 1092, 1063, 1040, 1018, 947, 916, 866, 839, 789, 752, 694; Accurate ESI(+) MS Calculated for [9+H], [C₇₀H₆₃N₂₄O₄], 1304.5464, found 1304.5437; Anal. Calcd (Obs) for C₇₀H₆₆N₂₄O₆: C, 62.77 (63.26); H, 4.97 (4.88); N, 25.10 (24.32); Mp: 70 °C glass trans., 95-100 °C liq.

Method B. A 2.0 mL THF solution of 0.040 g (0.15 mmol) bis(trimethylsilylethynyl)benzene and 0.14 mL of a 1.0 M NBu₄F in THF (0.14 mmol) was stirred for 30 min. The product mixture was partitioned between 50 mL each CH₂Cl₂ and H₂O, the organic phase is separated and the aqueous is extracted with an additional 50 mL CH₂Cl₂. The combined organics were dried over Na₂SO₄, filtered, and solvent was removed under vacuum, the residue (1,4-diethynylbenzene) was taken up in 10 mL THF and was transferred under nitrogen to a 4 mL nitrogen-purged solution of

THF/piperidine (1:1) containing 0.20 g (0.28 mmol) **2.4**, and 5 mol % each Pd(PPh₃)₂Cl₂ and CuI. After the mixture had been stirred 12 h at room temperature, it was worked up as described above to leave 0.10 g (0.074 mmol, 53 % based on NBu₄F) of **9·2H₂O** as a yellow solid. The characterization data were identical to those found described under Method A.

General Procedure for alkyne coupling reactions involving iron borate compounds.

A Schlenk flask is charged with the desired iron(II) (iodophenyl)tris(pyrazolyl)borate, Pd(PPh₃)₂Cl₂, terminal alkyne (XC₂H), THF and piperidine (ca 20 mL, between 4:1 to 2:1 v/v). The reaction vessel is then subjected to three freeze/pump/thaw cycles. The reaction mixture is frozen once more, the vessel is backfilled with N₂, CuI is added under a N₂ blanket. After the reaction flask is sealed with a septum reinforced by copper wire, it is frozen, evacuated, backfilled with nitrogen once more and then placed in a 60°C bath overnight. Then, the product mixture is adsorbed onto alumina, solvent is evaporated, and the alumina is added to a pad of fresh alumina. Eluting with hexanes eliminates any excess alkyne and homocoupled alkynyl impurities. Then, elution with CH₂Cl₂ affords the desired alkynylphenyl borate complex, Fe[(X-C₂C₆H₄)B(pz)₃]₂, in a fast moving purple band.

Fe[κ³(B)-(pz)₃CCH₂OCH₂-C₂-C₆H₄B(pz)₃]₂, (2.10). This compound was prepared in quantitative yield (312 mg) as a pink solid by using 0.231 g (0.261 mmol) Fe[IC₆H₄B(pz)₃]₂, 0.162 g (0.574 mmol) HC₂CH₂OCH₂C(pz)₃, 15 mg (8 mol %) Pd(PPh₃)₂Cl₂, 4 mg (8 mol %) CuI, 40 mL THF and 10 mL piperidine. An additional heating period of 8 h at 80°C was used in this case. Recrystallization by allowing a layer of MeOH to slowly diffuse into a CH₂Cl₂ solution at -20°C afforded pink-purple needles.

Mp, 220 °C dec., 255 °C liquifies; Anal. Calcd. (Obs.) For $C_{58}H_{52}N_{24}O_2B_2Fe$: C, 58.31 (57.71); H, 4.39 (4.12); N, 28.14 (27.84); 1H NMR (300 MHz, $CDCl_3$) δ 8.17 (part of AA'BB', J = 8 Hz, 4 H), 7.86 (d, J = 1 Hz, 6 H, H_3 -pz-C), 7.71 (br s, 6 H, H_5 -pz-B), 7.69 (part of AA'BB', 4 H), 7.51 (d, J = 2 Hz, 6 H, H_5 -pz-C), 7.02 (br s, 6 H, H_3 -pz-B), 6.39 (dd, J = 2,1 Hz, 6 H, H_4 -pz-C), 6.26 (br s, 6H, H_4 -pz-B), 5.35 (s, 4 H, OCH_2Cpz_3), 4.49 (s, 4 H, OCH_2CC); ^{13}C NMR (75.4 MHz, $CDCl_3$) δ 149.9, 141.6, 138.7, 135.1, 131.5, 131.1, 122.1, 106.8, 89.9, 87.7, 73.1, 60.3, 46.9; Accurate ESI(+) MS: Calcd. For M^+ : 1194.4260, Found: 1194.4302 .

$Fe[\kappa^3(B)-\{3,5-[(pz)_3CCH_2OCH_2]_2C_6H_3C_2\}C_6H_4B(pz)_3]_2$ (2.11). This compound was prepared in 91% yield (301 mg) as a pink-orange solid by using 0.158 g (0.178 mmol) $Fe[IC_6H_4B(pz)_3]_2$, 0.243 g (0.395 mmol) 1-(HC_2) $C_6H_3[3,5-CH_2OCH_2C(pz)_3]_2$, 25 mg (5 mol %) $Pd(PPh_3)_2Cl_2$, 6 mg (9 mol %) CuI , 10 mL THF and 5 mL piperidine. Mp, 310°C. Dec; Anal. Calcd. (Obs.) for $C_{94}H_{84}N_{36}O_4B_2Fe$: C, 60.72 (60.32); H, 4.55 (4.59); 27.12 (26.28); 1H NMR (300 MHz, $CDCl_3$) δ 8.92 (br s), 8.06 (br s), 7.72 (s, 12H, H_3 -pz-C), 7.67 (s), 7.49 (s, 12 H, H_5 -pz-C), 7.41 (m, overlapping), 7.02 (s), 6.40 (H_4 -pz-C), 6.36 (br, s, H_4 -pz-B), 5.20 (s, 8H, OCH_2Cpz_3) , 4.56 (s, 8 H, OCH_2CC); ESI(+) MS: Calcd. For M^+ : 1859, Found: 1859.

Attempted preparation of $Fe[\kappa^3(B)-4-[4'-(4-C_2C_6H_4)(2,2':6,2''-terpy)]C_6H_4B(pz)_3]_2$ (2.12) A mixture of 0.297 g (0.335 mol) $Fe[IC_6H_4B(pz)_3]_2$, 0.233 g (0.699 mmol) 4'-(4- $HC_2C_6H_4$)-2,2':6,2''-terpy, 12 mg (8 mol %) $Pd(PPh_3)_2Cl_2$, 2 mg (5 mol %) CuI , 3 mL THF and 3 mL piperidine was heated 8h at 70°C followed by 12h at room temperature. The resulting purple solid was collected by filtration, washed with three 10 mL portions MeOH, three 10 mL portions Et_2O and was air dried to afford 0.298 g of a very insoluble

(trace solubility in either refluxing tetrachloroethane or refluxing DMF) purple solid mixture of the mono- and disubstituted compounds as identified by High Res. ESI(+) TOF MS. Calcd (obs) for $\text{Fe}[\text{IC}_6\text{H}_4\text{B}(\text{pz})_3][(\text{terpy})\text{C}_6\text{H}_4\text{C}_2\text{C}_6\text{H}_4\text{B}(\text{pz})_3]$: 1091.2190 (1091.2190) and for $\text{Fe}[(\text{terpy})\text{C}_6\text{H}_4\text{C}_2\text{C}_6\text{H}_4\text{B}(\text{pz})_3]_2$ 1296.4338 (1296.4326).

2.5. References

1. a) G.F. Swiegers, T.J. Malefeste, *Chem. Rev.* **2000**, *100*, 3483. b) A.J. Blake, N.R. Champness, P. Hubberstey, W.S. Li, M.A. Withersby, M. Schröder, *Coord. Chem. Rev.* **1999**, *183*, 117. c) S.R. Batten, R. Robson, *Angew. Chem., Int. Ed. Engl.* **1998**, *37*, 1461. d) P.J. Stang, B. Olenyuk, *Acc. Chem. Res.* **1997**, *30*, 502. e) C.T. Chen, K.S. Suslick, *Coord. Chem. Rev.* **1993**, *128*, 293. f) R.D. Archer, *Coord. Chem. Rev.* **1993**, *128*, 49. g) N.R. Champness, M. Schröder, *Curr. Opin. Solid State Mater. Sci.* **1998**, *3*, 419.
2. a) P.S. Mukherjee, N. Das, P.J. Stang, *J. Org. Chem.* **2004**, *69*, 3526. b) K.W. Chi, C. Addicott, P.J. Stang, *J. Org. Chem.* **2004**, *69*, 2910. c) M. Fujita, S. Nagao, K. Ogura, *J. Am. Chem. Soc.* **1995**, *117*, 1649.
3. a) D.L. Reger, R.F. Semeniuc, V. Rassolov, M.D. Smith, *Inorg. Chem.* **2004**, *43*, 537. b) D.L. Reger, R.F. Semeniuc, M.D. Smith, *Inorg. Chem.* **2003**, *42*, 8137. c) D.L. Reger, R.F. Semeniuc, I. Silaghi-Dumitrescu, M.D. Smith, *Inorg. Chem.* **2003**, *42*, 3751. d) D.L. Reger, R.F. Semeniuc, M.D. Smith, *J. Organomet. Chem.* **2003**, *666*, 87. e) D.L. Reger, R.F. Semeniuc, M.D. Smith, *J. Chem. Soc., Dalton Trans.* **2003**, 285. f) D.L. Reger, R.F. Semeniuc, M.D. Smith, *J. Chem. Soc., Dalton Trans.* **2002**, 476. g) D.L. Reger, R.F. Semeniuc, M.D. Smith, *Inorg. Chem. Commun.* **2002**, *5*, 278. h) D.L. Reger, R.F. Semeniuc, M.D. Smith, *Inorg. Chem.* **2001**, *40*, 6545. i) D.L. Reger, T.D. Wright, R.F. Semeniuc, T.C. Grattan, M.D. Smith, *Inorg. Chem.* **2001**, *40*, 6212. j) D.L. Reger, T.C. Grattan, K.J. Brown, C.A. Little, J.J.S. Lamba, A.L. Rheingold, R.D. Sommer, *J. Organomet. Chem.* **2000**, *607*, 120.
4. K. Sonogashira, Y. Tohda, N. Hagihara, *Tetrahedron Lett.* **1975**, 4467.
5. D. L. Reger, J. R. Gardinier, W. R. Gemmill, M. D. Smith, A. M. Shahin, G. L. Long, L. Rebbouh, F. Grandjean, *J. Am. Chem. Soc.* **2005**, *127*, 2303-2316.
6. a) H.P. Dijkstra, M.D. Meijer, J. Patel, R. Kreiter, G.P.M. van Klink, M. Lutz, A.L. Spek, A. Canty, G. von Koten, *Organometallics* **2001**, *20*, 3159-3168. b) A.V. Rukavishnikov, A. Phadke, M.D. Lee, D.H. LaMunyo, P.A. Petukov, J.F. Keana, *Tetrahedron. Lett.* **1999**, *40*(35), 6353.
7. a) V. Grosshenny, F.M. Romero, R. Ziessel, *J. Org. Chem.* **1997**, *62*(5), 1491. b) P. Korall, A. Boerje, P.-O. Norrby, B. Aakermark, *Acta Chem. Scand.* **1997**, *51*(6/7), 760. c) C.A.G. Haasnoot, F. A. A. M. De Leeuw, C. Altona, *Tetrahedron*, **1980**, *36*, 2783.
8. D.L. Reger, J.R. Gardinier, M.D. Smith, A.M. Shahin, G.J. Long, L. Rebbouh, F. Grandjean, *Inorg. Chem.* **2005**, *44*, 1852-1867.
9. SMART Version 5.625 and SAINT+ Version 6.02a. Bruker Analytical X-ray Systems, Inc., Madison, Wisconsin, USA, 1998.

10. The DIRDIF99 program system. P.T. Beurskens, G. Beurskens, R. de Gelder, S. Garcia-Granda, R. Israel, R.O. Gould, J. M. M. Smits, Crystallography Laboratory, University of Nijmegen, The Netherlands. **1999**.
11. G.M. Sheldrick, SHELXTL Version 5.1; Bruker Analytical X-ray Systems, Inc., Madison, Wisconsin, USA, 1997.
12. PLATON, A Multipurpose Crystallographic Tool, Utrecht University, Utrecht, The Netherlands, A. L. Spek, **1998**.
13. C. Janiak, *J. Chem. Soc., Dalton Trans.* **2000**, 3885.
14. D.L. Reger, J.R. Gardinier, R.F. Semeniuc, M.D. Smith, *J. Chem. Soc., Dalton Trans.* **2003**, 1712.
15. a) W. Lu, M. C. W. Chan, N. Zhu, C. –M. Che, Z. He, K. –Y., *Chem. Eur. J.* **2003**, 9, 6155. b) T. Steiner, M. Tamm, *J. Organomet. Chem.* **1998**, 570, 235.
16. a) F. Ugozzoli, A. Arduini, C. Massera, A. Pochini, A. Secchi, *New J. Chem.* **2002**, 26, 1718. b) M. Freytag, P.G. Jones, B. Ahrens, A. K. Fischer, *New J. Chem.* **1999**, 12, 1137.
17. S. Trofimenko, *Scorpionates - The Coordination Chemistry of Polypyrazolylborate Ligands*, Imperial College Press; London, **1999**.
18. S. Trofimenko, J.C. Calabrese, J.S. Thompson, *Inorg. Chem.* **1987**, 28, 1507.
19. a) D. White, J. W. Faller, *J. Am. Chem. Soc.* **1982**, 104, 1548. b) C.P. Brock, M.K. Das, R.P. Minton, K. Niedenzu, *J. Am. Chem. Soc.* **1988**, 110, 817. c) C. Janiak, L.Braun, F. Girgsdies, *J. Chem. Soc., Dalton Trans.* **1999**, 3133. d) J.L. Kisko, T. Hascall, C. Kimblin, G. Parkin, *J. Chem. Soc., Dalton Trans.* **1999**, 1929. e) N.C. Hardin, J.C. Jeffery, J.A. McCleverty, L.H. Rees, M.A. Ward, *New J. Chem.* **1998**, 661. f) K. Niedenzu, S. Trofimenko, *Inorg. Chem.* **1985**, 24, 4222. g) F. Jäkle, K. Polborn, M. Wagner, *Chem. Ber.* **1996**, 129, 603. h) F. Fabrizi de Biani, F. Jäkle, M. Spiegler, M. Wagner, P. Zanello, *Inorg. Chem.* **1997**, 36, 2103. i) E. Herdtweck, F. Peters, W. Scherer, M. Wagner, *Polyhedron* **1998**, 17, 1149. j) S.L. Guo, F. Peters, F. Fabrizi de Biani, J.W. Bats, E. Herdtweck, P. Zanello, M. Wagner, *Inorg. Chem.* **2001**, 40, 4928. k) S.L. Guo, J.W. Bats, M. Bolte, M. Wagner, *J. Chem. Soc., Dalton Trans.* **2001**, 3572. l) S. Bieller, F. Zhang, M. Bolte, J.W. Bats, H.-W. Lerner, M. Wagner, *Organometallics* **2004**, 23, 2107. m) D.L. Reger, K.J. Brown, J.R. Gardinier, M.D. Smith, *Organometallics* **2003**, 22, 4973. n) D.L. Reger, R.P. Watson, J.R. Gardinier, M.D. Smith, *Inorg. Chem.* **2004**, 43, 6609-6619.

CHAPTER 3

SELECTIVE CLICK CHEMISTRY VIA MICROWAVE AS AN APPROACH TO NEW SMALL MOLECULES*

3.1 Introduction.

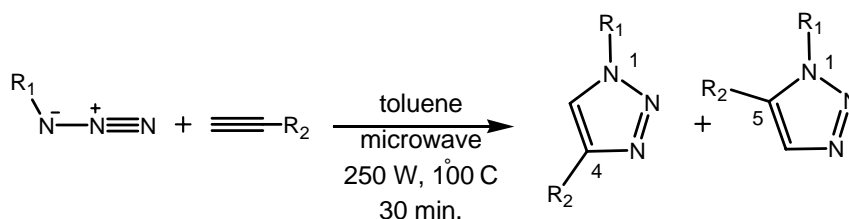
The 1,3-dipolar cycloaddition reaction of organic azides with alkynes, first investigated by Szeimies and Huisgen four decades ago,¹ gives stable 6π -aromatic 1,2,3-triazoles in high yields and under mild conditions. This transformation has been retooled by Sharpless as “click-chemistry” to synthesize biologically active species such as enzyme inhibitors² and is exploited to craft novel materials. Examples include click-functionalized dendrimers, polymers and dyes.³⁻⁵ The reaction of azides with alkynes is slow under thermal conditions, unless cyclooctyne is utilized,⁶ but Sharpless discovered that Cu(I) salts increase regioselectivity and reaction rate of the 1,3-dipolar cycloaddition of terminal alkynes with azides; copper acetylides coordinated to azides and/or triazoles are involved.²

Click chemistry is a set of powerful, reliable, and selective reactions for the rapid synthesis of useful new compounds and combinatorial libraries through heteroatom links.⁷ Click chemistry must be modular, wide in scope, give very high yields, and generate only inoffensive byproducts that can be removed by nonchromatographic

* Thanks to my collaborator Dr. Brian Englert for his tremendous help in this project.

methods.⁷ Required process characteristics include simple reaction conditions (insensitivity to oxygen and water), readily available starting materials and reagents, the use of benign solvents (such as water), and simple product isolation.⁷ Click reactions have a high thermodynamic driving force, usually greater than 20 kcal mol⁻¹. Processes such as these proceed rapidly to completion and also tend to be selective for a single product.⁷

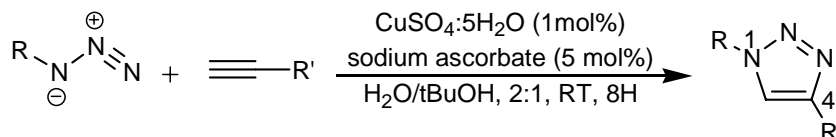
1,3-dipolar cycloadditions or Huisgen 1,3-dipolar cycloadditions¹ couple two unsaturated reactants to provide fast access to five-membered heterocycles. The cycloaddition of azides and alkynes to form triazoles is a very useful member of this family. Azides and alkynes are both highly energetic functional groups with narrow distributions of reactivity.¹⁻² Their weak acid-base properties make them nearly inert toward biological molecules, and they are even stable toward the conditions found inside living cells.⁸ Typically, under thermal conditions, this reaction yields a mixture of 1,4 and 1,5 triazoles (Scheme 3.1).



Scheme 3.1. Thermal 1,4 and 1,5 triazoles formation.

1,4-triazoles are useful in organic synthesis and drug design.⁹ One of the first reports of selectivity for the 1, 4-triazole was reported by Meldal using diisopropylamine and copper iodide on solid phase resins.^{9a} This approach led to the formation of only the 1,4 adduct. Sharpless has shown on various substrates that this reaction yields only the

1,4-triazole when using copper sulfate and sodium ascorbate (Scheme 3.2).⁸ Other reports have shown that the 1,3-dipolar cycloaddition even takes place within a reversibly formed, self-assembled capsule with absolute regioselectivity.^{9b}



Scheme 3.2. Copper catalyzed synthesis of 1,4-triazoles.

Azides have found wide use in industrial applications such as insecticides,¹⁰ fungicides,¹¹ optical brighteners,¹² corrosion inhibition of copper and copper alloys,¹³ photostabilizers for fibers, plastics and dyes,¹⁴ UV-screens for the protection of human skin,¹⁵ and photographic materials.¹⁶

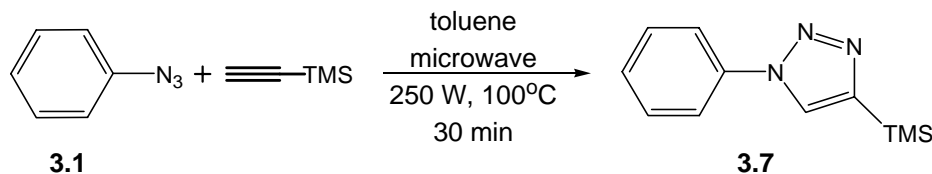
Not only their easy reactions with alkynes but also their broad potential uses in industry had encouraged us to explore azide chemistry by the click method. We began to explore the regioselectivity of this reaction and found that under microwave radiation the reactions of stannanes or silanes with azides were, in most cases, regioselective. We obtained excellent regioselectivity and were able to isolate 1,4-triazoles in high yields. We have synthesized a library of substituted triazoles (Table 3.1) and highlighted their use in further synthetic strategies.

Stannanes and silanes are useful in organic synthesis and can undergo a number of transformations.¹⁷ They can be easily transformed into iodides (Scheme 3.3).^{18,19} In our lab we frequently couple aromatic rings substituted with iodides to alkynes using the

Heck-Cassar-Sonogahira-Hagihara reaction.²⁰ We were intrigued with the idea of incorporating triazoles into larger structures and even in to polymers. Since trimethylsilyl and stannane functionalities could easily be exchanged for iodides, the only question that remained was, which triazoles could be prepared.

3.2 Results and Discussion.

Using various silane and stannane substituted acetylenes and azides, we were able to synthesize triazoles **3.7-3.48** (Scheme 3.1 and Table 3.1). In most cases the 1,4-triazole was easily isolated without a trace of the 1,5 adduct. Monomer **3.1** and TMS acetylene (TMSA) was reacted under thermal microwave (CEM discovery) conditions as seen in Scheme 3.3. Removal of toluene furnished **3.7** as very clean product and only 1,4 regioisomer in 30 min. TMSA can also be used as solvent and reagent at the same time.

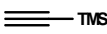
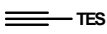
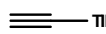
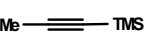

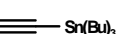
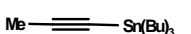
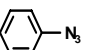
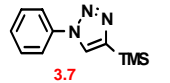
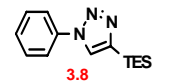
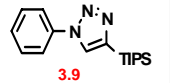
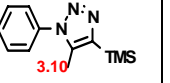
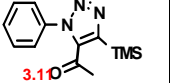
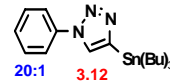
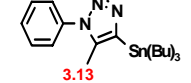

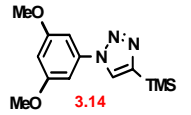
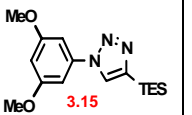
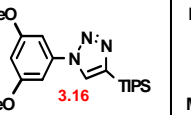
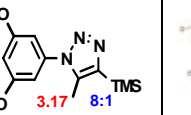
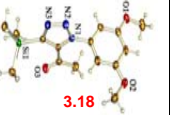
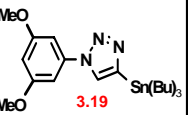
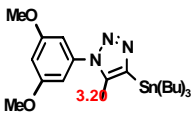
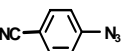
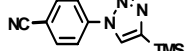
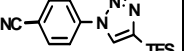
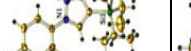

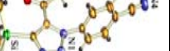
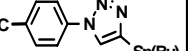
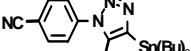
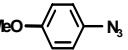
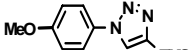
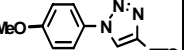
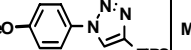
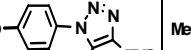
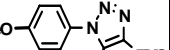
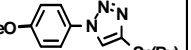
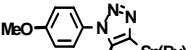
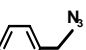
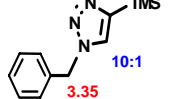
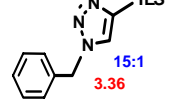
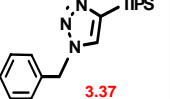
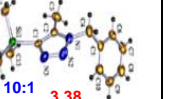
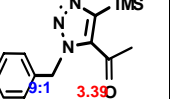
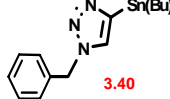
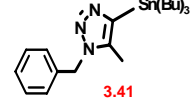
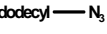
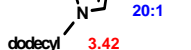
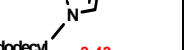

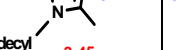
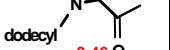
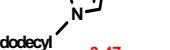
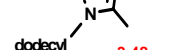


Scheme 3.3. Synthesis of **3.7** obtained under thermal conditions in a CEM discovery microwave system.

Single crystal analysis (Figure 3.1) assured our stereochemical assignments. The data show that only one type of regioisomer is present in crystal lattice. We also found that ¹H NMR data show regiospecificity on 1,4 triazole formation in most cases. The chemical shifts of H-5 proton on the triazole rings have chemical shifts between 7.20-8.15 ppm. This approach has many advantages that there is no catalyst need therefore

virtually no work up, only the removal of the solvent under vacuum is required, resulting in products which give accurate elemental analysis.

Table 3.1. Library of triazoles obtained under thermal conditions in a CEM discovery microwave system.

							
 3.1	 3.7	 3.8	 3.9	 3.10	 3.10	 20:1 3.12	 3.13
 3.2	 3.14	 3.15	 3.16	 3.17 8:1	 3.18	 3.19	 3.20
 3.3	 3.21	 3.22	 3.23	 3.24	 3.25	 3.26	 3.27
 3.4	 3.28	 15:1 3.29	 15:1 3.30	 9:1 3.31	 8:1 3.30	 14:1 3.33	 3.34
 3.5	 10:1 3.35	 15:1 3.36	 3.37	 10:1 3.38	 9:1 3.39	 3.40	 3.41
 3.6	 20:1 3.42	 3.43	 3.44	 15:1 3.45	 9:1 3.46	 3.47	 3.48

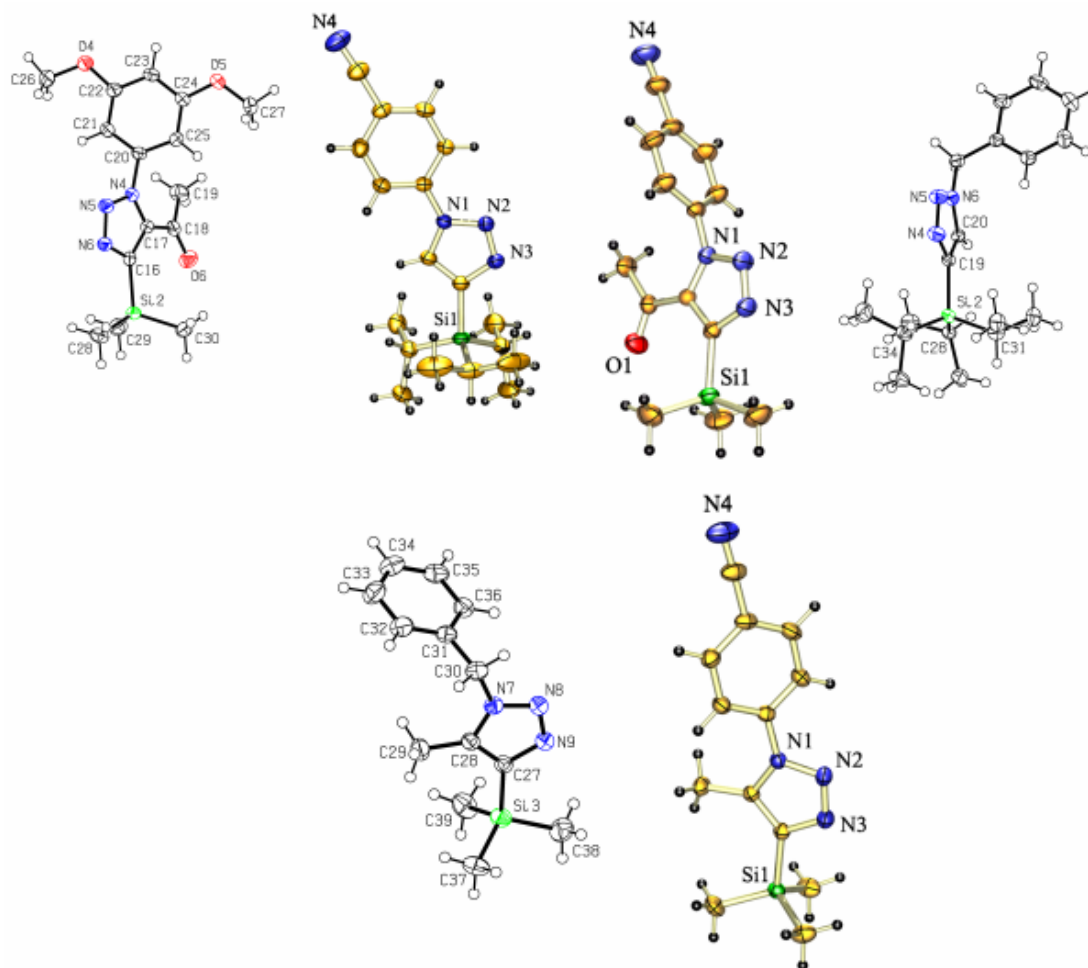
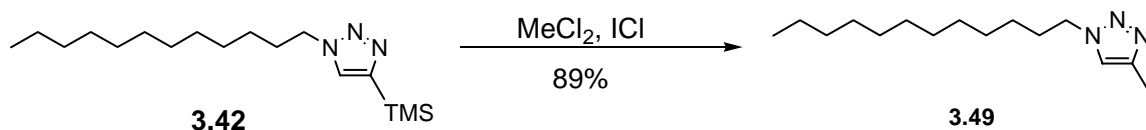


Figure 3.1. ORTEP plots of compounds **3.18**, **3.23**, **3.24**, **3.25**, **3.37**, and **3.38**.

In case of a mixture of 1,4 and 1,5-triazole product, we believe substitution of the azides play an important role. By having donor substitution on the aromatic ring, only 1,4-triazole formation was observed. When there is no substitution on the azide or an acceptor group is present, both 1,4 and 1,5 triazole formation occurred. We also believe steric hindrance plays a big role as well. When acetylene has bulkier group attached, the isomerization increases. When steric effect increases the regioselectivity increases in these systems.

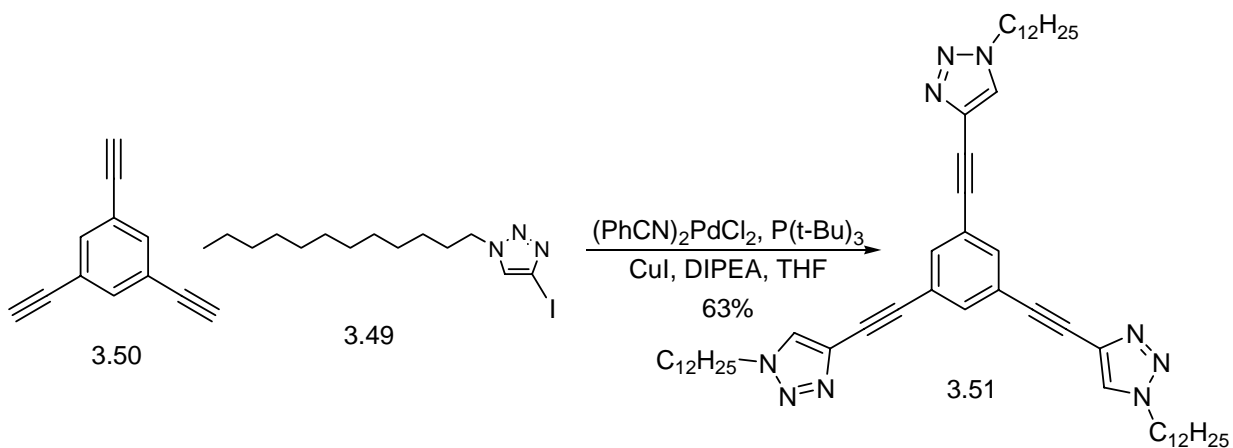
Iodine monochloride can be used to directly iodinate aromatic rings.²⁰ It can also be used to replace trimethylsilyl groups with iodines.¹⁹ Due to the ability of ICl to iodinate aromatic rings, we were unable to transform any triazoles containing aromatic rings into the corresponding iodines as planned.

Iodination of non aromatic triazoles by ICl worked well. In case of compound **3.42** was obtained in excellent yield. Though it is a 20:1 mixture of the 1,4 and 1,5 triazole, it can be purified. Due to the hardy nature of its precursor silane, treatment with iodine monochloride in dichloromethane gives **3.31** in a yield of 89 % (Scheme 3.4).



Scheme 3.4. Synthesis of iodine substituted 1,4-triazoles from the corresponding silanes.

Compound **3.49** could be coupled to 1,3,5-triethynyl benzene in the presence of Pd catalyst, CuI and triphenyl phosphine and THF to yield **3.51** in 63% yield as seen in Scheme 3.5. Compound **3.51** crystallizes easily out of ethanol and single crystal X-ray analysis reveals that the triazole rings are slightly twisted with respect to the central benzene ring (Figure 3.2). Two of the triazole rings are oriented with nitrogens on the same side of the molecule while the third triazole's nitrogens face the opposite side of the molecule.



Scheme 3.5. Use of iodine substituted triazole **3.51** to yield conjugated molecules.

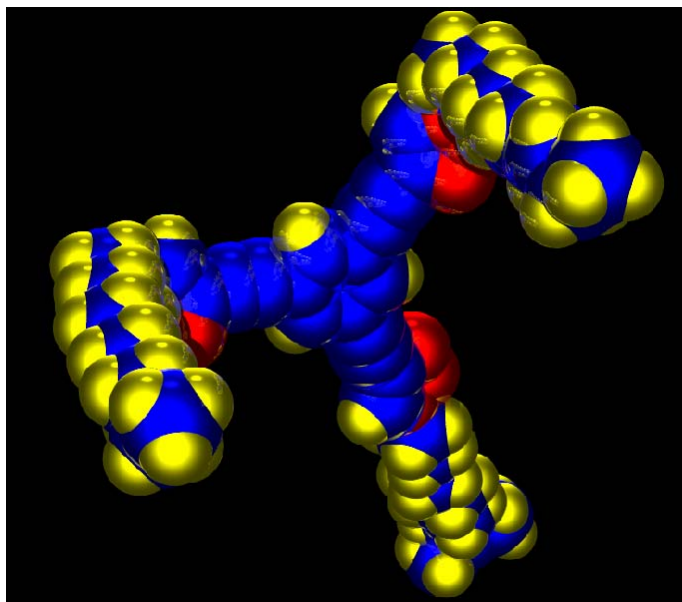
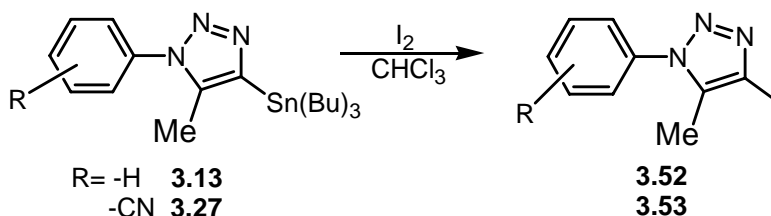


Figure 3.2. Single crystal X-ray analysis of **3.51** reveals that the triazole rings are slightly twisted with respect to the central benzene ring.

While compound **3.51** could be interesting for small molecule electronic devices, it would be more useful to have a larger selection of iodine substituted triazoles. Since iodine monochloride did not furnish the majority of iodines desired, we opted to synthesize the corresponding triazoles from the corresponding stannane compounds (Scheme 3.5).

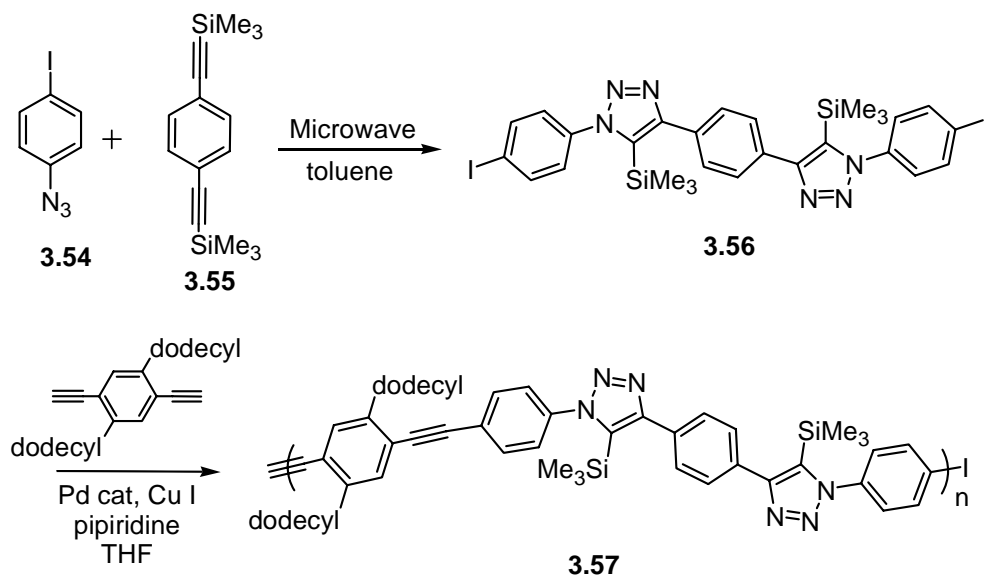


Scheme 3.6. Sythesis of iodinated triazole.

Using I_2 for iodination of aromatic triazoles offers the advantage of being able to obtain any of the desired iodo compounds without having to use iodine monochloride. Preliminary results indicate that molecular iodine can be used for the transformation, and the corresponding stannanes can be converted into the iodo compounds as seen in Scheme 3.6. Both **3.13** and **3.27** were reacted with iodine in chloroform at ambient temperature. Removal of tin salt was formed **3.52** and **3.53** in excellent yield. Compound **3.51** should be easily obtained via both synthetic routes in only slightly different overall yields.

The next logical step is to produce more conjugated molecules like poly-phenylene triazole employing the method as outlined. Synthesis starts from coupling *para*-iodophenyl azide **3.54** to bis alkynyl benzene **3.55** under microwave coupling conditions to furnish **3.56** in high yield as shown in Scheme 3.7. Monomer **3.56**

copolymerizes with 1,4-diethynyl-2,5-dimethylbenzene to give polymer **3.57**. This colorless polymer **3.57** is not very fluorescence in the solid state and blue fluorescence in chloroform.



Scheme 3.7. Synthesis of polyphenylenetriazoline.

Optical data of polymer **3.57** is shown in Figure 3.3. In case of methanol addition, emission maximum of polymer was blue shifted by 40 nm. Upon addition of aqueous HCl or TFA to a solution of **3.57** in chloroform, the emission maximum is bathochromically shifted by 20 nm. Protonation of the triazole ring increases the fluorescence efficiency and conjugation.

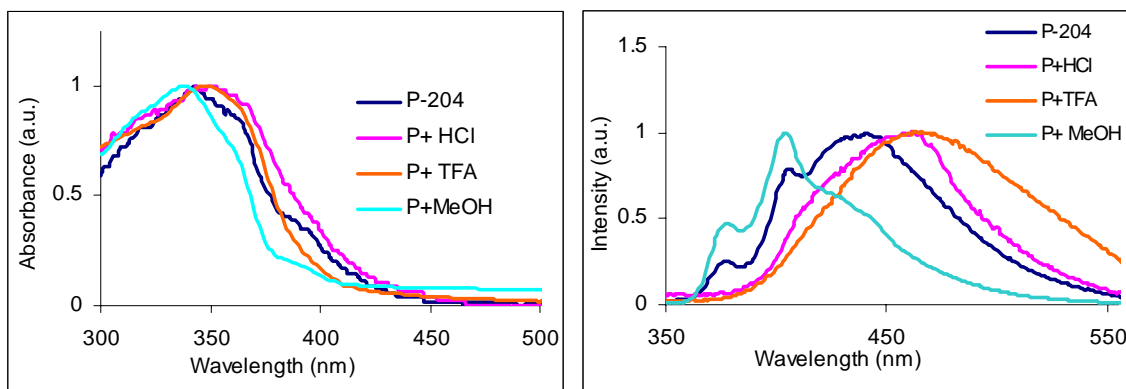


Figure 3.3. Optical data of polymer **3.57**

3.3 Conclusion.

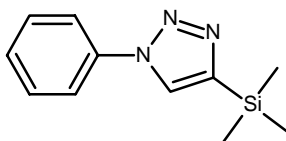
Initial work has been done detailing a promising approach to the synthesis of conjugated molecules. These methods allow incorporation of triazoles into small conjugated molecules and polymers. With further exploration, this could lead to the formation of materials useful for small molecule electronic devices or other applications. Two of the primary obstacles which must be overcome are the further conversion to the iodo substituted triazoles, as well as the ready made synthesis of a large library of these molecules and the further exploration of their properties. Due to the high yield and selectivity for one product, this chemistry would be an excellent choice for the functionalization of polymers.

3.4 Experimental

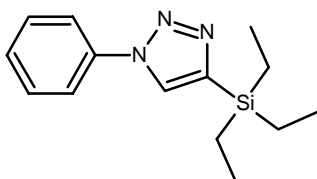
Instrumentation. The ^1H and ^{13}C NMR spectra were taken with a Varian 300 MHz or a Varian 400 MHz spectrometer using broadband probe. The ^1H chemical shifts are referenced to the residual proton peaks of CDCl_3 at δ 7.24(vs. TMS). The ^{13}C resonance is referenced to the central peak of CDCl_3 at δ 77.0 (vs. TMS). Azides **3.1-3.4** were prepared in accordance to published procedures.²¹

Compounds **3.5**, **3.6**, **3.35-3.48** were produced graciously by coworker Dr. Brian Englert. I would like to thank Dr. Brian Englert for his thought, work, and input on this project.

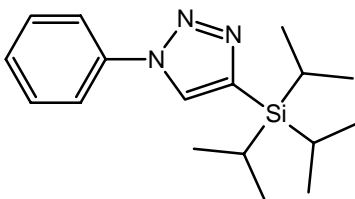
General procedure 1 for triazole formation: The corresponding azide (1 eq) and the corresponding acetylene (3 eq) were placed in a microwavable reaction vessel. Reactions which consisted of only reactants that were liquids at room temperature were performed with no solvent. Reactions in which one or more of the starting materials were solids were performed using toluene as a solvent. Starting materials were irradiated in a CEM discovery microwave system (250 watt, 155°C, 300 psi) for 25 minutes. The reaction vessel was allowed to cool to room temperature before being opened. Solvents were removed under vacuum, and solid products were crystallized and liquid products were distilled.



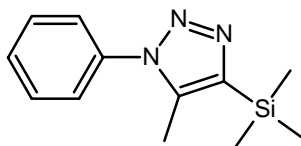
1-Phenyl-4-trimethylsilanyl-1*H*-1,2,3-triazole 3.7: Following the general procedure 1 outlined above azide **3.1** and corresponding acetylene were reacted to yield the 1, 4-triazole. The solvent was removed under reduced pressure to yield **3.7** as a colorless solid (82 %). ¹H NMR (CDCl₃): δ 7.93 (s, 1 H), 7.69 (m, 2 H), 7.48 (m, 2 H), 7.38 (m, 1 H), 0.34 (s, 9 H); ¹³C NMR (CDCl₃): δ 147.1, 136.9, 129.5, 128.3, 127.0, 120.6, -1.1; IR: ν 3740, 3137, 2953, 2894, 2247, 1957, 1878, 1747, 1600, 1505, 1464, 1207, 1156, 1044, 856, 744, 686, 632; MP: 99 °C.



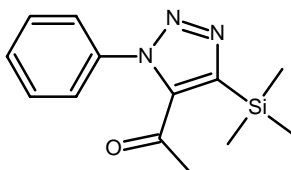
1-Phenyl-4-triethylsilanyl-1*H*-1,2,3-triazole 3.8: Following the general procedure 1 outlined above azide **3.1** and corresponding acetylene were reacted to yield the 1, 4-triazole. The solvent was removed under reduced pressure to yield **3.8** as a colorless solid (89 %). ¹H NMR (CDCl₃): δ 7.95 (s, 1 H), 7.66 (m, 2 H), 7.36 (m, 2 H), 7.26 (m, 1 H), 0.95 (t 9 H), 0.76 (q, 6 H); ¹³C NMR (CDCl₃): δ 144.0, 136.6, 129.2, 127.9, 127.3, 120.1, 7.1, 3.3; IR: ν 3124, 3060, 2950, 2871, 2401, 2237, 1950, 1676, 1599, 1509, 1503, 1463, 1413, 1238, 1147, 1039, 984, 908, 800, 718; MP: 108°C.



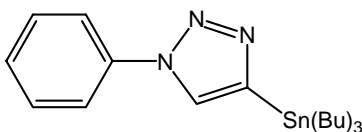
1-Phenyl-4-triisopropylsilanyl-1*H*-1,2,3-triazole 3.9: Following the general procedure 1 outlined above azide **3.1** and corresponding acetylene were reacted to yield the 1, 4-triazole. The solvent was removed under reduced pressure to yield **3.9** as a colorless solid (69 %). ¹H NMR (CDCl₃): δ 7.96 (s, 1 H), 7.75 (m, 2 H), 7.50 (m, 2 H), 7.40 (m, 1 H), 1.41 (m 3 H), 1.12 (d, 18 H); ¹³C NMR (CDCl₃): δ 142.7, 137.0, 129.5, 128.2, 127.8, 120.5, 18.7, 11.2; IR: ν 3122, 3059, 2962, 2864, 2253, 1955, 1885, 1676, 1597, 1506, 1463, 1456, 1339, 1202, 1148, 1073, 1047, 1017, 916, 883, 761, 757, 710, 693, 577; Anal. Calcd for C₁₇H₂₇N₃: C, 67.7; H, 9.03; N, 13.94. Found: C, 70.80; H, 9.65; N, 14.44%; MP: 53 °C.



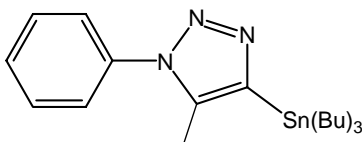
1-Phenyl-4-trimethylsilanyl-5-methyl-1*H*-1,2,3-triazole 3.10: Following the general procedure 1 outlined above azide **3.1** and corresponding acetylene were reacted to yield the 1, 4-triazole. The solvent was removed under reduced pressure to yield **3.10** as a colorless solid (71 %). ¹H NMR (CDCl₃): δ 7.56-7.48 (m, 3 H), 7.43 (m, 2 H), 2.33 (s, 3 H), 0.38 (s, 9 H), 1.41 (d, 18 H); ¹³C NMR (CDCl₃): δ 143.6, 138.8, 136.6, 129.6, 129.4, 125.5, 10.5, -0.54; IR: ν 3035 2955, 2482, 1596, 1590, 1502, 1406, 1392, 1300, 1291, 1270, 1248, 1099, 1071, 918, 838, 770, 681, 634; MP: 69 °C.



1-Phenyl-4-trimethylsilanyl-5-ethanonyl-1*H*-1,2,3-triazole 3.11: Following the general procedure 1 outlined above azide **3.1** and corresponding acetylene were reacted to yield the 1, 4-triazole. The solvent was removed under reduced pressure to yield **3.11** as a colorless solid (75 %). ¹H NMR (CDCl₃): δ 7.55 (m, 3 H), 7.46 (m, 2 H), 2.08 (s 3 H), 0.35 (s, 9 H); ¹³C NMR (CDCl₃): δ 191.0, 150.0, 143.0, 136.9, 130.5, 129.9, 125.6, 30.8, -1.0; IR: ν 3066, 2975, 2904, 1682, 1593, 1495, 1415, 1359, 1247, 1184, 1149, 1054, 1004, 963, 840, 768, 692; MP: 50 °C

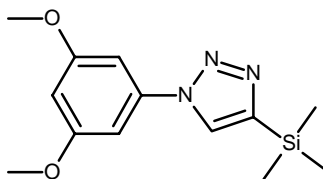


1-Phenyl-4-tributylstannanyl-1*H*-1,2,3-triazole 3.12: Following the general procedure 1 outlined above azide **3.1** and corresponding acetylene were reacted. The solvent was removed under reduced pressure and the remaining liquid was distilled under reduced pressure to yield product **3.12** as clear oil (67 %). ¹H NMR (CDCl₃): δ 7.98, 7.68, 7.42, 1.58, 1.36, 1.18, 0.92; ¹³C NMR (CDCl₃): δ 144.6, 140.5, 129.2, 128.9, 120.9, 120.2, 28.5, 27.6, 13.9, 10.6; IR: ν 2918, 2851, 1601, 1506, 1456, 1375, 1192, 1072, 1034, 872, 756.

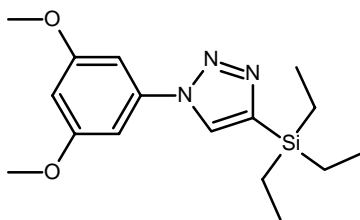


1-Phenyl-4- tributylstannanyl-5-methyl-1*H*-1,2,3-triazole 3.13: Following the general procedure 1 outlined above azide **3.1** and corresponding acetylene were reacted. The solvent was removed under reduced pressure and the remaining liquid was distilled under

reduced pressure to yield product **3.13** as yellow oil (89 %). ^1H NMR (CDCl_3): δ 7.45, 2.29, 1.56, 1.35, 1.17, 0.89; ^{13}C NMR (CDCl_3): δ 162.7, 144.1, 139.4, 137.0, 129.5, 129.1, 125.2, 29.4, 28.3, 27.6, 14.0, 10.1.

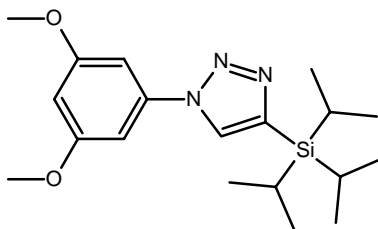


1-(3,5-dimethoxyphenyl)-4-trimethylsilanyl-1H-1,2,3-triazole 3.14: Following the general procedure 1 outlined above azide **3.2** and corresponding acetylene were reacted to yield the 1, 4-triazole. The solvent was removed under reduced pressure to yield **3.14** as a colorless solid (78 %). ^1H NMR (CDCl_3): δ 7.93 (s, 1 H), 6.78 (m, 2 H), 6.33 (m, 1 H), 3.67 (s, 6 H), 0.25 (s, 9 H); ^{13}C NMR (CDCl_3): δ 161.0, 146.7, 138.1, 127.0, 99.9, 98.8, 55.4, -1.3; IR: ν 3127, 2897, 2838, 1599, 1488, 1338, 1248, 1206, 1067, 988, 929, 839, 757, 680, 633; MP: 84°C.

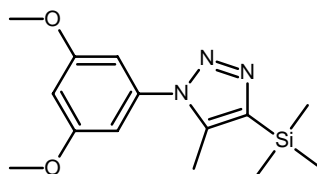


1-(3,5-dimethoxyphenyl)-4-triethylsilanyl-1H-1,2,3-triazole 3.15: Following the general procedure 1 outlined above azide **5.2** and corresponding acetylene were reacted to yield the 1, 4-triazole. The solvent was removed under reduced pressure to yield **3.15** as a colorless solid (86 %). ^1H NMR (CDCl_3): δ 7.91 (s, 1 H), 6.88 (m, 2 H), 6.43 (m, 1 H), 3.79 (s, 6 H), 0.99 (t 9 H), 0.84 (q, 6 H); ^{13}C NMR (CDCl_3): δ 161.1, 144.2, 138.3,

127.5, 99.9, 98.8, 55.5, 7.3, 3.5; IR: ν 3122, 2874, 1599, 1456, 1301, 1197, 1158, 1133, 1061, 1013, 928, 828; MP: 102 °C.



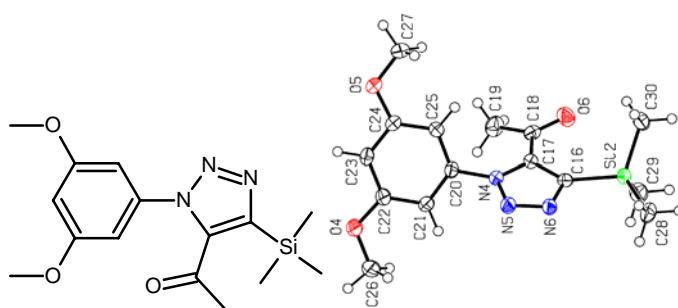
1-(3,5-dimethoxyphenyl)-4-triisopropylsilanyl-1H-1,2,3-triazole 3.16: Following the general procedure 1 outlined above azide **3.2** and corresponding acetylene were reacted to yield the 1, 4-triazole. The solvent was removed under reduced pressure to yield **3.16** as a colorless solid (89 %). ^1H NMR (CDCl_3): δ 7.93 (s, 1 H), 6.93 (m, 2 H), 6.43 (m, 1 H), 3.85 (s, 6 H), 1.41 (m 3 H), 1.13 (d, 18 H); ^{13}C NMR (CDCl_3): δ 161.3, 142.6, 138.4, 128.0, 100.0, 99.0, 55.7, 18.6, 11.2; IR: ν 3122, 2941, 2863, 1602, 1490, 1460, 1318, 1272, 1209, 1202, 1162, 1135, 1016, 883, 8318, 681, 653, 580, 519; Anal. Calcd for $\text{C}_{19}\text{H}_{31}\text{N}_3$: C, 63.12; H, 8.64; N, 11.62. Found: C, 63.13; H, 8.67; N, 11.71 %; MP: 83 °C.



1-(3,5-dimethoxyphenyl)-4-trimethylsilanyl-5-methyl-1H-1,2,3-triazole 3.17:

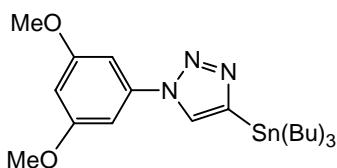
Following the general procedure 1 outlined above azide **3.2** and corresponding acetylene were reacted to yield the 1, 4-triazole. The solvent was removed under reduced pressure to yield **3.17** as a colorless solid (78 %). ^1H NMR (CDCl_3): δ 6.56 (s, 3 H), 3.81 (s, 6 H),

2.34 (s 3 H), 0.38 (s, 9 H); ^{13}C NMR (CDCl_3): δ 160.9, 143.3, 138.5, 137.7, 103.7, 101.1, 55.7, 10.2, -0.8; IR: ν 3115, 2960, 2838, 2108, 1614, 1590, 1432, 1348, 1251, 1205, 1158, 1105, 1028, 928, 839, 758, 678; MP: 97 $^\circ\text{C}$.



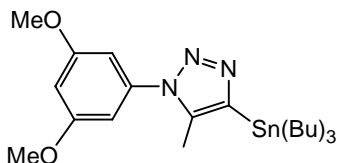
1-(3,5-dimethoxyphenyl)-4-trimethylsilanyl-5-ethanonyl-1*H*-1,2,3-triazole 3.18:

Following the general procedure 1 outlined above azide **3.2** and corresponding acetylene were reacted to yield the 1, 4-triazole. The solvent was removed under reduced pressure to yield **3.18** as a colorless solid (89 %). ^1H NMR (CDCl_3): δ 6.59 (m, 3 H), 3.82 (s, 6 H), 2.16 (s 3 H), 0.37 (s, 9 H); ^{13}C NMR (CDCl_3): δ 191.0, 161.2, 150.0, 142.7, 137.9, 137.7, 103.8, 102.1, 55.8, 30.4, -1.3; IR: ν 3081, 2959, 2841, 1677, 1616, 1612, 1593, 1476, 1358, 1245, 1158, 1142, 1058, 1019, 970, 926, 847, 838, 768, 696, 635, 539; Anal. Calcd for $\text{C}_{15}\text{H}_{21}\text{N}_3$: C, 56.40; H, 6.63; N, 13.15. Found: C, 56.58; H, 6.69; N, 13.16 %; MP: 121 $^\circ\text{C}$.



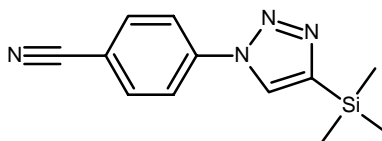
1-(3,5-dimethoxyphenyl)-4-tributylstannanyl-1*H*-1,2,3-triazole 3.19: Following the general procedure 1 outlined above azide **3.2** and corresponding acetylene were reacted. The solvent was removed under reduced pressure and the remaining liquid was distilled

under reduced pressure to yield product **3.19** as clear oil (86 %). ^1H NMR (CDCl_3): δ 7.92, 6.91, 6.44, 3.82, 1.57, 1.36, 1.18, 0.91; ^{13}C NMR (CDCl_3): δ 161.2, 145.7, 138.2, 127.8, 100.1, 98.9, 55.5, 29.3, 27.7, 14.0, 10.1; IR: ν 2953 2851, 2106, 1614 1601, 1489 1456, 1252, 1205, 1157 1063, 1018, 829.



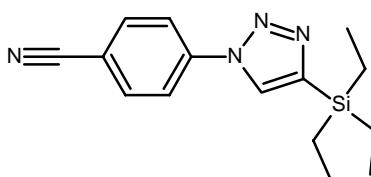
1-(3,5-dimethoxyphenyl)-4-tributylstannanyl-5-methyl-1H-1,2,3-triazole 3.20:

Following the general procedure 1 outlined above azide **3.2** and corresponding acetylene were reacted. The solvent was removed under reduced pressure and the remaining liquid was distilled under reduced pressure to yield product **3.20** as clear oil (94 %). ^1H NMR (CDCl_3): δ 6.60, 6.55, 3.83, 2.33, 1.91, 1.55, 1.34, 1.15 0.94; ^{13}C NMR (CDCl_3): δ 162.3, 143.6, 138.7, 127.8, 100.1, 98.8, 55.6, 29.3, 28.3, 27.5, 14.1, 10.3; IR: ν 2953 2851 2108, 1608 1597, 1456, 1340, 1229, 1205, 1157 1065, 968, 839.

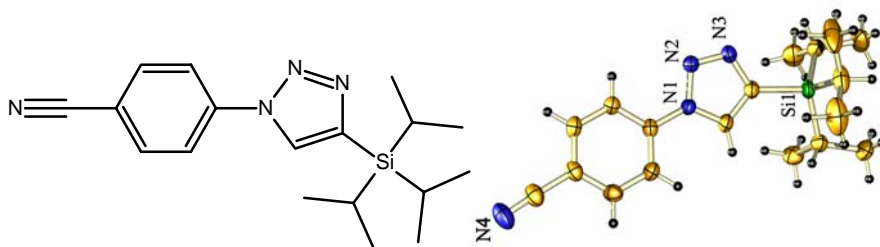


1-(4-benzonitrile)-4-trimethylsilanyl-1H-1,2,3-triazole 3.21: Following the general procedure 1 outlined above azide **3.3** and corresponding acetylene were reacted to yield the 1, 4-triazole. The solvent was removed under reduced pressure to yield **3.21** as a colorless solid (90 %). ^1H NMR (CDCl_3): δ 8.00 (s, 1 H), 7.91 (d, 2 H), 7.79 (d, 2 H), 0.35 (s, 9 H); ^{13}C NMR (CDCl_3): δ 148.2, 139.7, 133.7, 126.6, 120.6, 117.7, 111.9, -1.1;

IR: ν 3747, 3126, 3100, 2955, 2899, 2805, 2399, 2226, 1944, 1878, 1605, 1511, 1482, 1426, 1393, 1291, 1247, 1204, 1198, 1147, 1110, 1040, 984, 843, 822, 761, 705, 634, 557; MP: 130 °C.

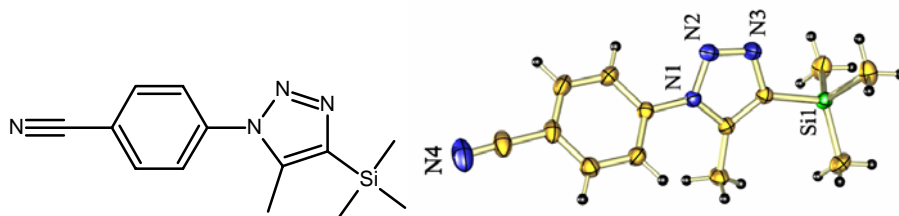


1-(4-benzonitrile)-4-triethylsilyl-1H-1,2,3-triazole 3.22: Following the general procedure 1 outlined above azide **3.3** and corresponding acetylene were reacted to yield the 1, 4-triazole. The solvent was removed under reduced pressure to yield **3.22** as a colorless solid (93 %). ^1H NMR (CDCl_3): δ 8.00 (s, 1 H), 7.94 (d, 2 H), 7.83 (d, 2 H), 1.03, (t 9 H), 0.89 (q, 6 H); ^{13}C NMR (CDCl_3): δ 145.9, 140.0, 134.0, 127.3, 120.9, 118.0, 112.2, 7.7, 3.8; IR: ν 3420, 3138, 3103, 3060, 2954, 2950, 2932, 2874, 2417, 2226, 1924, 1604, 1504, 1480, 1425, 1321, 1268, 1233, 1202, 1142, 1109, 1036, 1005, 984, 842, 829, 599, 556, 476; Anal. Calcd for $\text{C}_{15}\text{H}_{20}\text{N}_4$: C, 63.3; H, 7.1; N, 19.7. Found: C, 60.9; H, 4.1; N, 13.0 %; MP: 78 °C.

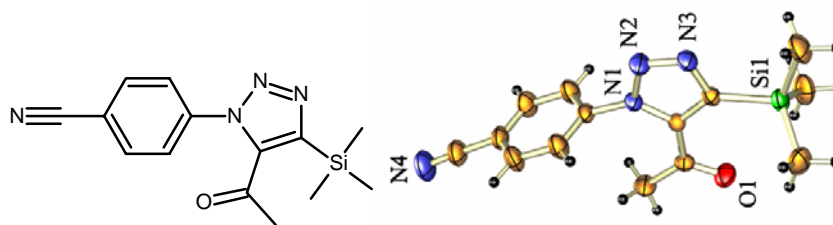


1-(4-benzonitrile)-4-triisopropylsilyl-1H-1,2,3-triazole 3.23: Following the general procedure 1 outlined above azide **3.3** and corresponding acetylene were reacted to yield the 1, 4-triazole. The solvent was removed under reduced pressure to yield **3.23**

as a colorless solid (91 %). ^1H NMR (CDCl_3): δ 8.08 (s, 1 H), 7.94 (d, 2 H), 7.76 (d, 2 H), 1.32, (m 3 H), 1.05 (d, 18 H); ^{13}C NMR (CDCl_3): δ 143.6, 139.6, 133.5, 127.5, 120.4, 117.6, 111.5, 18.4, 11.0; IR: ν 3830, 3082, 2946, 2865, 2840, 2227, 1928, 1800, 1606, 1516, 1508, 1480, 1460, 1427, 1395, 1204, 1145, 1037, 1017, 882, 845, 804, 683, 556, 519, 431; MP: 71 $^\circ\text{C}$.

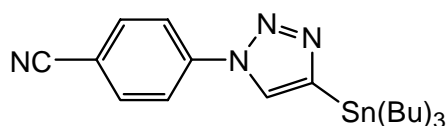


1-(4-benzonitrile)-4-trimethylsilanyl-5-methyl-1H-1,2,3-triazole 3.24: Following the general procedure 1 outlined above azide **3.3** and corresponding acetylene were reacted to yield the 1, 4-triazole. The solvent was removed under reduced pressure to yield **3.24** as a colorless solid (90 %). ^1H NMR (CDCl_3): δ 7.84 (d, 2 H), 7.63 (d, 2 H), 2.40 (s, 3 H), 0.39 (s, 9 H); ^{13}C NMR (CDCl_3): δ 144.5, 139.7, 138.3, 133.3, 125.4, 117.6, 112.8, 10.4, -0.9; IR: ν 3100, 2960, 2953, 2489, 2231, 1945, 1883, 1816, 1705, 1605, 1510, 1404, 1254, 1245, 1160, 1119, 1089, 1007, 972, 836, 765, 712, 637, 567; MP: 162 $^\circ\text{C}$.

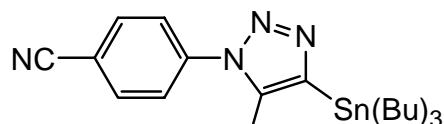


1-(4-benzonitrile)-4-trimethylsilanyl-5-ethanonyl-1H-1,2,3-triazole 3.25: Following the general procedure 1 outlined above azide **3.3** and corresponding acetylene were

reacted to yield the 1, 4-triazole. The solvent was removed under reduced pressure to yield **3.25** as a colorless solid (94 %). ^1H NMR (CDCl_3): δ 7.86 (d, 2 H), 7.59 (d, 2 H), 2.27 (s, 3 H), 0.44 (s, 9 H); ^{13}C NMR (CDCl_3): δ 190.7, 150.3, 142.4, 140.2, 133.8, 126.1, 117.6, 114.3, 31.4, -0.8; IR: ν 3053, 2958, 2233, 1943, 1817, 1677, 1608, 1513, 1478, 1435, 1425, 1412, 1361, 1303, 1251, 1243, 1156, 1100, 1057, 959, 848, 840, 756, 650, 570, 533; Anal. Calcd for $\text{C}_{14}\text{H}_{16}\text{N}_4$: C, 59.13; H, 5.67; N, 19.70. Found: C, 61.78; H, 7.40; N, 19.61 %; MP: 147 °C.

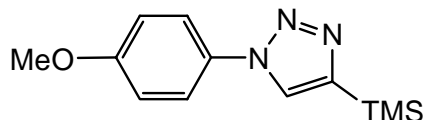


1-(4-benzonitrile)-4-tributylstannanyl-1H-1,2,3-triazole 3.26: Following the general procedure 1 outlined above azide **3.3** and corresponding acetylene were reacted to yield the 1, 4-triazole. The solvent was removed under reduced pressure and the product **3.26** was collected as yellow solid (72 %). ^1H NMR (CDCl_3): δ 8.04, 7.89, 7.70, 1.48, 1.24, 1.07, 0.80; ^{13}C NMR (CDCl_3): δ 146.5, 140.1, 133.9, 128.0, 120.7, 118.0, 111.7, 29.1, 27.5, 13.9, 10.4; IR: ν 3115, 2953, 2905, 2868, 2376, 2230, 1608, 1518, 1446, 1375, 1325, 1198, 1176, 1074, 1038, 966, 847; MP: 71 °C.

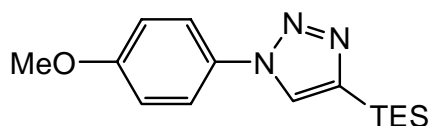


1-(4-benzonitrile)-4-tributylstannanyl-5-methyl-1H-1,2,3-triazole 3.27: Following the general procedure 1 outlined above azide **3.3** and corresponding acetylene were reacted. The solvent was removed under reduced pressure and the remaining liquid was distilled

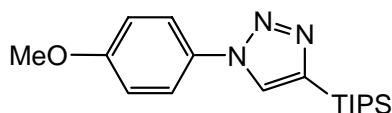
under reduced pressure to yield product **3.27** as clear oil (93 %). ^1H NMR (CDCl_3): δ 7.85, 7.67, 2.40, 1.55, 1.30, 1.16, 0.95; ^{13}C NMR (CDCl_3): δ 145.8, 140.7, 139.8, 133.1, 125.3, 118.0, 112.4, 29.4, 27.6, 14.0, 10.2; IR: ν 2915, 2868, 2230, 1923, 1680 1607 1506, 1456, 1400, 1375, 1246, 1153, 1072, 970, 843.



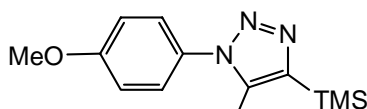
1-(4-methoxyphenyl)-4-trimethylsilanyl-1H-1,2,3-triazole 3.28: Following the general procedure 1 outlined above azide **3.4** and corresponding acetylene were reacted to yield the 1, 4-triazole. The solvent was removed under reduced pressure and the product **3.28** was collected as brown-yellow solid (91 %). ^1H NMR (CDCl_3): δ 7.85, 7.63, 7.00, 3.86, 0.37; ^{13}C NMR (CDCl_3): δ 159.7, 147.1, 130.7, 127.6, 122.5, 114.8, 55.8, 0.7; IR: ν 2957, 2052, 1884, 1610, 1522, 1456, 1304, 1246, 1205, 1103, 1030, 839; MP: 66 °C.



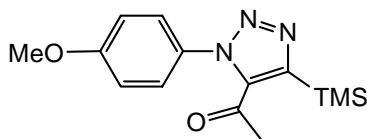
1-(4-methoxyphenyl)-4-triethylsilanyl-1H-1,2,3-triazole 3.29: Following the general procedure 1 outlined above azide **3.4** and corresponding acetylene were reacted. The solvent was removed under reduced pressure and the remaining liquid was distilled under reduced pressure to yield product **3.29** as yellow o oil (79 %). ^1H NMR (CDCl_3): δ 7.86, 7.64, 7.05, 3.87, 1.03, 0.89; ^{13}C NMR (CDCl_3): δ 159.6, 144.3, 130.7, 128.0, 122.4, 114.8, 55.8, 7.7, 3.9; IR: ν 2951 2874, 1518, 1456, 1302, 1252, 200, 1038, 1011, 831.



1-(4-methoxyphenyl)-4-triisopropylsilyl-1H-1,2,3-triazole 3.30: Following the general procedure 1 outlined above azide **3.4** and corresponding acetylene were reacted. The solvent was removed under reduced pressure and the remaining liquid was distilled under reduced pressure to yield product **3.30** as yellow oil (88%). ^1H NMR (CDCl_3): δ 7.89, 7.66, 7.00, 3.82, 1.13, 1.11; ^{13}C NMR (CDCl_3): δ 157.5, 144.5, 131.2, 128.7, 122.4, 55.3, 1.32, 1.05; IR: ν 2941, 2862, 1518, 1452, 1250, 1202, 1171, 1040, 883, 831.

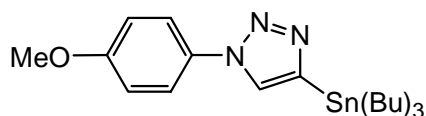


1-(4-methoxyphenyl)-4-trimethylsilyl-5-methyl-1H-1,2,3-triazole 3.31: Following the general procedure 1 outlined above azide **3.4** and corresponding acetylene were reacted to yield the 1, 4-triazole. The solvent was removed under reduced pressure and the product **3.31** was collected as brown solid (83 %). ^1H NMR (CDCl_3): δ 7.63, 6.99, 3.86, 2.29, 0.38; ^{13}C NMR (CDCl_3): δ 159.6, 147.2, 130.5, 127.7, 122.5, 114.7, 55.8, 29.6, 0.78; IR: ν 2955, 2833, 2102, 1890, 1599, 1508, 1441, 1300, 1244, 1167, 1036, 835; MP: 78 $^\circ\text{C}$.

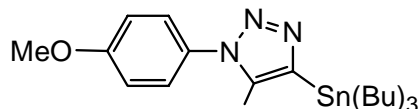


1-(4-methoxyphenyl)-4-trimethylsilyl-5-ethanonyl-1H-1,2,3-triazole 3.32: Following the general procedure 1 outlined above azide **3.4** and corresponding acetylene

were reacted. The solvent was removed under reduced pressure and the remaining liquid was distilled under reduced pressure to yield product **3.32** as yellow solid (73 %). ^1H NMR (CDCl_3): δ 7.64, 7.00, 3.86, 2.21, 0.41; ^{13}C NMR (CDCl_3): δ 191.2, 159.7, 147.2, 130.7, 127.8, 122.4, 114.8, 55.8, 30.9, 0.7; IR: ν 2955, 2833, 2102, 1890, 1599, 1508, 1441, 1300, 1244, 1167, 1036, 835; MP: 78 $^\circ\text{C}$.



1-(4-methoxyphenyl)-4-tributylstannanyl-1H-1,2,3-triazole 3.33: Following the general procedure 1 outlined above azide **3.4** and corresponding acetylene were reacted. The solvent was removed under reduced pressure and the remaining liquid was distilled under reduced pressure to yield product **3.33** as yellow oil (95 %). ^1H NMR (CDCl_3): δ 7.80, 6.87, 3.71, 1.55, 1.33, 1.16, 0.84; ^{13}C NMR (CDCl_3): δ 145.0, 130.8, 128.2, 122.2, 114.7, 55.7, 29.9, 29.5, 27.3, 14.1, 10.1; IR: ν 2955, 2926, 2849, 1518, 1456, 1302, 1250, 1184, 1038, 831.



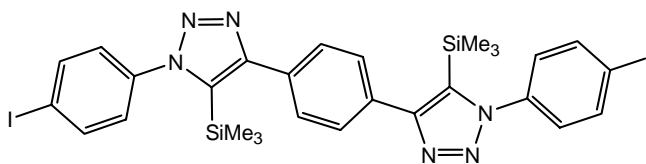
1-(4-methoxyphenyl)-4-tributylstannanyl-5-methyl-1H-1,2,3-triazole 3.34: Following the general procedure 1 outlined above azide **3.4** and corresponding acetylene were reacted. The solvent was removed under reduced pressure and the remaining liquid was distilled under reduced pressure to yield product **3.34** as yellow oil (67 %). ^1H NMR (CDCl_3): δ 7.88, 7.24, 6.89, 3.72, 2.21, 1.60, 1.35, 1.15, 0.92; ^{13}C NMR (CDCl_3): δ 159.6,

145.0, 130.7, 128.1, 122.1, 114.7, 55.8, 29.6, 27.3, 14.2, 10.1; IR: ν 2922, 2851, 1500, 1464, 1364, 1300, 1252, 1171, 1076, 1032, 970, 833.

Synthesis of iodides from silanes and stannanes. The corresponding silane or stannane and ICl (in the case of the silane) ground iodine (in the case of the stannane) (2-5 eq) were placed in a round bottom flask and stirred for 48 h. The reaction mixture was poured onto aqueous sodium sulfate and stirred until yellow. The organic layer was washed with water and dried over magnesium sulfate. The solvent was removed under vacuum and the crude product purified by recrystallization followed by chromatography over silica gel.

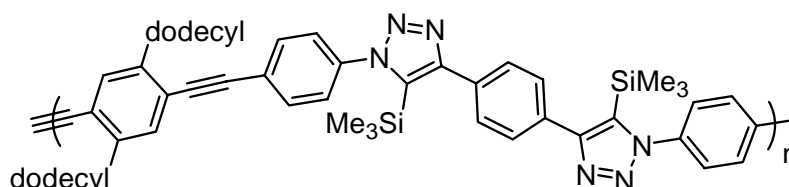
3.52. ^1H NMR (CDCl_3): δ 7.55, 7.43, 2.34; ^{13}C NMR (CDCl_3): δ 136.7, 136.4, 130.1, 129.8, 125.0, 90.8, 28.2.

3.53. ^1H NMR (CDCl_3): δ 7.88, 7.65, 2.42; ^{13}C NMR (CDCl_3): δ 139.6, 133.8, 125.2, 117.7, 114.0, 92.0, 11.1.



Compound 3.56 Mixture of 1-Azido-4-iodo-benzene 250 mg (0.51mmole) and 1,4-diethynyl-benzene 138 mg (1.02 mmole) in 3mL toluene were charge into microwavable reaction vessel. Mixture was irradiated in a CEM discovery microwave system (250 watt, 155°C, 300 psi) for 25 minutes. The reaction vessel was allowed to cool to room temperature before being opened. Solvents were removed under vacuum, and off-white products 216 g (82%) was collected. ^1H NMR (CDCl_3): δ 7.66, 7.21, 6.99, 0.21; ^{13}C

NMR (CDCl₃) δ: 145.9, 142.0, 138.4, 136.0, 130.3, 126.5, 94.6, 0.4; IR: ν 3080, 3036, 2953, 2893, 1911, 1792, 1657, 1491, 1418, 1389, 1248, 1178, 1142, 1057, 991, 845, 827, 762, 717, 638, 607, 488; Mp. 262-264 °C.



Polymer 3.57: To an oven dried 50 mL Schlenk flask, **5** (162 mg, 0.314 mmol) and didodecyl-*p*-diacetylbenzene (145 mg, 0.314 mmol) were dissolved in THF (2.0 mL). 5 mol % Pd(PPh₃)₂Cl₂, 5 mol % CuI, and piperidine (5.0 mL) were added to the mixture. The reaction mixture was stirred and kept at 30°C for 24 h. The solution was poured into a mixture of chloroform (100.0 mL) and water (100.0 mL). The organic layer was washed three times with water (100 mL). The aqueous layer was washed twice with chloroform (50 mL), and the organic layers were combined. To the resultant organic layer, methanol (600 mL) was added to precipitate the polymer. Suction filtration was produced an off-white polymer (0.170 g, 84 %). ¹H NMR (CDCl₃): δ 7.45, 7.27, 2.75, 1.64, 1.22, 0.84, 0.23; ¹³C NMR (CDCl₃): δ = 145.9, 142.5, 142.1, 138.5, 135.8, 132.3, 130.6, 128.2, 126.5, 124.7, 122.5, 92.9, 90.4, 34.4, 32.2, 31.0, 30.0, 29.7, 23.0, 14.5, -0.4; IR: ν 3434, 2924, 2852, 1628, 1512, 1458, 1072, 849, 800; Φ_F=0.13.

3.5 References.

1. Huisgen R.; Szeimies G.; Moebius L.; *Chem. Ber.* **1967**, *100*, 2494.
2. Rostovtsev V.V.; Green L.G.; Fokin V.V.; Sharpless K.B.; *Angew. Chem.* **2002**, *41*, 2596, b) Loren J.C.; Sharpless K.B.; *Synthesis* **2005**, 1514-1520. c) Rodionov V.O.; Fokin V.V.; Finn M.G.; *Angew. Chem.* **2005**, *44*, 2210-2215.
3. Wooley K.L.; Hawker C.J.; *Top. Curr. Chem.* **2005**, *245*, 287-305. b) Helms B.; Mynar J.L.; Hawker C.J.; Frechet J.M.J.; *J. Am. Chem. Soc.* **2004**, *126*, 15020-15021.
4. Englert B.C.; Bakbak S.; Bunz U.H.F.; *Macromolecules* **2005**, *38* (14), 5868-5877.
5. a) Sivakumar K.; Xie F.; Cash B.; Long S.; Barnhill H.N.; Wang Q.; *Org. Lett.* **2004**, *6*, 4603 - 4606. b) Binder W.H.; Kluger C.; *Macromolecules* **2004**, *37*, 9321-9330. c) Tsarevsky N.V.; Sumerlin B.S.; Matyjaszewski K.; *Macromolecules* **2005**, *38*, 3558-3561.
6. Agard N.J.; Prescher J.A.; Bertozzi C.R.; *J. Am. Chem. Soc.* **2004**, *126*, 15046-15047.
7. Kolb, H. C.; Finn, M. G.; and Sharpless, B. K. *Angew. Chem. Int. Ed.* **2001**, *40*, 2004-2021.
8. Wang, Q.; Chan, T. R.; Hilgraf, R.; Fokin, V. V.; & Sharpless, B. K.; Finn, M. G. *J. Am. Chem. Soc.* **2003**, *125*, 3192-3193.
9. a) Tornoe, C. W.; Christensen, C.; & Meldal, M. *J. Org. Chem.* **2002**, *67*, 3057-3064. b) Chen, J.; & Rebek, J. *Org. Lett.* **2002**, *4*, 327-329.
10. Boddy, I.K.; Briggs, G.G.; Harrison, R.P.; Jones, T.H.; O'Mahony, M.J.; Marlow, I.D.; Roberts, B. G.; Willis, R.J. Bardsley, R.J. *Reid. Pestic. Sci.*, **1996**, *48*, 189.
11. Buechel, K. H.; Gold, H.; Frohnberger, P. E.; Kasperd, H., *Ger. Pat.* **1975**, 2407305.
12. Guenther, D.; Nestler H. J.; Roesch, G.; Schinzel, E.; *Cherm. Abstr.* **1980**, *93*, 73786.
13. Abdennabi, A. M. S.; Abdulhadi, A. I.; Abu-Orabi, S. T.; Saricimen, H. *Corrosion Sci.* **1996**, *38*, 1791.
14. Rody, J.; Slongo, M.; *Chem. Abstr.*, **1981**, *95*, 197267.

15. Strobel, A. F.; Whitthouse, M. L.; *Chem. Abstr.*, **1971**, 76, 99674.
16. Fan, W. Q.; Kitritzky, A. R., *InComprehensive Heterocyclic Chemistry II*; Kitritzky, A. R.; Rees C. W.; Scriven, E. F. V.; *Elsevier Science*: Oxford, **1996**, 4, 1-126.
17. Rostovtsev, V. V.; Green, L. G.; Fokin, V. V.; & Sharpless, B. K *Angew. Chem. Int. Ed.* **2002**, 41, 2596-2599.
18. Shen, Xianfeng; Ho, Douglas M.; Pascal, Robert A., Jr. *J. Am. Chem. Soc.* **2004**, 126 (18), 5798-5805.
19. Choi, Joon Hun; Choe, Yearn Seong; Lee, Kyung-Han; Choi, Yong; Kim, Sang Eun; Kim, Byung-Tae. *Carbohydrate Research.* **2003**, 338 (1), 29-34.
20. Murphy, R. A.; Kung, H.F.; Kung, M.; and Billings, J. *J. Med. Chem.* **1990**, 33, 171-178.
21. a)Kurumi, M.; Sasaki, K.; Takata, H.; Nakayama, T., *Heterocycles*, **2000**, 53, No. 12, 2809-2819. b) Teguiche, M.; Lamara, K.; Smalley, R. K., *Journal de la Societe Algerienne de Chimie*, 2003, 13(1), 19-27. c) Liu, Q.; Tor, Y., *Organic Letters*, 2003, 5, No.14, 2571-2572.

CHAPTER 4

CLICK-CHEMISTRY AS A POWERFUL TOOL FOR THE CONSTRUCTION OF FUNCTIONALIZED POLY(P-PHENYLENEETHYNYLENE)S: COMPARISON OF PRE- AND POSTFUNCTIONALIZATION SCHEMES.*

4.1 Introduction

The post-polymerization functionalization of conjugated polymers is a useful technique in which a specific polymer backbone is post-synthetically altered. Leclerc¹ has executed this concept elegantly in the polythiophene series by polymerization of an active-ester containing thiophene monomer, while Holdcroft² has developed the post-polymerization halogenation of polythiophenes. These approaches allow introduction of molecular diversity late, in the final step, of the synthetic sequence and are therefore highly efficient compared to the introduction of functional elements during the synthesis of specific monomers. Additionally, postfunctionalization schemes allow the introduction of groups that might not be compatible with the polymerization conditions. Fast assembly of libraries of polymers and introduction of different and potentially sensitive functional groups are some of the advantages of post polymerization functionalization. The caveat with postfunctionalization is the requirement of high yielding and specific

* Thanks to my collaborator Dr. Brian Englert for his tremendous help in this project

reactions; errors in the functionalization of monomers can be corrected by the appropriate purification steps, while a polymer synthesized by postfunctionalization processes can not be purified further.

Huisgen and Szeimies³ investigated the 1,3-dipolar cycloaddition of azides to alkynes. Triazoles are the only product of this reaction. Sharpless recognized the potential of this transformation and retooled the dipolar cycloaddition as “Click Chemistry” for the construction of biologically active molecules.⁴ The high yield and the specificity of this transformation make it appealing, not only for synthesis of small molecules but as well for the functionalization of polymers as reported very recently by Hawker and Frechet⁵ in the attachment of dendrons to non-conjugated polymers.

4.2 Results and Discussion

PPEs are valuable due to their dramatic chromic responses.⁶⁻⁸ They have been utilized in sensory schemes and in semiconductor devices including but not restricted to light emitting diodes^{7a,b} and photodiodes.⁸ However, postfunctionalization schemes on PPEs have only sparsely been carried out.⁶ As a consequence it is of significant interest to develop an efficient platform that could allow the manipulation of PPE's properties in a post polymerization modification approach (Figure 4.1). In this contribution a PPE scaffold, **4.3**, is introduced that allows to “click on” different functional groups by a 1,3-dipolar cycloaddition. The polymers made by the postmodification approach were compared to those of the same structure but made by a conventional approach (Figure 4.1). This allows the evaluation of the click process as tool to functionalized conjugated polymers. Important (specific) questions are if the postfunctionalization process selects

the alkyne appendage over the backbone alkynes, and if the conversion of the appended alkynes is complete and if it occurs with a similar regiochemical 1,4-control as reported for the copper catalyzed 1,3-dipolar cycloaddition (Figure 4.1).

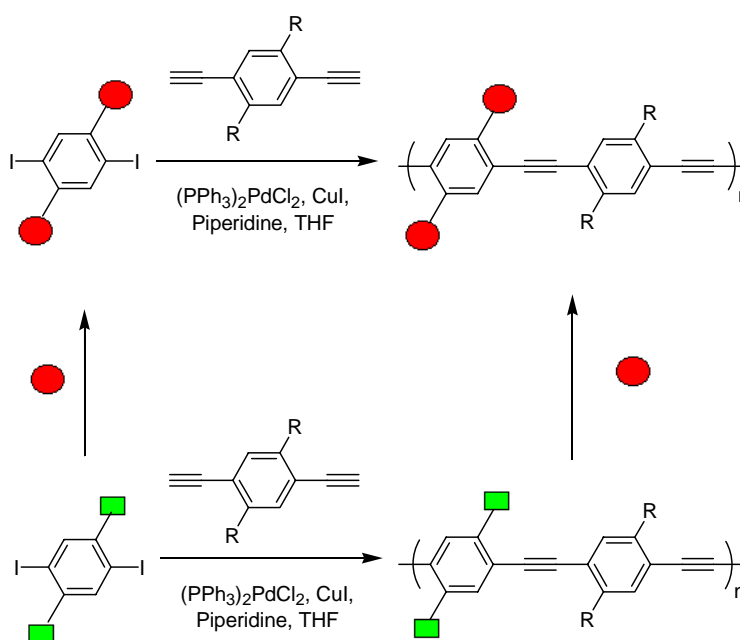
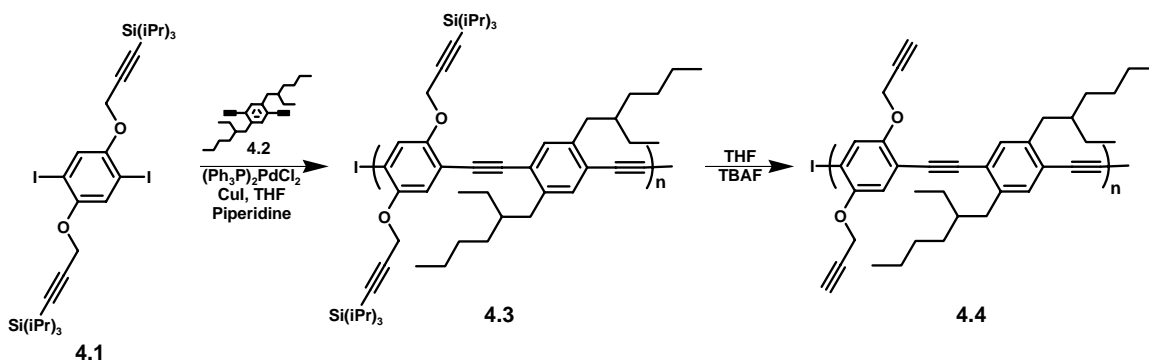


Figure 4.1. Post and prepolymerization functionalization strategies.

Synthesis and Characterization of Polymers

Polymer **4.3** and **4.4** were synthesized by Dr. Brian Englert as shown in Scheme 4.1. Both polymers **4.3** and **4.4** are yellow. **4.3** has a degree of polymerization (P_n) of 64 (gel permeation chromatography, $M_n = 65 \times 10^3$, $M_w/M_n = PDI = 4.4$). Gel permeation chromatography shows a decrease of P_n to 46 ($M_n = 24 \times 10^3$, $PDI = 1.6$). We believe that the decreased solubility of **4.4** as compared to that of **4.3** leads to a removal of higher

molecular weight polymer chains during the filtration step that is necessary for the preparation of GPC samples.



Scheme 4.1. Synthesis of the polymer **4.4**.

^1H NMR and ^{13}C NMR spectra of **4.3** and **4.4** were obtained in the presence of chromium acetylacetonate (cracac) as relaxing agent. The proton NMR spectrum of **4.4** resembles that of **4.3** but does a) not show a signal for the TIPS groups, b) shows an additional signal for the free alkyne groups at $\delta = 2.58$ ppm c) shows a shift in the arene protons that are now spaced and resonate at 7.17 and 7.40 ppm. The IR spectrum of **4.4** shows a strong band at 3301 cm^{-1} , which is diagnostic for the presence of a terminal alkyne. Additionally two bands at 2202 and 2122 cm^{-1} can be attributed to the $\text{C}\equiv\text{C}$ stretch band of the backbone and the free alkyne respectively.

The optical spectra of **4.3** and **4.4** are shown in Figure 4.2 and Table 4.1. The solution spectra of **4.3** and **4.4** are typical for PPEs. The solid-state spectra of **4.3** and **4.4** are strikingly different. The removal of the TIPS groups leads to a 12 nm red shift (577 cm^{-1}) in absorption. This red shift could be either a sign of increased planarization or of

inter chromophore interaction that would give testimony to the formation of weak electronic aggregates between PPE chains on top of a significant contribution of chain planarization (1475 cm^{-1}). The solid-state emission of **4.4** shows an excimer band at 533 nm that is not present in the solid-state spectrum of **4.3**, reinforcing the notion of some interchain interactions in exist in **4.4** at least in the solid state.⁹

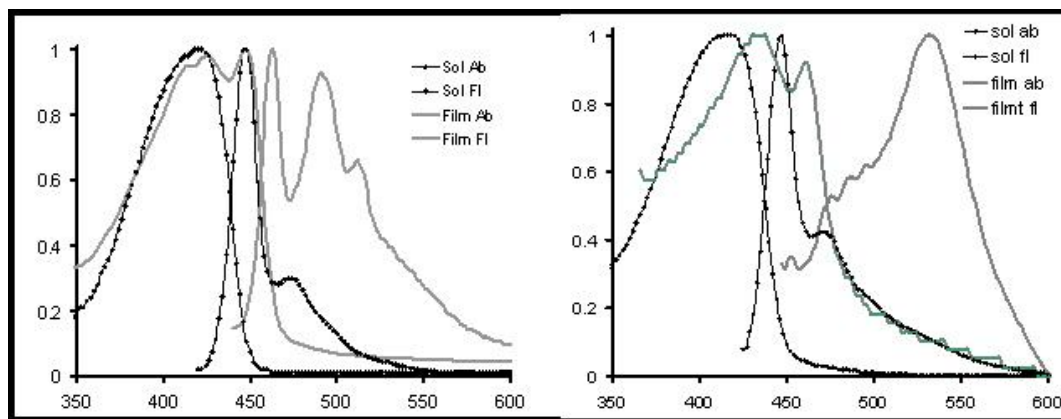
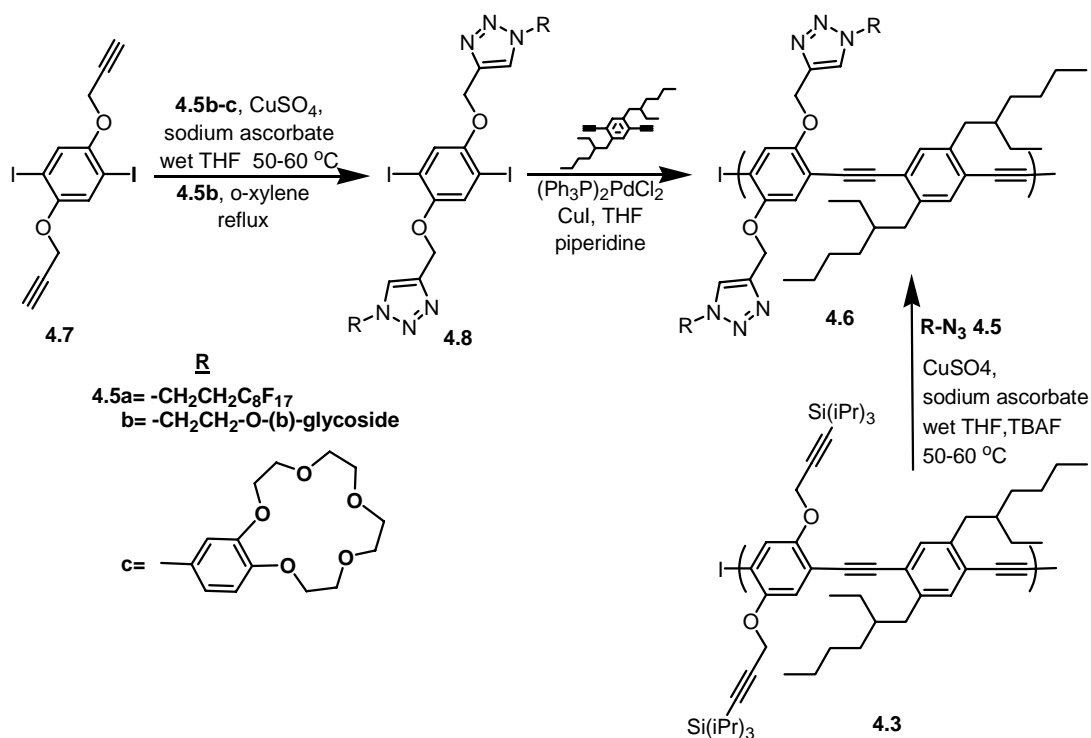


Figure 4.2. UV-vis and emission spectra of polymer **4.3** (left) and polymer **4.4** (right) in chloroform solution and in the solid state (Absorption and emission maxima see Table 1).

The successful formation of **4.4** allowed the investigation of its reaction with different azides. In a first experiment direct reaction of **4.4** with **4.5a** was investigated under microwave irradiation, but the low solubility of polymer **4.4** in organic solvents led to a material that was only to a moderate extent triazole functionalized. It was found that an in situ deprotection with tetrabutylammoniumfluoride (TBAF) and coupling procedure was a much better way of obtaining the 1,3-dipolar cycloadducts. Reaction of **4.3** with the azides **4.5a-c** in the presence of copper sulfate, TBAF and sodium ascorbate in wet THF (5% water) as solvent gave the functionalized PPEs **4.6a-c** in yields of 75-96 %

after 48h at 40-60 °C. Without the addition of copper sulfate and sodium ascorbate the reaction did not proceed as well. As a consequence, postmodification reactions were performed in the presence of copper sulfate and sodium ascorbate. Workup is performed by threefold precipitation of the formed polymer into methanol to remove the starting azide reagent. The yields of the postfunctionalization reactions are high and shown in Table 4.1.

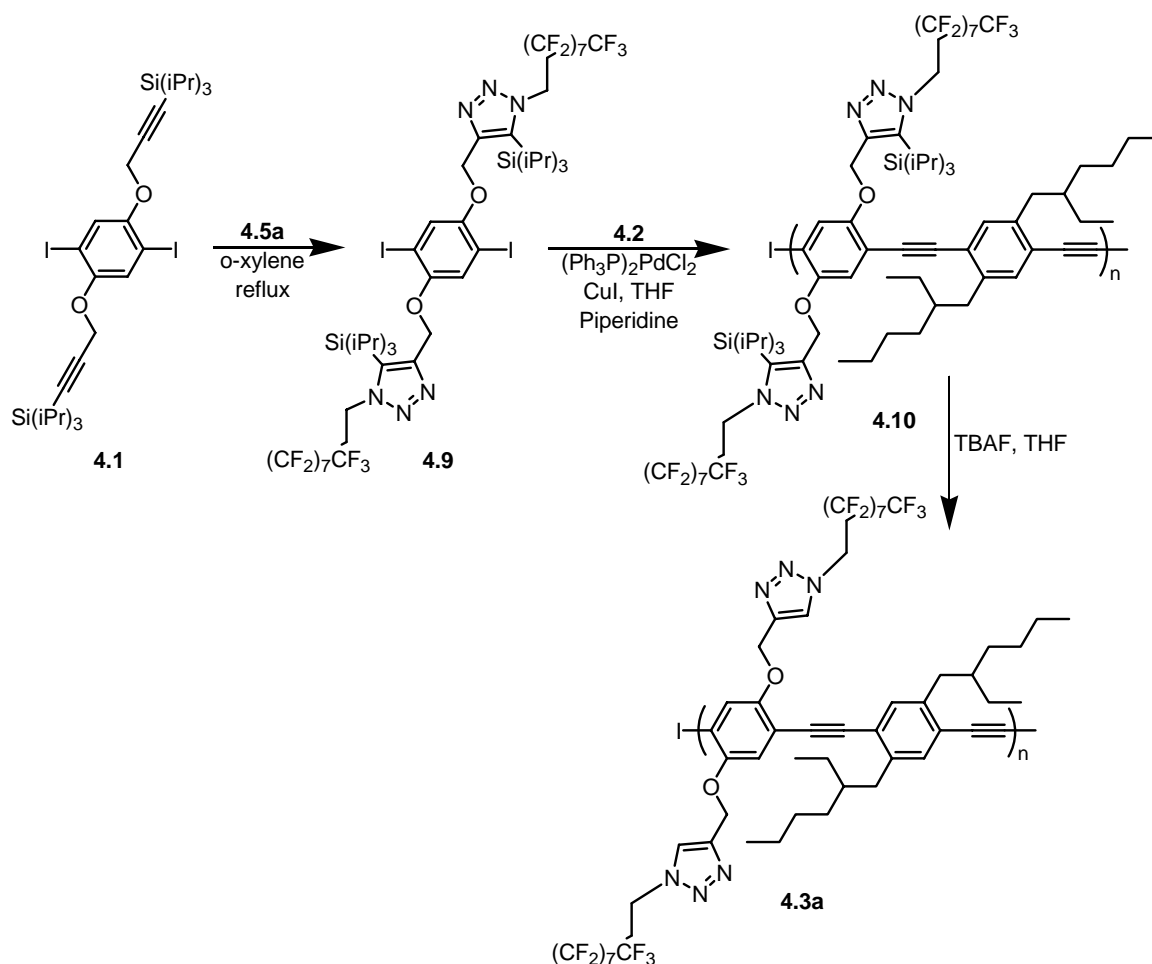


Scheme 4.2. In situ generation of **4.4** and its reaction with azides **4.5a-c** yielding **4.6a-c** and prefunctionalization approach towards **4.6a-c**.

Reactions carried out with azides **4.5a-c** afforded polymers **4.6a-c** of which were completely functionalized according to ^1H , ^{13}C NMR, and IR. This was confirmed by the synthesis of the same polymers **4.6a-c** by a more conventional approach (Scheme 4.2).

These “premodified” polymers afforded a standard the postmodified PPEs could be compared to. The completely postmodified polymers **4.6a-c** had no peaks in the ^1H NMR at 2.55 ppm for the terminal alkyne. Signals for the newly formed triazoles are present at 7.5-8.0 ppm. Signals from the triazole carbon nuclei are easily visible at 140-150 ppm and 120-130 ppm in the ^{13}C NMR spectrum of the functionalized polymers. The peak at 3294 cm^{-1} has disappeared in the IR spectra of the postfunctionalized polymers. The excess of azide reagent **4.5** was removed completely by threefold precipitation of the polymers **4.6** into methanol, according to IR spectroscopy where the strong azide band at 2100 cm^{-1} had disappeared.

Reaction of **4.7** with azides **4.5b-c** afforded monomers **4.8b-c**. Reaction with diyne **4.2** under standard conditions furnished the polymers **4.6b-c** in excellent yields (Table 4.1). Monomer **4.8a** was obtained by this method but due to lack of solubility could neither be characterized nor purified. An alternate approach employing the reaction of **4.1** with azide **4.5a** under thermal conditions afforded monomer **4.9** (Scheme 4.3). Polymerization of **4.9** with **4.2** under standard conditions affords **4.10** in almost quantitative yields. The presence of the triisopropylsilyl groups can be confirmed by the presence of two signals between $\delta = 10$ and 20 ppm in the ^{13}C NMR spectrum of **4.10**. Deprotection of **4.10** with TBAF yielded polymer **4.3a** as a moderately soluble yellow solid.



Scheme 4.3. Synthesis of polymer **4.3a** via a prefunctionalized strategy starting from monomer **4.3**.

Regioisomers

At room temperature, the copper catalyzed process is typically regioselective favoring the 1,4-triazole. We opted to perform these copper catalyzed reactions between 40-60°C as we observed improved yields in monomers and higher degrees of functionalization in polymeric systems. Under these conditions **4.10b**, **4.10c**, were obtained as approximate 2:1 mixtures of the 1,4- to the 1,5-regioisomers. The regioisomers were not separable by flash chromatography and therefore used as mixtures.

Due to decrease in resolution, when going from monomer to polymer, we are not able to assess the regiochemistry of the polymers **4.6** at all by NMR spectroscopy, and therefore can not make an assessment of the regioselectivity of this process in the postfunctionalization process. Only in the formation of the sterically hindered monomer **4.9** full regioselectivity is observed, only the 1,4-product is formed.

Characterization of functionalized polymers 4.6a-c

It was of interest to study the influence of postmodification on the molecular weight **4.6**. We find PPEs decreases in molecular weight when converting **4.3** into **4.6** (**4.3**: 63.6×10^3 ; $10.8 \times 10^4 > \mathbf{4.6} > 8.5 \times 10^3$) and polydispersity (**4.3**: 4.4 to between $4.4 > \mathbf{4.6} > 1.5$) with respect to platform polymer **4.3** (Table 1). This is possibly due to differences in solubility between **4.3** and the post functionalized polymers **4.6**. Material is lost during the filtration step required for GPC due to aggregated and/or insoluble parts of **4.6** as discussed for polymer **4.3**. GPC ultrafilters are yellowish in appearance after filtration of solutions of **4.6a-c**. The decreased polydispersity is an excellent indication for the loss of material during filtration.

To rule out the possibility of diyne formation, i.e. crosslinking, as a reason for observed insolubility, we treated polymer **4.4** with TBAF, copper sulfate and sodium ascorbate in wet THF (5% water) in the presence of air. Only after heating to reflux for 24 h we observed a material with moderate diyne linkages. Because the material was still soluble the amount of cross-linking must be moderate. The signals of the diyne linkages are however visible in ^{13}C NMR due to their shorter relaxation time as compared to the signals attributed to the main chain. These signals that can be assigned to diyne

formation were not observed in any of the postfunctionalized polymers **4.6a-c** synthesized under nitrogen with the scrupulous exclusion of oxygen.

The possibility of incorporation of triazole groups into the backbone of the PPEs as a cause for the decreased solubility was also considered. Control experiments were performed in which didodecyl-PPE was treated at 40°C for 16 h with an excess of dodecyl azide under standard postfunctionalization conditions. After precipitation into methanol only unfunctionalized PPE was isolated according to ^1H NMR, ^{13}C NMR and UV-vis spectroscopy, strongly suggesting that attack on the backbone-alkynes is not favored under the current reaction conditions.

There is precedence for decreased solubility of click-functionalized polymers: Kluger et al. performed postfunctionalization of poly(oxynorbornenes)¹⁰ and noted dramatic differences in solubility between polymers functionalized with 1,4-triazoles and those not. In some cases, GPC data for these polymers could not be obtained due to limited solubility. Matyjaszewski et al. has recently modified polymers of acrylonitrile with click-type chemistry to form tetrazoles and also noted marked differences in solubility between polymers modified by click chemistry and those not modified by click chemistry.¹¹ It is however surprising that the attachment of dodecyl chains or Frechet-type dendrons leads to a decrease in solubility. A possible explanation is that the presence/incorporation of the triazole group per se reduces the solubility of any polymer.

Table 4.1. Optical Properties, Yields, Degree of Polymerization and Degree of Functionalization of 4.3, 4.4 and 4.6

<i>Polymer</i>	Yield	M_n (PDI)	Degree of Postfunctionalization	Absorption (CHCl₃) [nm]	Absorption (Film) [nm]	Emission (CHCl₃) [nm]	Emission (Film) [nm]
4.3	87%	63.6 x 10 ³ 4.43	na	422	450,426	448	462, 490, 512
4.4	95%	24.4 x 10 ³ 1.64	>95%	420	462, 438	447	533
4.10	91%	25.5 x 10 ⁴ 4.25	>95%	406	410	447	450
4.6a pre	82%	71.7 x 10 ³ 4.44	na	416	422	449	483
4.6a post	94%	25.4 x 10 ³ 2.56	>95%	418	435	448	479
4.6b pre	93%	24.5 x 10 ³ 1.01	na	421	433	454	470
4.6b post	76%	22.6 x 10 ³ 2.39	>95%	424	431	454	470, 523
4.6c pre	93%	16.2 x 10 ⁴ 7.70	na	408	416	452	470
4.6c post	82%	10.8 x 10 ⁴ 1.49	>95%	412	426	450	452, 470

Optical properties of functionalized polymers 4.6a-c

The optical properties of polymers **4.6a-c** were examined and compared with their pre-modified counterparts. In solution, absorption and fluorescence maxima of structurally identical polymers **4.6a-c** occur at similar wavelengths (± 2 nm). It is interesting to note that the largest difference in absorption is found when comparing platform polymer **4.4** to functionalized polymers. For all polymers (**4.6**), both pre and post-functionalized, blue shifts in absorption are observed when compared to **4.4** (Table 1). Polymer **4.10** with TIPS groups attached to the pendent triazole moieties as an extreme case has a solution absorption maxima of 406 nm, which is blue shifted by 6 to 24 nm of the absorption maxima of post and pre-polymers **4.6a-c** (Figure 4.3). The solid-state emission of **4.10** is almost unchanged to that obtained in solution. We assume that the increased steric demand of the TIPS groups forces the PPEs into a non-planar ground state.^{12, 13}

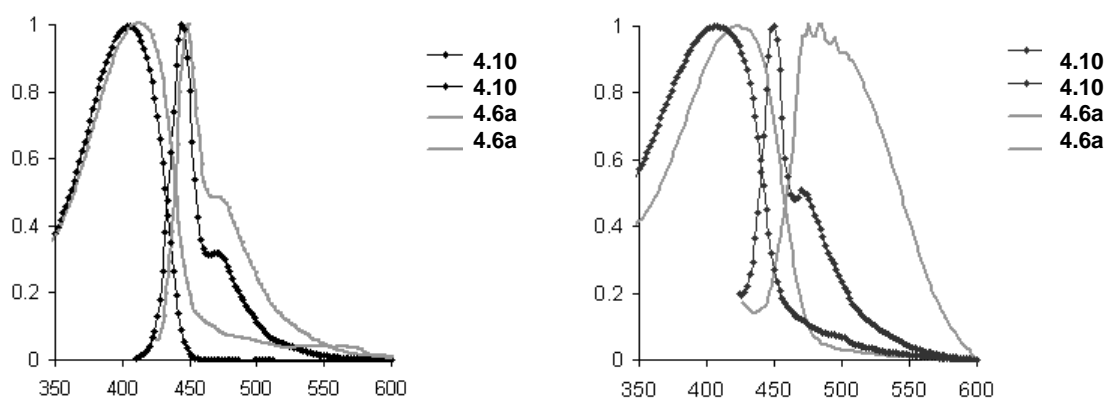


Figure 4.3. UV-vis and emission spectra of polymer **4.6a** conventional and polymer **4.10** in chloroform and in the solid state. The only difference is the TIPS group attached to the triazole units.

The solution emission spectra of polymers **4.6a-c** vary only slightly and are almost superimposable.⁹ All of the investigated polymers **4.3**, **4.4**, **4.6**, **4.10** have the same backbone. In the solid state, i.e. in thin films their absorption spectra vary considerably. The polymer **4.4** shows an absorption maximum at 462 nm, while the TIPS-substituted **4.10** has a solid state absorption maximum located at 410 nm. All of the other, triazole-functionalized polymers, **4.6**, show absorption maxima ranging from 416-436 nm. It is interesting to note that the red shift in the absorption spectra of **4.6a-c** when going from solution into the solid state, is quite small, only 6-17 nm. That is unusual, because the precursor polymer **4.4**, featuring the same backbone shows a shift of 42 nm when going from solution into the solid state. The differences in the thin film UV-spectra between pre- and postfunctionalized polymers **4.6a-c** of identical structure is small, and as a rule the absorption of the post-functionalized samples is 8-13 nm red shifted.

The introduction of the triazole unit into the side chains of the PPEs **4.6** and the PPE **4.10** influences their absorption insofar as a more twisted conformations of the main chain must be assumed resulting in the presence of nonplanar ground states. In the case of **4.10** the large TIPS substituent will probably lead to an additional twist of the main chain and the conformation of **4.10**'s backbone in solution and in the solid state will be very similar. The subtle differences between the absorption of the pre vs. the postfunctionalized triazole-substituted PPEs **4.6a-c** is possibly due to differences in the ratio of 1,4- and 1,5-isomers.

DSC of functionalized polymers 4.6a-c

The thermal behavior of polymers **4.6a-c** was investigated between 0-250°C by differential scanning calorimetry (DSC). Polymers **4.3**, **4.4**, **4.6a**, **4.6b** and **4.6c** show slow decomposition and no phase transitions. When comparing polymers synthesized by a post and pre-modification strategy it is important to note that the conventional and the click polymers **4.6** often have different degrees of polymerization but identical substituents and are therefore expected to behave differently. Longer polymer chains would melt at higher temperatures. As discussed above slightly differing polymer structures such as the presence of 1,5-triazoles would also be expected to cause differences in the solid state properties of these polymers.

4.3 Conclusion

We have produced a series of PPEs (**4.6a-c**) by employing click chemistry in both pre and post-polymerization functionalization approaches. In examples where the structural repeat unit of the polymer was the same, the optical properties of these polymers in solution proved to be identical. Differing thin-film optical and thermal behavior properties result from differing degrees of polymerization and small amounts of triazole regioisomers. Click chemistry provided a means to completely functionalize PPEs via a postmodification strategy. While all of these triazole-functionalized polymers aggregate, their absorption spectra are quite insensitive to the aggregation process, which suggests that triazole-functionalized PPEs may find attractive applications in biological sensing schemes.¹⁴

4.4 Experimental

Instrumentation. The ^1H and ^{13}C NMR spectra were taken on a Varian 300 MHz or a Bruker 400 MHz spectrometer using a broadband probe. The ^1H chemical shifts are referenced to the residual proton peaks of CDCl_3 at δ 7.24 and DMSO at δ 2.49. The ^{13}C resonances are referenced to the central peak of CDCl_3 at δ 77.0 and DMSO at δ 39.5. Chromium(III)acetylacetonate was used when obtaining ^{13}C NMR data for all polymers. UV-VIS measurements were made with a Shimadzu UV-2401PC recording spectrophotometer. Fluorescence data was obtained with a Shimadzu RF-5301PC spectrofluorophotometer. A Headway Research Model PWM32 instrument was used to spin-coat dilute chloroform solutions of polymers onto quartz slides for thin film experiments. 1,4-Diiodo-2,5-dihydroquinone,¹³ 1,4-diethynyl-2,5-bis(2-ethylhexyl)-benzene **4.2**,¹³ **4.5a-c**,¹² and **4.7**¹³ were prepared and characterized in accordance to published procedures.

I would like to thank Dr. Brian Englert for his tremendous help in this project.

General Procedure for Conversion of Halide to Azide: In a round bottom flask the corresponding organic halide was dissolved in acetone, 10 eq of sodium azide were added, and the mixture was heated to reflux for 24 h, cooled to room temperature and the solvent was removed under vacuum. Following aqueous work up the crude products were purified by column chromatography on silica gel with dichloromethane:hexane as an eluent.

Synthesis of polymer 4.6a (post-polymerization functionalization): Polymer **4.3** (0.100 g, 0.118 mmol) and azide **4.5a** (0.231 g, 0.471 mmol) were dissolved in THF (15 mL) under nitrogen purge in an oven dried Schlenk flask. The flask was flushed with nitrogen, frozen and evacuated three times after which CuSO₄ (0.5 mg, 2 μmol), L-Ascorbic acid sodium salt (4 mg, 19 μmol), and tetrabutylammoniumfluoride (0.25 mL, 1M solution in THF, containing ca. 5% water) were added. The mixture was allowed to stir at 60°C for 48 h. The solvent was removed under vacuum. The mixture was re-dissolved in dichloromethane, washed with 1N HCl, 1N NH₄OH and water. The organic layer was dried over MgSO₄ and the solvent was removed. The resulting polymer was dissolved in dichloromethane and precipitated out of methanol to yield **4.6a** (0.168 g, 94%) as a yellow solid. ¹H NMR (CDCl₃): δ 7.64 (m, 2H), 7.26 (m, 2H), 7.17 (m, 2H), 5.34 (m, 4H), 4.64 (m, 4H), 2.82 (m, 4H), 1.25 (m, 20H), 0.84 (m, 12H). ¹³C NMR (CDCl₃): δ 153.0, 144.5, 141.2, 133.2, 122.2, 118.2, 114.9, 110.6, 94.8, 90.1, 63.8, 57.9, 42.3, 40.3, 38.3, 32.3, 31.7, 29.7, 28.6, 25.5, 22.9, 18.3, 13.8, 11.0, 10.6. IR: ν 3311, 3259, 2961, 2443, 2204, 1702, 1592, 1505, 1456, 1415, 1356, 1316, 1258, 1076, 1015, 887, 799, 752, 707, 658. GPC (polystyrene standards) M_n = 25.4 x 10³, PDI = 2.56.

Synthesis of 4.9: Diiodo compound **4.1** (1.00 g, 1.33 mmol) and azide **4.5a** (2.93 g, 5.99 mmol) were dissolved in *o*-xylene under nitrogen purge in an oven dried Schlenk flask. The mixture was allowed to stir at reflux for 48 h. The solvent was removed under vacuum and the crude product purified by chromatography on silica gel (1:3, ethylacetate:hexane) to yield **4.9** as a colorless solid and single regioisomer (2.01 g, 86 %). ¹H NMR (CDCl₃): δ 7.25 (s, 2H), 5.06 (s, 4H), 4.74 (t, 4H), 3.04 (m, 4H), 1.43 (m,

6H), 1.09 (m, 36H). ^{13}C NMR (CDCl_3): δ 152.4, 142.3, 137.0, 123.0, 85.8, 60.8, 40.7, 31.8, 18.8, 18.5, 11.5, 1.1. ^{19}F NMR (CDCl_3): -82.1, -115.4, -123.0, -123.2, -124.1, -124.5, -127.5. IR: ν 3090, 2947, 2867, 2725, 2464, 2363, 2105, 2002, 1692, 1467, 1458, 1375, 1352, 1233, 1207, 1150, 1055, 1000, 883, 848, 711, 647. MS Calculated for, $[\text{C}_{50}\text{H}_{56}\text{F}_{34}\text{I}_2\text{N}_6\text{O}_2\text{Si}_2]$, 1728.9; found 1729.4; MP: 146-150°C.

Synthesis of polymer 4.10 (pre-polymerization functionalization): Monomer **4.9** (single regioisomer) 1.00 g, 0.574 mmol) and 2,5-ethylhexyl-1,4-diethynylbenzene **4.2** (0.203 g, 0.579 mmol) were dissolved in dichloromethane (2 mL) and piperidine (2 mL) in an oven dried Schlenk flask. The flask was flushed with nitrogen, frozen and evacuated three times after which $(\text{Ph}_3\text{P})_2\text{PdCl}_2$ (20 mg, 29 μmol), and CuI (6 mg, 29 μmol) were added. The mixture was allowed to stir at room temperature for 48 h. The solvent was removed and the mixture dissolved in dichloromethane, washed with 1N HCl, 1N NH_4OH , and water. The organic layer was dried over MgSO_4 and the solvent removed. The resulting polymer **4.10** was dissolved in dichloromethane and precipitated out of methanol three times to yield a yellow solid (1.42 g, 91 %). ^1H NMR (CDCl_3): δ 7.26 (m, 4H), 7.18 (m, 2H), 5.35 (m, 4H), 4.66 (m, 4H), 2.80 (m, 4H), 1.24 (m, 18H), 1.01 (m, 42H) 0.82 (m, 12H). ^{13}C NMR (CDCl_3): δ 152.7, 141.9, 141.4, 137.4, 133.2, 122.5, 117.3, 114.7, 113.2, 110.5, 95.6, 88.8, 60.4, 44.8, 40.4, 38.1, 32.2, 31.6, 28.6, 25.4, 22.8, 18.3, 13.7, 11.3, 10.5. IR: ν 2962, 2867, 2726, 2357, 2205, 1506, 1460, 1412, 1367, 1259, 1092, 1018, 872, 797, 658. GPC (polystyrene standards) $M_n = 25.5 \times 10^4$, PDI = 4.25.

Synthesis of Polymer 4.6a (pre-polymerization functionalization): Polymer **4.10** (0.5 g, 0.331 mmol) was dissolved in THF (50 mL) under nitrogen purge in an oven dried Schlenk flask. Under nitrogen tetrabutylammoniumfluoride (3 mL, 1M solution in THF, containing ca. 5% water) was added slowly over 5 min. The mixture was stirred for 24 hours. The solvent was removed under vacuum and the resulting solid dissolved in dichloromethane and washed with water. The organic layer was dried under MgSO_4 , filtered and the solvent removed to afford **4.3a** as a yellow solid (0.398 g, 96 %). ^1H NMR (CDCl_3): δ 7.65-7.51 (m, 2H), 7.25 (m, 2H), 7.18 (m, 2H), 5.32 (m, 4H), 4.63 (m, 4H), 2.82 (m, 4H), 1.24 (m, 20H), 0.83 (m, 12H). ^{13}C NMR (CDCl_3): δ 152.7, 140.8, 132.9, 122.8, 117.1, 114.3, 112.7, 100.7, 94.5, 89.6, 67.5, 63.1, 42.0, 40.0, 37.8, 31.8, 28.2, 25.0, 22.5, 17.9, 13.5, 10.2. IR: ν 2959, 2863, 2206, 1691, 1614, 1463, 1223, 1027, 883, 744, 709, 652. GPC (polystyrene standards) M_n 71.7 $\times 10^3$, PDI = 4.44.

Synthesis of Polymer 4.6b (post-polymerization functionalization): Polymer **4.3** (0.100 g, 0.118 mmol) and azide **4.5b** (88.4 mg, 0.355 mmol) were dissolved in THF (15 mL) under nitrogen purge in an oven dried Schlenk flask. The flask was flushed with nitrogen and frozen and evacuated three times after which CuSO_4 (0.5 mg, 2 μmol), sodium ascorbate (4 mg, 19 μmol), and tetrabutylammoniumfluoride (0.25 mL, 1M solution in THF, containing ca. 5% water) were added. The mixture was stirred at 50°C for 48 h. The solvent was removed and the mixture dissolved in dichloromethane, washed with 1N HCl, 1N NH_4OH , and water. The organic layer was dried over MgSO_4 and the solvent removed under vacuum. The resulting polymer was dissolved in hot DMSO and precipitated out of methanol (three times) to yield **4.6b** (0.093 g, 76 %) as a

yellow solid. ^1H NMR (DMSO): δ 7.56-7.50 (m, 4H), 7.41 (m, 2H), 5.73 (m, 2H), 4.92 (m, 2H), 4.59 (m, 6H), 4.01 (m, 12H), 3.18 (m, 12H), 1.91 (m, 32H), 1.73 (m, 6H), 1.55 (m, 16H), 1.25 (m, 6H), 0.84 (m, 12H). ^{13}C NMR (TCE): δ 152.6, 141.7, 132.6, 124.6, 117.5, 102.8, 93.9, 90.3, 74.4, 72.9, 69.8, 67.0, 60.8, 57.3, 48.1, 30.1, 27.8, 24.8, 22.6, 18.7, 13.2, 10.3. IR: ν 3544, 3309, 2948, 2866, 2528, 2200, 2102, 1730, 1625, 1436, 1382, 1203, 1118, 1076, 1041, 862, 740, 555, 453, 412. GPC (polystyrene standards) M_n = 22.6×10^3 , PDI = 2.39.

Synthesis of 4.8b: Diiodo compound **4.7** (1.00 g, 2.28 mmol) and azide **4.5b** (2.00 g, 4.79 mmol) were dissolved in THF under nitrogen purge in an oven dried Schlenk flask. The flask was flushed with nitrogen, frozen and evacuated three times after which CuSO_4 (6 mg, 22.8 μmol) and sodium ascorbate (45 mg, 228 μmol) were added. The mixture was allowed to stir at 50°C for 48 h. The solvent was removed and the mixture dissolved in dichloromethane, washed with 1N HCl, 1N NH_4OH , and water. The organic layer was dried over MgSO_4 . The solvent was removed under vacuum and the crude product purified by chromatography on silica gel (1:1, ethylacetate:dichloromethane) to yield **4.8b** as a colorless crystalline solid (1.81 g, 62 %). ^1H NMR (CDCl_3): δ 7.78 (s, 2H), 7.41 (s, 2H), 7.24 (s, 2H), 5.15 (m, 6H), 4.49 (m, 12H), 3.95 (m, 4H), 3.68 (m, 4H), 1.97 (m, 24H). ^{13}C NMR (CDCl_3): δ 170.3, 169.8, 169.1, 169.0, 152.5, 143.1, 124.2, 123.7, 100.4, 86.5, 72.3, 71.8, 70.8, 68.1, 67.6, 64.4, 61.6, 50.1, 20.7, 20.5. IR: ν 3557, 3479, 3454, 3086, 2955, 2876, 2739, 2450, 2419, 2109, 2028, 1961, 1916, 1732, 1645.17, 1482, 1320, 1172, 993, 952, 907, 854, 795, 753, 696, 649, 602. MS Calculated for, $[\text{C}_{44}\text{H}_{54}\text{I}_2\text{N}_6\text{O}_{22}]$, 1272.74; found 1273.1; MP: $156\text{-}160^\circ\text{C}$.

Synthesis of polymer 4.6b (pre-polymerization functionalization): Monomer **4.8b** (0.230 g, 0.251 mmol) and 2,5-ethylhexyl-1,4-diethynylbenzene **4.2** (0.088 g, 0.251 mmol) were dissolved in dichloromethane (2 mL) and piperidine (2 mL) in an oven dried Schlenk flask. The flask was flushed with nitrogen, frozen and evacuated three times after which (Ph₃P)₂PdCl₂ (3 mg, 5 μmol), and CuI (1 mg, 5 μmol) were added. The mixture was allowed to stir at room temperature for 48 h. The solvent was removed and the mixture dissolved in dichloromethane, washed with 1N HCl, 1N NH₄OH, and water. The organic layer was dried over MgSO₄ and the solvent removed. The solvent was concentrated and the polymer precipitated out of H₂O (50:50) twice to yield **4.6b** (0.241 g, 93%). ¹H NMR (DMSO): δ 7.56 (m, 2H), 7.50 (m, 2H), 7.41 (m, 2H), 5.72 (m, 2H), 4.91 (m, 2H), 4.59 (m, 6H), 4.01 (m, 12H), 3.18 (m, 12H), 1.91 (m, 32H), 1.70 (m, 6H), 1.54 (m, 16H), 1.26 (m, 6H), 0.87 (m, 6H). ¹³C NMR (DMSO): δ 152.7, 141.9, 140.7, 132.6, 124.5, 122.3, 117.7, 113.7, 111.9, 102.7, 93.8, 85.9, 76.48, 73.0, 69.9, 66.6, 61.0, 58.1, 49.4, 31.5, 27.8, 24.9, 21.9, 13.2, 10.2. IR: ν 3577, 3454, 3258, 3126, 2956, 2924, 2806, 2710, 2201, 1960, 1644, 1598, 1513, 1466, 1401, 1279, 1213, 1163, 1023, 991, 870, 804. GPC (polystyrene standards) M_n = 24.5 x 10⁴, PDI = 1.01.

Synthesis of 4.8c: Diiodo compound **4.7** (0.500 g, 1.14 mmol) and azide **4.5c** (1.05 g, 3.39 mmol) were dissolved in THF under nitrogen purge in an oven dried Schlenk flask. The flask was flushed with nitrogen, frozen and evacuated three times after which CuSO₄ (3 mg, 11 μmol) and sodium ascorbate (23 mg, 114 μmol) were added. The mixture was allowed to stir at 50°C for 48 h. The solvent was removed and the mixture dissolved in

dichloromethane, washed with 1N HCl, 1N NH₄OH, and water. The organic layer was dried over MgSO₄. The solvent was removed under vacuum and the crude product purified by chromatography on silica gel (10:1, ethylacetate:hexane) to yield **4.8c** as a colorless crystalline solid (0.651 g, 53 %). ¹H NMR (CDCl₃): δ 7.77 (m, 2H), 7.23 (m, 2H), 7.56 (m, 4H), 6.78 (t, 2H), 5.14 (m, 4H), 4.11 (m, 8H), 3.87 (m, 8H), 3.61 (m, 16H). ¹³C NMR (CDCl₃): δ 152.9, 135.5, 130.1, 124.8, 124.4, 118.5, 114.8, 111.4, 107.4, 86.8, 78.9, 71.9, 71.0, 69.9, 61.1, 58.2. IR: ν 3259, 2954, 2871, 2360, 2115, 1734, 1600, 1518, 1455, 1349, 1223, 1021, 801. MS Calculated for, [C₄₀H₄₆I₂N₆O₁₂], 1056.6; found 1057.2; MP: 162-164°C.

Synthesis of polymer 4.6c (post-polymerization functionalization): Polymer **4.3** (0.100 g, 0.188 mmol) and azide **4.5c** (0.116 g, 0.375 mmol) were dissolved in THF under nitrogen purge in an oven dried Schlenk flask. The flask was flushed with nitrogen, frozen and evacuated three times after which CuSO₄ (0.5 mg, 1.9 μmol), L-Ascorbic acid sodium salt (4 mg, 18.7 μmol), and tetrabutylammoniumfluoride (0.25 mL, 1M solution in THF, containing ca. 5% water) were added. The mixture was allowed to stir at 40°C for 48 h. The solvent was concentrated and the polymer precipitated out of methanol:H₂O (50:50) twice to yield **4.6c** (0.149 g, 82%). ¹H NMR (CDCl₃): δ 8.01 (m, 1H), 7.63 (m, 1H), 7.38 (m, 2H), 6.86 (m, 2H), 4.80 (m, 4H), 4.13 (m, 8H), 3.89 (m, 8H), 3.73 (m, 16H), 2.75 (m, 4H), 2.55 (m, 2H), 1.76 (m, 2H), 1.55 (m, 16H), 1.28 (m, 6H), 0.84 (m, 6H). ¹³C NMR (TCE): δ 153.5, 150.0, 144.9, 141.7, 133.6, 130.6, 120.7, 118.1, 114.3, 112.5, 107.1, 94.9, 90.1, 70.4, 69.6, 64.5, 53.23, 40.4, 38.5, 32.4, 28.8, 25.6, 22.6,

14.0, 10.9. IR: ν 3642, 3561, 3515, 3412, 2930, 2857, 2351, 2205, 1644, 1592, 1504, 1445, 1263, 1138, 1130. GPC (polystyrene standards) $M_n = 108.4 \times 10^3$, PDI = 1.49.

Synthesis of Polymer 4.6c (Pre-polymerization functionalization): Monomer **4.9c** (0.301 g, 0.280 mmol) and 2,5-ethylhexyl-1,4-diethynylbenzene **4.2** (99.2 mg, 0.283 mmol) were dissolved in dichloromethane (2 mL) and piperidine (2 mL) in an oven dried Schlenk flask. The flask was flushed with nitrogen, frozen and evacuated three times after which $(\text{Ph}_3\text{P})_2\text{PdCl}_2$ (10 mg, 14 μmol), and CuI (3 mg, 14 μmol) were added. The mixture was allowed to stir at room temperature for 48 h. The solvent was removed and the mixture dissolved in dichloromethane, washed with 1N HCl, 1N NH_4OH , and water. The organic layer was dried over MgSO_4 and the solvent removed. The resulting polymer was dissolved in dichloromethane and precipitated out of methanol three times to yield **4.6c** (0.309 g, 93 %) as a yellow solid. ^1H NMR (CDCl_3): δ 8.01 (m, 2H), 7.26 (m, 10H), 5.39 (m, 4H), 4.14 (m, 16H), 3.75 (m, 16H), 2.68 (m, 4H), 1.24 (m, 16H), 0.84 (m, 12H). ^{13}C NMR (CDCl_3): δ 153.0, 144.4, 142.6, 141.2, 135.0, 133.0, 131.7, 130.3, 120.4, 117.2, 113.2, 112.0, 106.3, 95.0, 89.8, 70.7, 70.7, 68.8, 63.7, 40.1, 38.0, 32.1, 30.5, 28.4, 25.2, 22.7, 13.8, 10.5. IR: ν 2958, 2207, 1604, 1510, 1453, 1261, 1101, 1018, 933, 802. GPC (polystyrene standards) $M_n = 16.2 \times 10^4$, PDI = 7.70.

4.5 References:

1. Bernier, S.; Garreau, S.; Bera-Aberem, M.; Gravel, C.; Leclerc, M. *J. Am. Chem. Soc.* **2002**, *124*, 12463.
2. a) Li, Y. N.; Vamvounis, G.; Holdcroft, S. *Chemistry of Materials*. **2002**, *14*, 1424. b) Li, Y. N.; Vamvounis, G.; Yu, J. F.; Holdcroft, S. *Macromolecules* **2001**, *34*, 3130.
3. a) Huisgen, R.; Szeimies, G.; Moebius, L. *Chem. Ber.* **1967**, *100*, 2494. b) Huisgen, R.; Knorr, R.; Moebius, L.; Szeimies, G. *Chem. Ber.* **1965**, *98*, 4014.
4. a) Lewis, W. G.; Green, L. G.; Grynszpan, F.; Radic, Z.; Carlier, P. R.; Taylor, P.; Finn, M. G.; Sharpless, B. K. *Angew. Chem. Int. Ed.* **2002**, *41*, 1053. b) Rostovtsev, V. V.; Green, L. G.; Fokin, V. V.; Sharpless, B. K. *Angew. Chem. Int. Ed.* **2002**, *41*, 2596.
5. a) Wu, P.; Feldman, A. K.; Nugen, A. K.; Hawker, C. J.; Scheel, A.; Voit, B.; Pyun, J.; Frechet, J. M. J.; Sharpless, B. K.; Fokin, V. V. *Angew. Chem. Int. Ed.* **2004**, *43*, 2. b) Helms, B.; Mynar, J. L.; Hawker, C. J.; Frechet, J. M. J. *J. Am. Chem. Soc.* **2004**, *126*, 15020.
6. a) Wagner, M.; Nuyken, O. *Macromolecules* **2003**, *36*, 6716. b) Wagner, M. Nuyken, O., *J. Macromol. Sci. A*. **2004**, *41*, 637. Wang, Y. Q.; Wilson, J. N.; Smith, M. D.; Bunz, U. H. F. *Macromolecules* **2004**, *37*, 970. c) Wilson, J. N., Wang, Y. Q.; Lavigne, J. J.; Bunz, U. H. F. *Chem Commun*, **2003**, 1626. d) Disney, M. D.; Zheng, J.; Swager, T. M.; Seeberger, P. H. *J. Am. Chem. Soc.* **2004**, *126*, 13343. e) Hecht S.; Khan A. *Angew. Chem.* **2003**, *42*, 6021. f) Breen, C. A.; Deng, T.; Breiner, T.; Thomas, E. L.; Swager, T. M. *J. Am. Chem. Soc.* **2003**, *125*, 9942.
7. a) Kraft, A.; Grimsdale, A. C.; Holmes, A. B. *Angew. Chem.* **1998**, *37*, 402. b) Pschirer, N. G.; Miteva, T.; Evans, U.; Roberts, R. S.; Marshall, A. R.; Neher, D.; Myrick, M. L.; Bunz, U. H. F. *Chem. Mater.* **2001**, *13*, 2691. c) Schmitz, C.; Posch, P.; Thelakkat, M.; Schmidt, H. W.; Montali, A.; Feldman, K.; Smith, P.; Weder, C. *Adv. Funct. Mater.* **2001**, *11*, 41.
8. Xu, Y.; Berger, P. R.; Wilson, J. N.; Bunz, U. H. F. *Appl. Phys. Lett.* **2004**, *85*, 4219.

9. a) Bunz, U. H. F.; Wilson, J. N.; Bangcuyo C. *ACS Symp. Ser.* **2005**, 888, 147. b) Halkyard, C. E.; Rampey, M. E.; Kloppenburg, L.; Studer-Martinez, S. L.; Bunz, U. H. F. *Macromolecules* **1998**, 31, 8655. c) Wilson, J. N.; Steffen, W.; McKenzie, T. G.; Lieser, G.; Oda, M.; Neher, D.; Bunz, U. H. F. *J. Am. Chem. Soc.* **2002**, 124, 6830. d) Kim, J. S.; Swager, T. M. *Nature* **2001**, 411, 1030. e) Miteva, T.; Palmer, L.; Kloppenburg, L.; Neher, D.; Bunz, U. H. F. *Macromolecules*, **2000**, 33, 652.
10. Binder, W. H.; Kluger, C. *Macromolecules*, **2004**, 37, 9321.
11. Tsarevsky, N. V.; Bernaerts, K. V.; Dugour, B.; Du Prez, F. E.; Matyjaszewski, K. *Macromolecules* **2004**, 37, 9308.
12. a) Englert, B. C.; Smith, M. D.; Hardcastle, K. I.; Bunz, U. H. F.; *Macromolecules*; **2004**, 37, 8212.
13. a) Bunz, U. H. F. *Chem. Rev.* **2000**, 100, 1605. b) Wilson, J. N.; Waybright, S. M.; McAlpine, K.; Bunz, U. H. F. *Macromolecules* **2002**, 35, 3799. c) Huang, W. Y.; Gao, W.; Kwei, T. K.; Okamoto, Y. *Macromolecules* **2001**, 34, 1570. d) Sluch, M. I.; Godt, A.; Bunz, U. H. F.; Berg, M. A. *J. Am. Chem. Soc.* **2001**, 123, 6447.
14. Breitkamp, R. B.; Tew, G. N. *Macromolecules* **2004**, 37, 1163.

CHAPTER 5

1,3-DIPOLAR CYCLOADDITION FOR POLY(ARYLENETRIAZOLENE)S AND NANOSTRUCTURED SEMICONDUCTORS BY HEATED PROBE TIPS

5.1 Introduction

The generation of nanostructured organic semiconductors is a critical technology in key areas that include device miniaturization, photovoltaic materials, photonic bandgap materials, and electronic circuitry.¹⁻⁵ Almost any area of high tech materials profits from the generation of nanostructures. An elegant way to generate nanostructures in soft materials is the use of heated atomic force microscope (AFM) cantilever tips, which allow the reversible or irreversible writing of nanostructures in thin films.⁶ We have pushed this concept a step further to generate an organic semiconducting material utilizing heat from a cantilever tip to induce a thermal 1,3-dipolar cycloaddition of a suitable aromatic diazide with a diethynylbenzene derivative. Simple methods of actively generating organic semiconductor nanostructures are rare and often rely on self assembly processes such as the ribbon and wire formation of substituted PPEs shown by Müllen and Rabe,⁷ monolayer self-assembly and electron beam lithography.^{8,9}

The 1,3-dipolar cycloaddition of terminal alkynes with azides has been investigated by Szeimies and Huisgen almost forty years ago.¹⁰ Recently this powerful reaction was

catalytically re-tooled as “Click” chemistry by Sharpless to synthesize biologically active species such as enzyme inhibitors and is exploited to craft novel materials.¹¹ He discovered that Cu(I) salts increase regioselectivity and reaction rate of the 1,3-dipolar cycloaddition of terminal alkynes with azides as shown in Scheme 1. Copper acetylides coordinates to azides and/or triazoles.

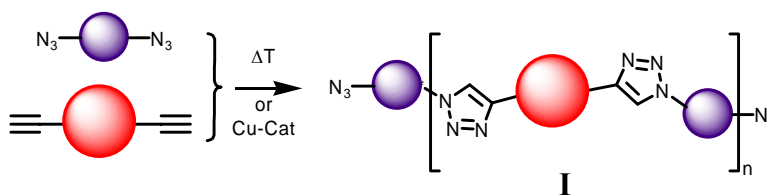
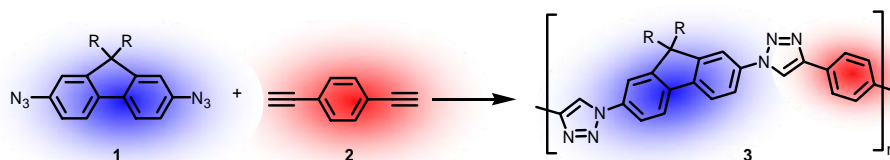


Figure 5.1. Synthesis of o poly(arylenetriazolyne)(PArT) by click chemistry



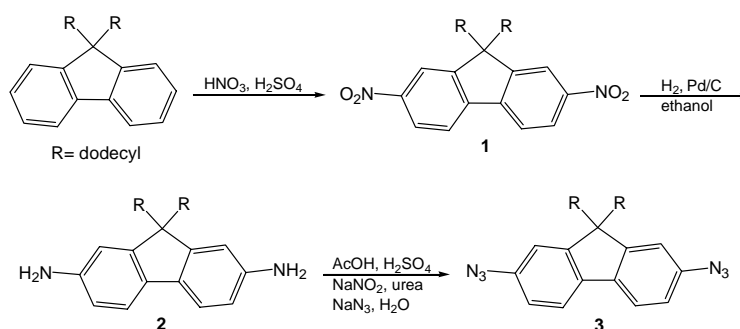
Scheme 5.1. Synthesis of a conjugated polymer by a 1,3-dipolar cycloaddition

While a slew of materials applications have been investigated by Hawker and others, the synthesis of conjugated polymers by 1,3-dipolar cycloadditions has been conspicuously absent.¹² Only one example has been reported.¹³ Herein, we describe a) the synthesis of conjugated fluorescent polymers by the thermal and Cu-catalyzed 1,3-dipolar cycloadditions of terminal diynes with aromatic diazides, and b) nanostructured

organic semiconductors by nanoscale thermal processing of mixed diazide/dialkyne thin films with a heated AFM cantilever tip.

5.2 Result and Discussion

The monomer synthesis was started from didodecyl fluorene which was synthesized according to literature procedures.¹⁴ Nitration of didodecyl fluorene in the presence of concentrated sulfuric acid and fuming nitric acid furnishes **5.1** in good yield. Hydrogenation was done in a pressurized steel autoclave, **5.1** in ethanol and Pd/C catalyst to furnish diamino fluorene **5.2** in a clean reaction. The diamine compound **5.2** was converted to fluorine diazide **5.3** under acidic conditions by using concentrated sulfuric acid, acetic acid and sodium azide.¹⁵ This diazide was used in polymerization without further purification because of its excellent purity. Reactions are outlined in Scheme 5.2.

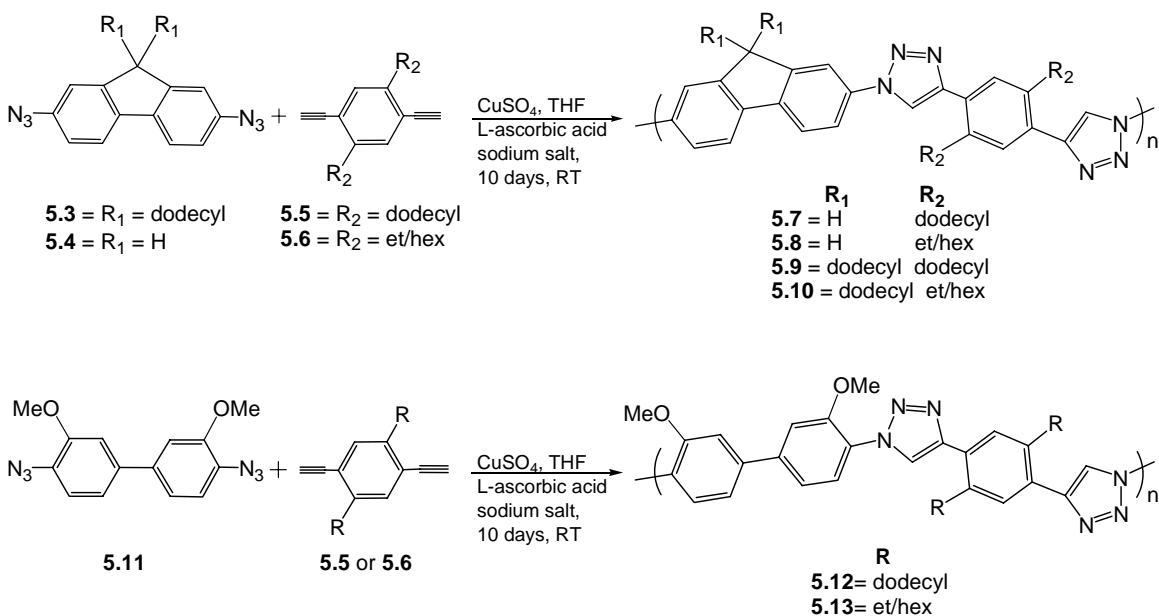


Scheme 5.2. Synthesis of didodecyl diazide fluorene monomer.

Reaction of the didodecyl-2,7-diazidofluorene **5.3** and 2,7-diazidofluorene **5.4** as cycloaddition partners for **5.5** and **5.6** produced polymers **5.7-5.10** in the presence of THF, copper sulfate and sodium ascorbate in excellent yields as yellowish or off white powders that precipitated out of solution as seen in Scheme 5.3.^{16,17} The

poly(arylenetriazolylene)s (PArTs) **5.7-5.8** are only moderately soluble in chloroform and THF, while **5.9** and **5.10** show increased solubility due to the larger concentration of alkyl chains.

The bisazide **5.11** was obtained by the reaction of 3,3'-dimethoxy-biphenyl-4,4'-diamine with trifluoromethanesulfonyl azide.^{22,23} Subsequent reaction of **5.11** with **5.5** or **5.6** in the presence of copper sulfate and sodium ascorbate in THF solution furnished the PArTs **5.12** and **5.13** (Scheme 5.3) at room temperature in excellent yields after precipitation from methanol (Table 1).¹⁶ The formed PArT are of relatively low molecular weight and exceeding 10^4 due to lack of solubility of the PArTs in THF employed as solvent. If the unsubstituted fluorenediazide **5.4** is used, a polymer with a significant fraction of insoluble material is isolated. However, most of the other PArTs are soluble in chloroform or dichloromethane.



Scheme 5.3. Copper catalyzed synthesis of **5.7-5.10** and **5.12** and **5.13**.

Table 5.1. Substituent key, optical and analytical data for polymers **5.3-5.6, 5.8** and **5.9**.

Polymer	R ¹	R ²	Yield	λ_{max} abs [nm]	λ_{max} em [nm]	Φ	M _n	PDI
5.7	H	dodecyl	92 %	322	358, 371	N/A	insoluble	
5.8	H	ethex	80 %	322	357, 370	0.41	1.9 x 10 ³	2.1
5.9	dodecyl	dodecyl	92 %	329	359, 376	0.38	5.7 x 10 ³	2.2
5.10	dodecyl	ethex	87 %	328	358, 375	0.48	8.7 x 10 ³	5.8
5.12	N/A	dodecyl	86 %	314	379	N/A	insoluble	
5.13	N/A	ethex	88 %	314	379	0.48	5.1 x 10 ³	5.5

According to ¹H and ¹³C NMR spectroscopy, the PArTs display regular 1,4-substitution around the triazole unit. The PArTs are non-fluorescent in the solid state but blue fluorescent in solution. The quantum yield of emission of the soluble representatives is around 0.4 (quinine sulfate/2-aminopyridine-standard). Their absorption maxima are between 314-330 nm and the emission maxima are recorded between 370-379 nm, often accompanied by shoulders at 357-359 nm as seen in Figure 5.2. The optical properties are practically independent from the molecular weight of the PArTs suggesting that the used building blocks lead to species with localized HOMO and LUMO. This effect will be discussed later in detail. A noteworthy observation is the red shift in emission upon

addition of acid to the PArTs. Figure 5.3 shows the emission spectra of polymer **5.9** upon protonation.

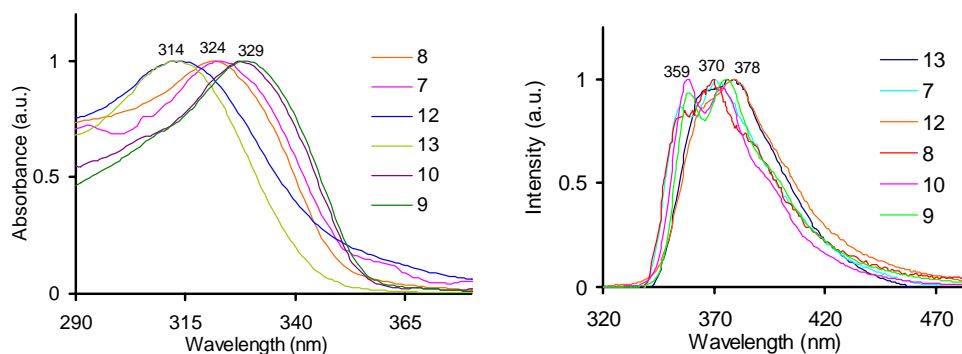


Figure 5.2. Absorption and emission spectra of **5.7-5.13** in chloroform.

Upon addition of aqueous HCl to a solution of **5.8** in chloroform, the emission intensity increases and the emission maximum is bathochromically shifted by 80 nm towards 435 nm as shown in Figure 5.4. Protonation of the triazole ring increases the fluorescence efficiency and conjugation.

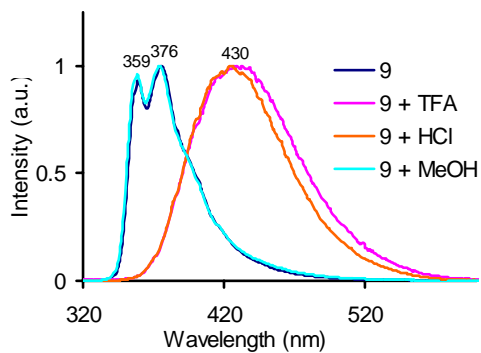


Figure 5.3. Emission spectra of **5.9** in chloroform, upon addition of methanol and acids.

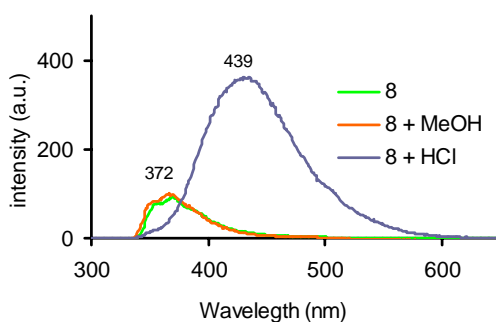
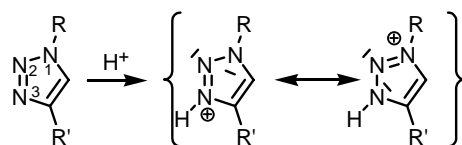


Figure 5.4. Emission spectra of 5.8 in chloroform and hydrochloric acid addition to a solution.

What is the reason for a) the molecular weight independence of the optical data and b) the observed significant red shift upon protonation? Quantum chemical model calculations (SPARTAN B3LYP 6-31G**//6-31G**) on 1,4-diphenyl-1,2,3-triazole explained both issues: a) the high band gap and the length independence of the optical properties are due to a distinct localization of the FMO on different parts of the molecule; the HOMO is predominantly located on the former alkyne and LUMO is located on the former azide part of the cycloadduct. b) Protonation in the 3-position (Scheme 5.4) of the triazole gives the most stable azaallylic imidazolinium type cation, which has a lower HOMO-LUMO gap and a more delocalized FMOs.



Scheme 5.4. Protonation of triazole ring.

An important aspect is the temperature at which the thermal 1,3-dipolar cycloaddition proceeds at a reasonable rate to give PArTs of significant molecular weight. Differential scanning calorimetry (DSC) experiments revealed that mixtures of **5.3** and **5.6** undergo exothermic reaction at 184 °C with 52614.69 kcal energy lost for one mol of triazole formation (Figure 5.5) to give the cycloadduct **5.10** by thermal reaction in the solid state. The heat balance and the analysis of the DSC traces provide an excellent analytical tool to optimize the reaction conditions of 1,3-dipolar cycloadditions in the solid state. The residue in the crucible was off-white and slightly fluorescent, testimony to the efficient 1,3-dipolar cycloaddition of **5.5** with **5.4** as opposed to thermal polymerization of the diyne units, which would have led to colored or dark materials.

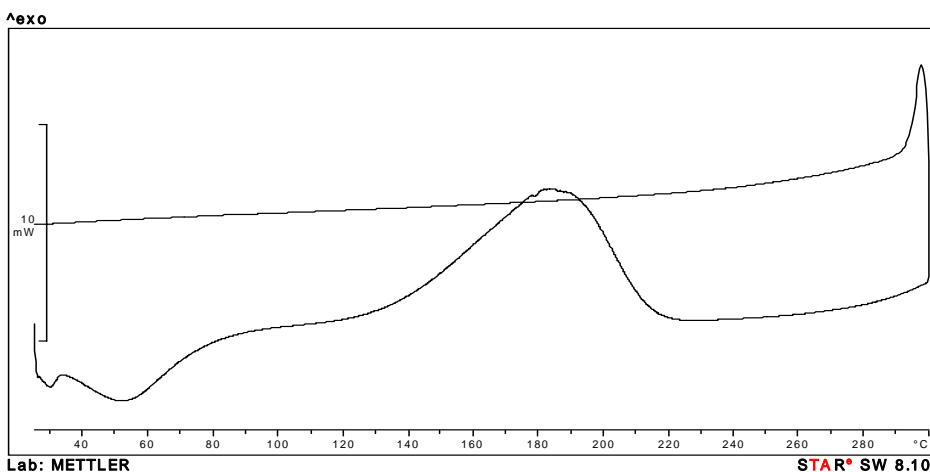


Figure 5.5. DSC data for mixture of **5.4** and **5.5**.

Processing

An exciting aspect of the in situ click chemistry is the potential for the formation of organic semiconductors in the solid state; thermal 1,3-dipolar cycloadditions are facile at

enhanced temperatures.¹³ Monomers **5.3**, **5.4** and **5.5** are crystalline. An attractive feature of the PArTs is their synthesis by co-melting and thermal polymerization. In collaboration with Prof. King^{20,21} in Mechanical Engineering at GaTech a heated AFM cantilever was used to write a feature into a non-sticky film of diazide and diyne monomers to give nanostructured organic semiconductor (PArT) features. A solid solution of two crystalline pre-annealed monomers would be excellent materials because crystalline materials have higher thermal conductivity and tend to stick less to hot cantilevers. This technology allowed thin films of azide and alkyne monomer to locospecifically polymerize into nanostructured PArT surfaces and patterns, a process useful for semiconductor and memory application. Figure 5.6 shows the experiment where a combination of diazide **5.3** and diyne **5.6** was spin cast on a quartz glass to give an 80 nm thick film. The mixed monomer film was structured and at the same time polymerized to give PArT **5.10** by an AFM cantilever heated to 230 °C. Well resolved elements with sharp edges result.

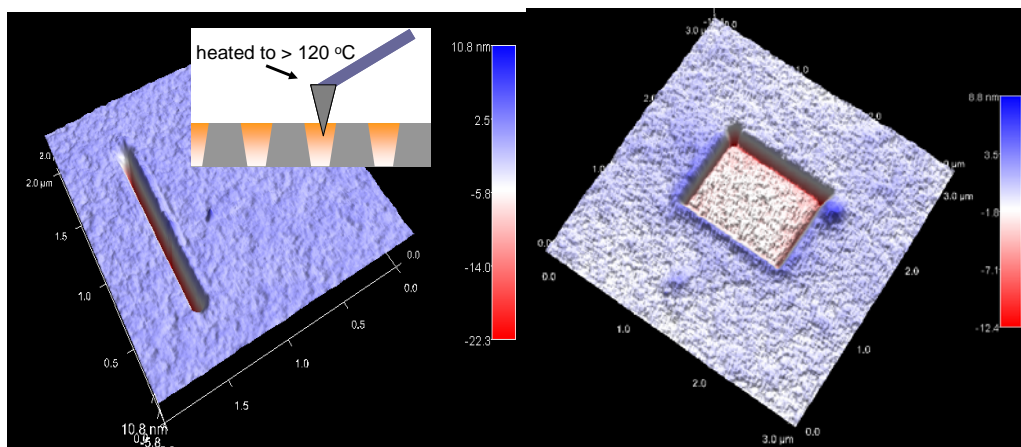


Figure 5.6. Heated cantilever writing (230 °C) on an 80 nm thin film of a mixture of the diyne **5.6** and diazide **5.3** on a cover slip.

Heated cantilevers will generate semiconducting PArT features on a 50 nm – 5 micron scale by click chemistry. Neither delamination nor ripping of the films is observed. The left image was obtained by multiple heating cycles and shows a line approx. 20 nm deep, 60 nm wide and 1.5 μm long, while the right hand side image shows a more shallow, 8 nm deep and 1 μm x 1 μm large square obtained by area cantilevering.

Band gap and electronic engineering:

A fascinating aspect of most of these cycloadducts is the localization of their FMOs, i.e. HOMO and LUMO on different parts of the molecules. Figure 5.7 shows the HOMO and the LUMO of the 1,3-dipolar cycloadduct 1,4-diphenyl-1,2,3-triazole. The HOMO is mostly located on the side of the former dipolarophile, while the LUMO is located on the side of the former 1,3-dipole. To reduce the band gap, one should use the natural distribution of the HOMO and LUMO orbital coefficients and attach donor and acceptor groups to the alkyne, and the azide, respectively.



Figure 5.7. HOMO (left) and the LUMO (right) of the 1,3-dipolar cycloadduct phenylacetylene and phenyl azide. Calculations: Dr. Bunz

Figure 5.8. displays the calculated FMOs of the pentameric model **11**, with a resulting band gap of 2.96 eV. Distyrylbenzene has a calculated band gap of 3.39 eV (HO -5.18 eV, LUMO -1.79 eV), suggesting that correct do-acc substitution allows to decrease the band gap of PArTs to any desired value. Donor and acceptor substitution will be the key for the successful use of PArTs and while single chains will not be strongly conjugated, 3d-conjugation in the solid state is expected for strongly donor-acceptor substituted PArTs.²⁵ If the functionalities are inverted, i.e the adduct of (dimethylamino)phenylazide and diethynylpyrazine is calculated, this isomeric form of **11** shows its HOMO at -5.16 eV and its LUMO at -1.40 eV with a resulting band gap of 3.66 eV. DFT calculations as performed here give excellent ground state structures and orbital energies, but only a rough idea about absorption and emission spectra, due to the neglect of configuration interaction and excited state contributions. However, donor and acceptor substitution will define the electronics of PArTs.

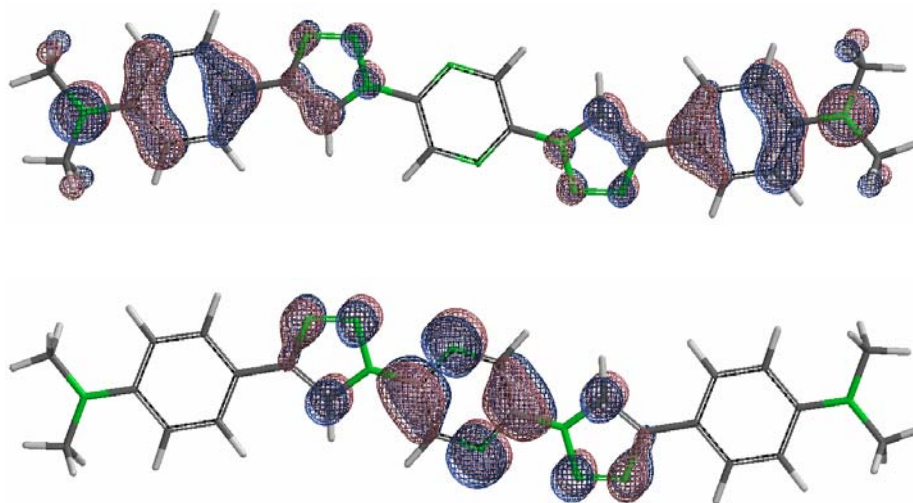
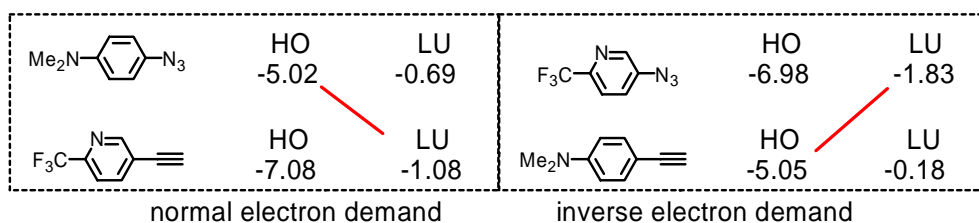


Figure 5.8. HOMO (-4.97 eV, top) and the LUMO (-2.01 eV; Gap = 2.96 eV, bottom) of the 1,3-dipolar cycloadduct **11** ((dimethylamino)phenylacetylene and 2,5-pyrazinediazide).

One additional issue is the electronic characteristics of azide and alkyne. Thermal 1,3-dipolar cycloadditions work well if an electron accepting alkyne and an electron rich azide are employed. However, according to DFT calculations, the inverse electron demand 1,3-dipolar cycloaddition should have very similar primary FMO interactions as the cycloaddition with normal electron demand. We would therefore assume that this combination should work well. In the case of the copper catalyzed click reactions, electronic demand does not seem to play a large role or is altered by the formation copper acetylides.



Conclusions

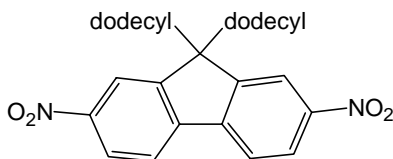
Both thermal and Cu-catalyzed 1,3-dipolar cycloadditions are discussed here to make conjugated oligomers and polymers. The cycloaddition is atom economic; there is no side- or byproducts and allows the introduction of virtually any function into PArTs possible. The reaction can be performed in solution, in the solid state or in thin films, with or without copper catalysts. In thin (20-80 nm) films, locospecific reaction by a heated AFM cantilever results in the in situ formation of nanoscale organic semiconductor features from azides and alkynes for potential device applications such as

thin film transistors. This powerful strategy should lead to nanostructured and classically soluble organic semiconductors and generate a significant impact in the chemistry and physics of conjugated polymers. Azide-alkyne cycloadditions are promising but need further development to give useful organic semiconductors.

Experimental

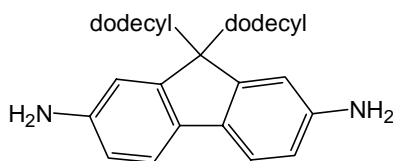
Instrumentation. The ^1H and ^{13}C NMR spectra were taken on a Varian 300 MHz and 75 MHz (^{13}C). The ^1H chemical shifts are referenced to the residual proton peaks of CDCl_3 at δ 7.24. The ^{13}C resonances are referenced to the central peak of CDCl_3 at δ 77.0 and. IR data were collected by a Shimadzu FTIR-8400S infrared spectrophotometer. UV-VIS measurements were made with a Shimadzu UV-2401PC recording spectrophotometer. Fluorescence data were obtained with a Shimadzu RF-5301PC spectrofluorophotometer. Fluorescence quantum yields were determined in relation to quinine sulfate ($\approx 10^{-6}$ M in 0.1M H_2SO_4 , $\Phi_F = 0.54$) according to reference.²⁶ 9,9-Didodecyl-9H-fluorene¹⁴, 2,7-diazido-9-H-fluorene¹⁵ and 4,4'-Diazido-3,3'-dimethoxy-biphenyl¹⁵ were synthesized and characterized in accordance to published procedures.

I would like to thank Shubham Saxena for his help on AFM measurements.

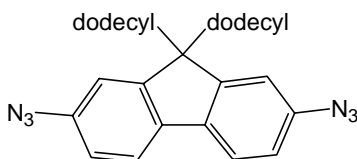


9,9-Didodecyl-2,7-dinitro-9H-fluorene 5.1: In a 250 mL round bottom flask, 9,9-didodecyl-9H-fluorene (10.0 g, 19.9 mmol) was added to a mixture of concentrated sulfuric acid (50.0 mL) and fuming nitric acid (50.0 mL) at 0°C . The mixture was stirred at room temperature for 2.5 h then the reaction was stopped. Mixture was poured into ice-water and extracted with CH_2Cl_2 and water. The organic layer was dried over MgSO_4 and the solvent removed. Product was collected as off-white solid (11.8 g, 72 %). ^1H NMR (CDCl_3): δ 8.34, 8.26, 7.93, 2.10, 1.21-1.04, 0.82, 0.55; ^{13}C NMR (CDCl_3): δ 153.7, 148.6, 144.9, 123.8, 121.8, 118.7, 56.7, 40.0, 32.0, 30.0, 29.8, 29.7, 29.4, 24.0, 22.8,

14.3; IR: ν 3101, 3926, 2852, 1921, 1794, 1612, 1591, 1524, 1466, 1340, 1130, 1072, 899, 831, 785, 739.



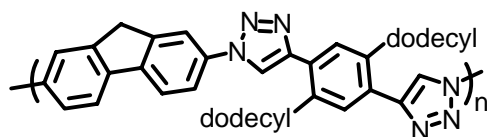
9,9-Didodecyl -9H-fluorene-2,7-diamine 5.2: Solution of 9,9-Didodecyl-2,7-dinitro-9H-fluorene (6.73 g, 80 %) in ethanol and Pd/C catalyst was added to a hydrogen bomb vessel. Vessel was pressurized and the pressure was released for 3 times. Finally hydrogen bomb was filled with pressurized H₂ (2000 psi) and the vessel was heated to 50 °C for 2 days. Reaction was stopped and solvent was evaporated. The mixture was filtered over celite, the filter cake was washed with CH₂Cl₂ then the filtrate was evaporated and dried. (5.73 g, 80 %, brown oil). ¹H NMR (CDCl₃): δ 7.35, 6.63, 6.61, 3.59, 1.84, 1.21, 1.06, 0.90, 0.68; ¹³C NMR (CDCl₃): δ 115.8, 144.8, 133.3, 119.3, 114.1, 110.3, 54.8, 41.2, 32.2, 30.5, 30.0, 29.8, 29.6, 29.5, 24.0, 23.0, 14.4; IR: ν 3462, 3369, 3213, 2924, 2851, 1850, 1618, 1583, 1468, 1327, 1298, 1244, 1130, 858, 808; Mp= 56.



2,7-Diazido-9,9-didodecyl-9H-fluorene 5.3: In a 500 mL round bottom flask, 9,9-dimethyl-9H-fluorene-2,7-diamine (5.00 g, 9.38 mmol) was added to a mixture 40.0 mL AcOH and 20.0 mL concentrated H₂SO₄. Then sodium nitrite (1.38 g, 20.0 mmol) in 20.0 mL water was added drop wise to a mixture at 0°C. After 10 min of stirring, urea was

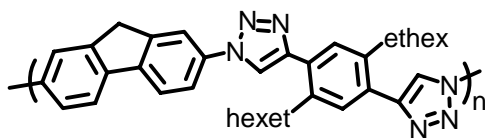
added to the mixture to remove excess sodium nitrite and finally sodium azide (1.10 g, 20.0 mmol) was added. The reaction was stirred at 0°C for 3 h. and mixture was poured into ice water. Aqueous sodium hydroxide was added and the mixture extracted with ethyl acetate. The organic layer was dried over MgSO₄ and the solvent removed to give product as yellow solid (5.11 g, 93 %). ¹H NMR (CDCl₃): δ 7.61, 7.00, 6.95, 1.92, 1.27-1.05, 0.91-0.84, 0.57; ¹³C NMR (CDCl₃): δ 152.8, 138.9, 120.8, 118.1, 113.8, 55.7, 40.6, 32.1, 30.1, 29.7, 29.5, 27.1, 23.9, 22.9, 14.3; IR: ν 3204, 2924, 2851, 2401, 2100, 1859, 1610, 1581, 1462, 1441, 1375, 1294, 1140, 1090, 889, 804, 721, 669; Mp= 38.

General Procedure for Polymers: Diethynyl and diazide monomers (1:1 equiv.) and sodium ascorbate (5 mol %) were dissolved in THF (5 mL) under flow of nitrogen into a flame dried Schlenk flask. The flask was flushed with flow of nitrogen for 15 min and the mixture was frozen and evacuated for three times and CuSO₄ (5 mol %) was added. The mixture was allowed to stir at ambient temperature for 5 days. The THF was removed under vacuum and the mixture was dissolved in dichloromethane, washed with 1N HCl, 1N NH₄OH, and water. The organic layer was dried over MgSO₄ and the solvent removed. The resulting polymer was dissolved in chloroform and precipitated out of methanol.

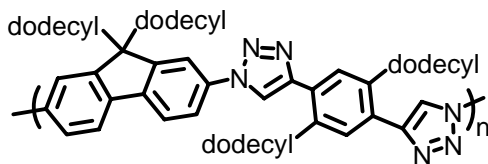


Polymer 5.7: 0.142 g (92 %), insoluble green-yellow solid. ¹³C NMR (solid-state): δ = 199.8, 185.0, 143.9, 142.2, 138.4, 134.4, 126.6, 118.3, 51.9, 29.3, 22.5, 13.7; IR: ν 3437,

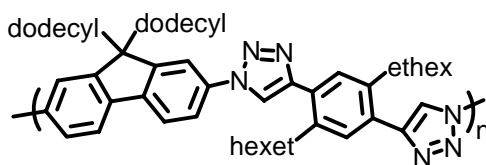
2922, 2651, 1616, 1461, 1363, 1225, 1153, 1034, 808; $\Phi_F = 0.29$; $\lambda_{\text{max abs}} = 322$, $\lambda_{\text{max flu}} = 371$.



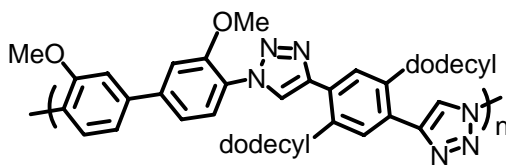
Polymer 5.8: 0.137 g (80 %), yellow solid. ^1H NMR (CDCl_3): δ 8.17, 8.10, 7.99, 7.88, 7.60, 7.44, 4.16, 2.79, 1.56, 1.25, 0.86; ^{13}C NMR (solid-state): δ =145.3, 139.4, 135.1, 126.6, 119.0, 65.8, 60.3, 53.4, 36.5, 28.6, 24.4, 13.4, 9.8; IR: ν 3439, 3306, 3130, 2957, 2924, 2101, 1616, 1589, 1483, 1460, 1259, 1221, 1095, 1040, 1011, 816; GPC (polystyrene standards): $M_n = 1975$, $M_w/M_n = 2.08$, $P_n = 3.3$; $\Phi_F = 0.41$; $\lambda_{\text{max abs}} = 322$, $\lambda_{\text{max flu}} = 370$.



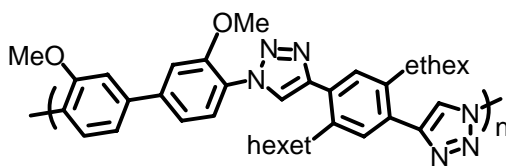
Polymer 5.9: 0.261 g (83%), yellow solid. ^1H NMR (CDCl_3): δ 8.20, 7.96, 7.91, 7.82, 7.73, 2.94, 2.14, 2.04, 1.72, 1.25, 1.17, 0.86; ^{13}C NMR (CDCl_3): δ 153.4, 148.1, 140.5, 138.9, 136.8, 131.4, 129.5, 121.3, 119.6, 115.6, 56.5, 56.1, 40.6, 33.8, 32.2, 31.6, 29.9, 24.2, 24.0, 22.9, 14.3; IR: ν 3433, 2953, 2918, 2849, 2104, 1612, 1470, 1377, 1296, 1227, 1034, 1011, 889, 812, 717; GPC (polystyrene standards): $M_n = 5693$, $M_w/M_n = 2.20$, $P_n = 5.4$; $\Phi_F = 0.38$; $\lambda_{\text{max abs}} = 329$, $\lambda_{\text{max flu}} = 376-358$.



Polymer 5.10: 0.278 g (87 %), off-white solid. ^1H NMR (CDCl_3): δ 8.20, 7.93, 7.81, 7.60, 2.90, 2.12, 1.59, 1.17, 0.82; ^{13}C NMR (CDCl_3): δ 153.3, 148.3, 140.6, 138.1, 136.9, 132.8, 129.9, 121.4, 120.2, 119.6, 115.6, 56.5, 40.7, 40.4, 37.7, 32.6, 32.1, 30.2, 29.7, 29.5, 28.9, 25.8, 24.2, 23.3, 22.9, 14.3, 11.0; IR: ν 3452, 2953, 2924, 2852, 2106, 1614, 1473, 1464, 1377, 1225, 1036, 1011, 820, 727; GPC (polystyrene standards): $M_n = 8753$, $M_w/M_n = 5.80$, $P_n = 9.4$; $\Phi_F = 0.48$; $\lambda_{\text{max abs}} = 328$, $\lambda_{\text{max flu}} = 375\text{--}358$.



Polymer 5.12: 0.220 g (86 %), insoluble red-brown solid. ^{13}C NMR (solid-state): δ = 148.7, 144.9, 137.5, 127.1, 123.7, 109.0, 53.5, 41.4, 29.6, 22.7, 13.8; IR: ν 3431, 2940, 2662, 2119, 1628, 1458, 1244, 1205, 1034, 936, 845, 808, 722; $\Phi_F = 0.22$; $\lambda_{\text{max abs}} = 314$, $\lambda_{\text{max flu}} = 379$.



Polymer 5.13: 0.161 g (88 %), off-white solid. ^1H NMR (CDCl_3): δ 8.35, 8.07, 7.66, 7.42, 7.36, 4.04, 2.87, 1.61, 1.25, 0.82; ^{13}C NMR (CDCl_3): δ = 151.3, 146.9, 142.2, 137.7, 132.4, 130.1, 126.4, 125.8, 124.1, 120.5, 111.4, 56.6, 40.3, 37.8, 32.6, 28.9, 25.8, 23.4, 14.5, 11.0; IR: ν 2955, 2928, 2856, 2120, 1607, 1578, 1508, 1460, 1381, 1319,

1250, 1220, 1182, 1140, 1095, 1030, 984, 810; GPC (polystyrene standards): $M_n = 1835$,
 $M_w/M_n = 70.54$, $P_n = 8.0$; $\Phi_F = 0.48$; $\lambda_{\text{max abs}} = 314$, $\lambda_{\text{max flu}} = 379$.

References:

- 1) (a) Janata, J.; Josowicz, M. *Nature Mater.* **2003**, *2*, 19-24.
- 2) (a) Wilson, J. N.; Bangcuyo, C. G.; Erdogan, B.; Myrick, M. L.; Bunz, U. H. F. *Macromolecules* **2003**, *36*, 1426-1428. (b) Song L, Bly, R. K.; Wilson, J. N.; Bakbak, S.; Park, J. O.; Srinivasarao, M.; Bunz U. H. F. *Adv. Mater.* **2004**, *16*, 115-119.
- 3) (a) Lovinger, A. J.; Rothberg, L. J. *J. Mater. Res.* **1996**, *11*, 1581-1592. (b) Horowitz, G. *J. Mater. Res.* **2004**, *19*, 1946-1962.
- 4) Roberson LB, Poggi MA, Kowalik J, Smestad GP, Bottomley LA, Tolbert LM, *Coord. Chem. Rev.* **2004**, *248*, 1491-1499.
- 5) (a) Dong, B.; Krutschke, M.; Zhang, X.; Chi, L. F.; Fuchs, H. *Small* **2005**, *1*, 520-524. (b) Li, G. F.; Martinez, C.; Semancik, S. *J. Am. Chem. Soc.* **2005**, *127*, 4903-4909
- 6) (a) Charest, J. L. Bryant, L. E. Garcia, A. J. King, W. P. *Biomaterials* **2004** *25*, 4767-4775. (b) Rowland, H. D.; King, W. P. *J. Micromechanics and Microengineering* **2004**, *14*, 1625-1632. (c) Nelson, B. A.; King, W. P.; Gall, K. *Appl. Phys. Lett.* **2005**, *86*, Art.103108.
- 7) (a) Samori, P.; Francke, V.; Müllen, K.; Rabe, J. P. *Chemistry Eur. J.* **1999**, *5*, 2312-2317. (b) Perahia D.; Traiphol, R.; Bunz, U. H. F. *Macromolecules* **2001**, *34*, 151-155.
- 8) (a) Dhirani, A. A.; Zehner, R. W.; Hsung, R. P.; Guyot-Sionnest, P.; Sita, L. R. *J. Am. Chem. Soc.* **1996**, *118*, 3319-3320. (b) Tour, J. M. *Acc. Chem. Res.* **2000**, *33*, 791-804.
- 9) Angelopoulos, M. *IBM Res. Dev.* **2001**, *45*, 57-75
- 10) (a) Huisgen, R.; Knorr, R.; Moebius, L.; Szeimies, G. *Chem. Ber.* **1965**, *98*, 4014-4019. (b) Huisgen R, Szeimies G, Moebius L, *Chem. Ber.* **1967**, *100*, 2494-2501,
- 11) Rostovtsev, V. V.; Green, L. G.; Fokin, V. V.; Sharpless K. B. *Angew. Chem.* **2002**, *41*, 2596-2599.

- 12) (a) Wooley, K. L.; Hawker, C. J. *Top. Curr. Chem.* **2005**, *245*, 287-305. (b) Helms, B.; Mynar, J. L.; Hawker, C. J.; Frechet, J. M. J. *J. Am. Chem. Soc.* **126**, 15020-15021, 2004 (c) Englert, B. C.; Bakbak, S.; Bunz, U. H. F, *Macromolecules* **2005**, *38*, 5868-5877. (d) Binder, W. H.; Kluger, C. *Macromolecules* **2004**, *37*, 9321-9330. (e) Scheel, A. J.; Komber, H.; Voit, B. I. *Macromol. Rapid Commun.* **2004**, *25*, 1175-1180. (f) Parrish B, Breitenkamp RB, Emrick T, *J. Am. Chem. Soc.* **2005**, *127*, 7404-7410. (g) Tsarevsky, N. V.; Sumerlin, B. S.; Matyjaszewski, K. *Macromolecules* **2005**, *38*, 3558-3561.

- 13) van Steenis, D. J. V. C.; David, O. R. P.; van Strijdonck, G. P. F.; van Maarseveen, J. H.; Reek, J. N. H. *Chem. Commun.* **2005**, 4333-4335.

- 14) Soloducho, J.; Roszak, S.; Chyla, A.; Tajchert, K., *New Journal of Chemistry* **2001**, 25(9), 1175-1181.

- 15) Itaya A.; Inoue T.; Yamamoto T.; Nobutou T.; Miyasaka H.; Toriumi M.; Ueno T., *Journal of Materials Chemistry*, **1996**, 6(5), 705-710.

- 16) Bräse, S.; Gil, C.; Knepper, K.; Zimmermann, V. *Angew. Chem.* **2005**, *44*, 5188-5240.

- 17) Bunz, U. H. F. *Chem. Rev.* **2000**, *100*, 1605-1644 and cited references.

- 18) (a) Liu Q.; Tor Y. *Org. Lett.* **2003**, *14*, 2571-2572. (b) Andersen J.; Madsen U.; Bjorkling F.; Liang X.F. *Synlett.* **2005**, 2209-2213.

- 19) Brase S.; Gil C.; Knepper K.; Zimmermann V. *Angew. Chem.* **2005**, *44*, 5188-5240.

- 20) (a) Piner R.D.; Zhu J.; Xu F.; Hong S. H., Mirkin C.A , *Science* **1999**, *283*, 661-663. (b) Lee K.B., Park S.J., Mirkin C.A., Smith J.C., Mrksich M., *Science* **2002**, *295*, 1702-1705. (c) Hong S.H., Zhu J., Mirkin C.A., *Science* **1999**, *286*, 523-525. (d) Hamley I.W., *Angew. Chem.* **2003**, *42*, 1692-1712.

- 21) Sheehan P.E., Whitman L.J., King W.P., Nelson B.A. *Appl. Phys. Lett.* **2004**, *85*, 1589-1591.

- 22) (a) Scherf U., *Top. Curr. Chem.* **1999**, *201*, 163-222. (b) Bunz U.H.F., *Chem. Rev.* **2000**, *100*, 1605-1644. (c) McCullough R.D., *Adv. Mater.* **1998**, *10*, 93. (d) Leclerc M., Faid K., *Adv. Mater.* **1997**, *19*, 1087-1094.

- 23) (a) Charrins S., Brettreich M., Wudl F., *Synthesis* 2002, 1191-1194. (b) Orita A., Haskegawa D., Nakano T., Otera J., *Chemistry Eur. J.* 2002, 8, 2000-2004.
- 24) Charrins S., Brettreich M., Wudl F., *Synthesis* 2002, 1191-1194.
- 25) (a) Godt A., *J. Org. Chem.* **1997**, 62, 7471-7474. (b) Francke V., Mangel T., Müllen K., *Macromolecules* 1998, 31, 2447-2453. (c) Xu C., Yamada H., Wakamiya A., Yamaguchi S., Tamao K., *Macromolecules* **2004**, 37, 8978-8983.
- 26) The experimental details for the determination of the quantum yields were obtained from: <http://www.jobinyvon.com/usadivisions/Fluorescence/applications/quantumyieldstrad.pdf>

CHAPTER 6

SOLID STATE POLYMERIZE THIOPHENES

AND THIO-DERIVATIVES

6.1 Introduction

Poly (ethylenedioxythiophene)s (PEDOT) are the most widely studied conjugated polymers because of their high conductivity for their use as hole injecting layers in light emitting diodes, solar cells and semiconductor device fabrications.¹

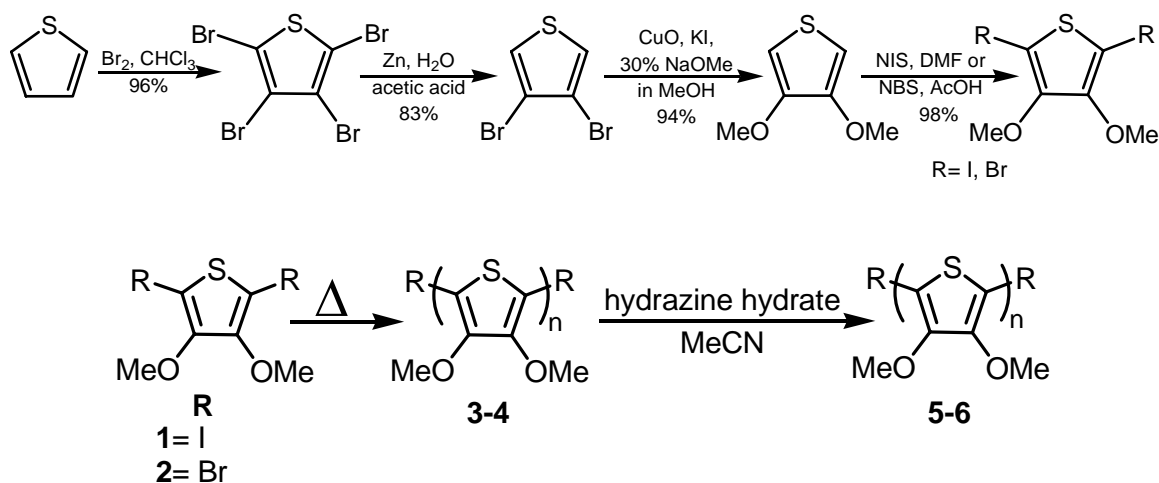
In general, perfect polymeric structure is only possible by single crystal polymerization.² Traditional PEDOT synthesis has limitations especially in molecular order. Compared to traditional polymerization methods (in presence of solvent and catalyst), solid state polymerization via single crystal or powder has great advantages because no further purification is necessary, and the formed polymer has a high degree of molecular order and often shows less defect.

Solid-state polymerization of the most widely studied conduction polymer, polythiophene was first reported by Wudl and coworkers.³ They demonstrated the solid state polymerization of 2,5-dibromo-3,4-ethylenedioxythiophene (DBEDOT). Since this initial discovery, more studies utilizing solid state synthesis have been reported.⁴ This new synthetic route could lead to inexpensive and facile device fabrication by incorporation of well-defined polymers.

Here, we are reporting a facile solid state synthesis of polydialchoxythiophene. This solvent and catalyst free polymerization of dihalo dialchoxythiophenes furnishes a doped conducting polymer. We explain the synthesis of a new polymer with diiodo and dibromo derivatives and give full characterization of polymers.

6.2 Results and Discussions:

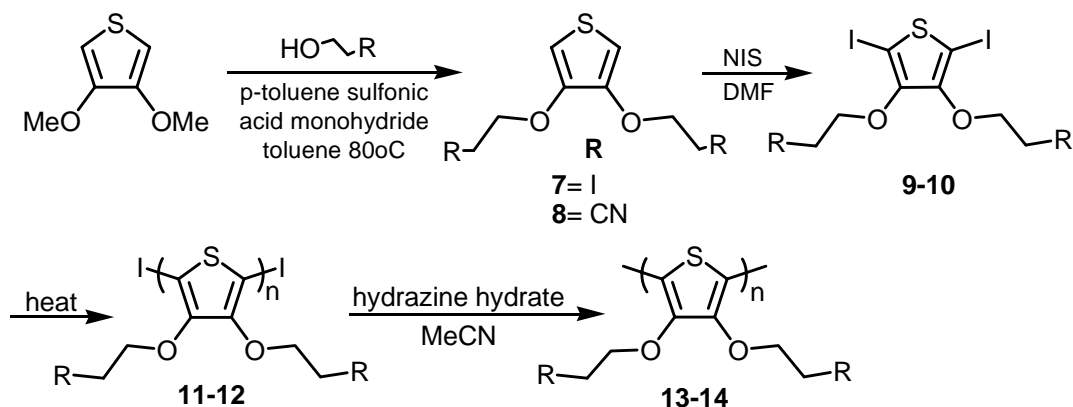
Synthesis of poly 2,5-dihalo-3,4-dimethoxythiophene is seen in Scheme 6.1. The monomer 4,5-dihalo-3,4-dimethoxythiophenes (**1-2**) were synthesized according to literature procedure.⁵ Monomer 4,5-diiodo-3,4-dimethoxythiophene **1** is very soluble in all common organic solvents and is stable in solution. The colorless powder monomer **1** was stored in the dark at room temperature, which then formed black film. This black material is very different from monomer and is no longer soluble in organic solvents. Following the same synthetic route, 5,5-dibromo-3,4-dimethoxythiophene **2** was also left in the dark at room temperature for several days to form **4**. Heating **2** to below its melting point also furnished polymer **4** in several days.



Scheme 6.1. Synthesis of solid state doped polymers **3-4** and natural **5-6**.

This phenomenon can be explained as the solid-state polymerization of thiophene. Wudl clarifies that this solid state reaction is autocatalytic and the strong oxidant, bromine/iodine are driving force for this type of polymerization.^{4b} Bromine or iodine were released during polymerization to form doped polymers. The exact mechanism of the polymerization has not been proved.

The doped polymers were dried under vacuum for several hours and then stirred in 50 % aqueous hydrazine hydrate in CH₃CN overnight, then filtered, washed with CH₃CN and dried under vacuum (Scheme 6.1). A dark brown-black color natural polymer was collected.



Scheme 6.2. Synthesis of Polymer 13 and 14.

We now know that not only DBEDOT but also 2,5-diiodo and 2,5-dibromo thiophenes goes in to solid state polymerization. Next we would like to extent aliphatic 3,4-substitution on thiophene to understand more of mechanism of this solid state polymerization. Synthesis of polymers **13** and **14** was outlined in Scheme 6.2. Compound **7** was synthesized from trans esterification reaction of dimethoxythiophene and 2-

oidoethanol in acidic reaction condition. Then **7** was iodinated at 2,5- position with using N-iodosuccinimide (NIS) to furnish **9** in clean reaction. Monomer **9** was left at ambient temperature for several days to form black in soluble doped polymer **11** and polymer **11** was treated with hydrazine hydrate in CH₃CN overnight to obtain dark brown natural polymer **13** as seen in Figure 6.1. Polymer **14** was synthesized by following the same synthetic route.

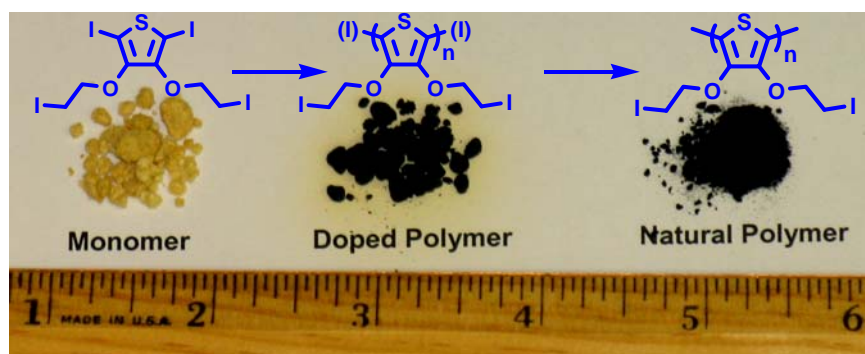
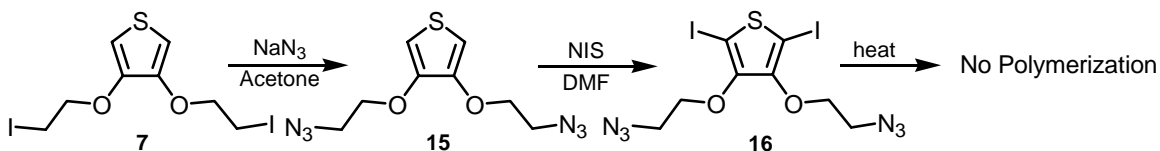


Figure 6.1 . Pictures of monomer **9** (left), polymer **11** (middle) and **12** (right).

7 was refluxed with sodium azide in acetone to give azide substitute derivative **15**. Iodination of **15** with NIS furnishes compound **16**. Monomer **16** was left at ambient temperature and heated to below melting point however no polymerization was observed. (Scheme 6.3)



Scheme 6.3. Synthetic route of azide polymer.

Polymerizations were not affected by air, vacuum or light. Solid-state ^{13}C NMR, FT-IR and powder XRD techniques were used to confirm the structure of the polymers. Due to the lack of solubility of these polymers GPC measurements can not be performed.

Compounds **1-2** were characterized by NMR, FT-IR, and melting point. Single crystal data was obtained from compound **1** by slow evaporation of hexane solution. The crystal structure of monomer **1** and its matrix is seen in Figure 6.2. This crystal data could reveal information to explain how this solid state polymerization occurs. The distances between iodines (I—I distance) was measured in the crystal structure as I1---I1: 3.812 Å (x2), 4.415 Å (x2) and I1---I2: 4.249 Å, 4.295 Å (Van der Waals radius of I = 1.98 Å), which is not shorter than Van der Waals distance but iodine are very close to each other and in the matrix they are in the plane and on the top of each other.

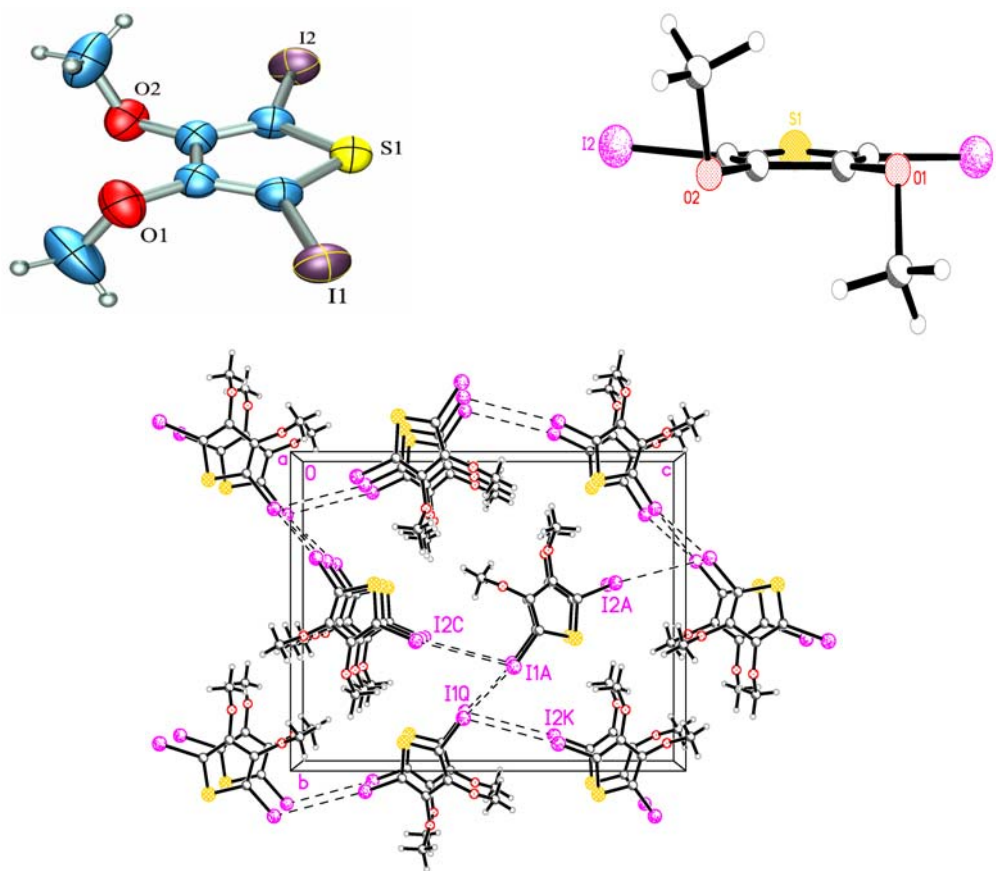


Figure 6.2. Crystal structure of monomer **1**.

Powder XRD data of monomer **1** and polymer **3** are very different from each other. Powder of monomer **1** shows very crystalline property. In case of polymer **3**, broad spectrum reveals that material is no longer crystalline. (Figure 6.3) FTIR spectra of monomer **1**, doped **3** and natural **5** polymers were shown in Figure 6.4. Vibration of C2 and C5 give peaks at 900 cm^{-1} and 1000 cm^{-1} in the monomer spectra. These peaks disappear in the polymers **3** and **5** which indicate polymerization occur at 2 and 5 positions of thiophenes.

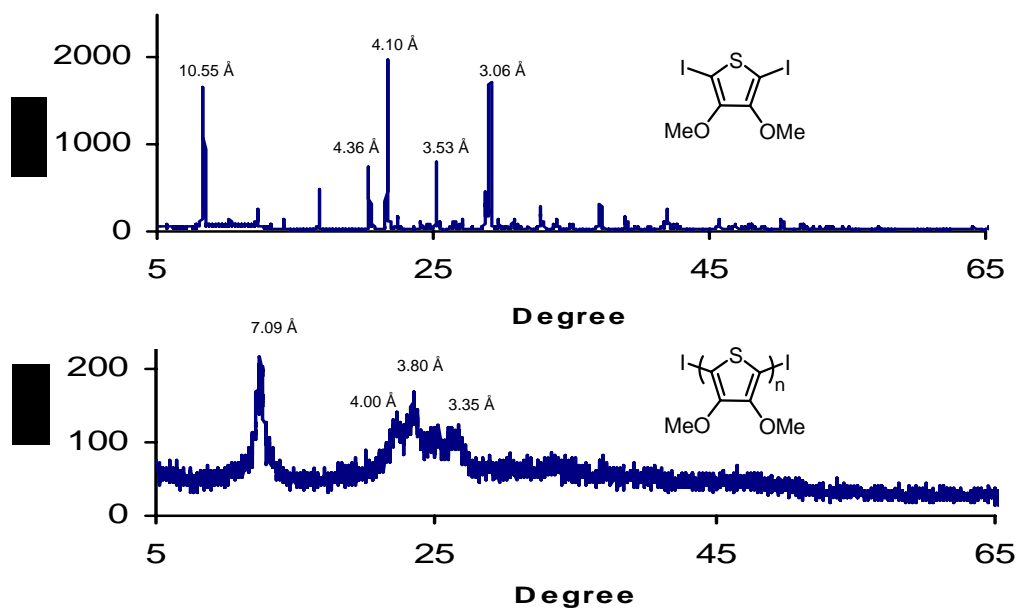


Figure 6.3. XRD data of monomer **1** and polymer **3**.

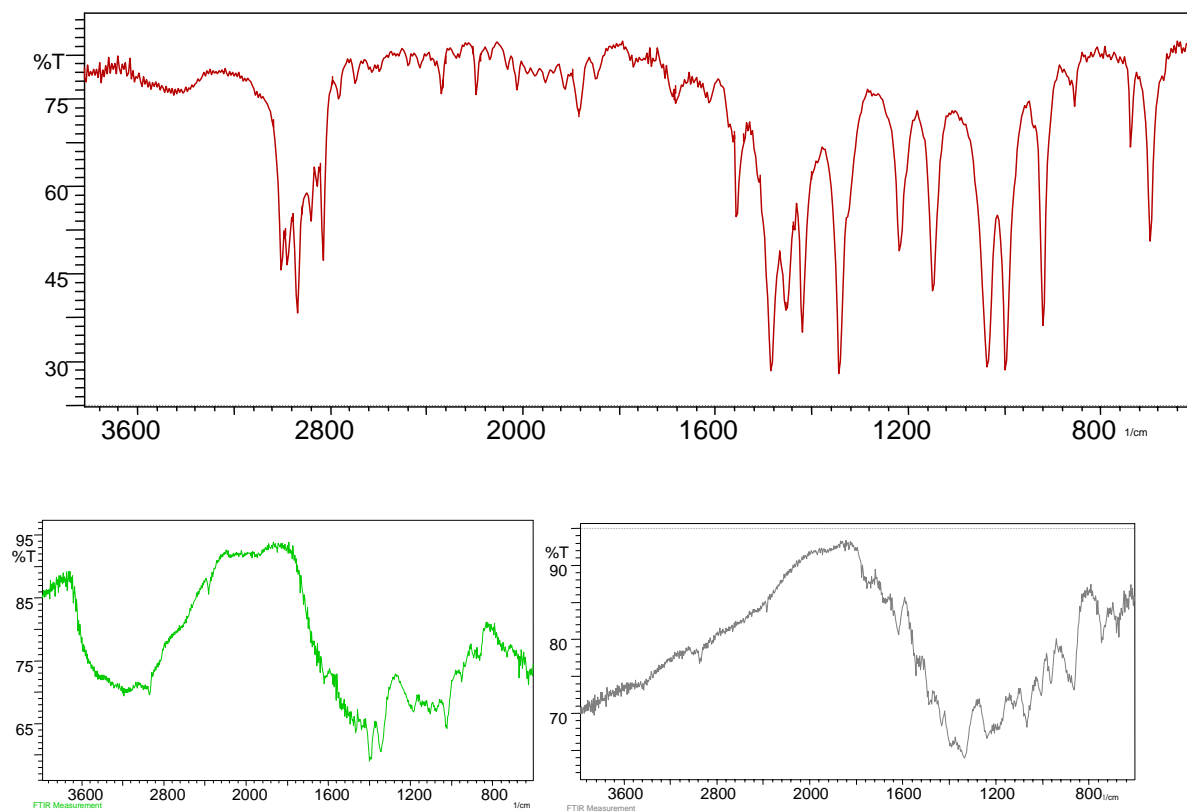


Figure 6.4. IR data of monomer **1** (top), polymer **3** (middle) and **5** (bottom).

Solid state ^{13}C NMR spectroscopy was studied to understand the structure of polymers. Since bromine or iodine was present in the doped polymer, strong magnetic broadening was seen in ^{13}C NMR spectroscopy (Figure 6.5-6.6). In natural polymer better resolution was observed. For both natural and doped polymer aliphatic carbon peaks do not shift during polymerization. Only big shifts was seen for 2,5-C atoms after polymerization.

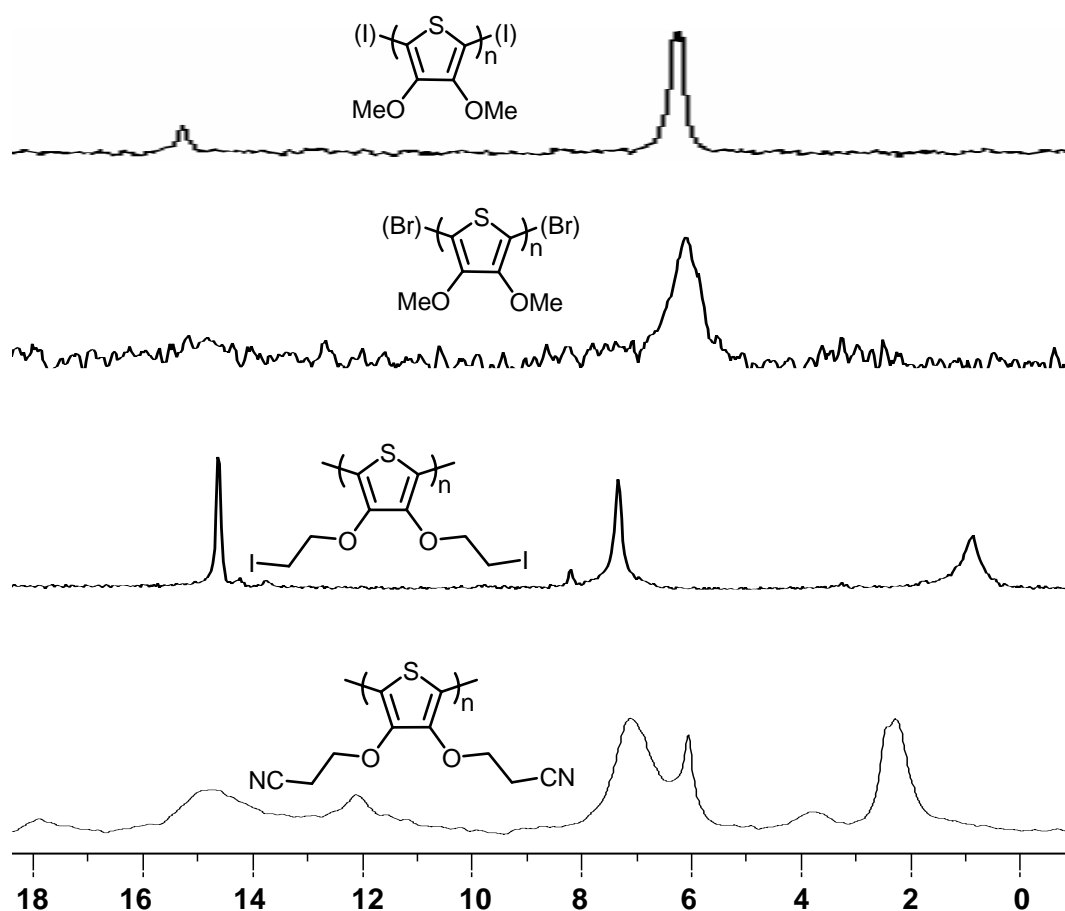


Figure 6.5. Solid state ^{13}C NMR data of doped polymer 3, 4, 11 and 12.

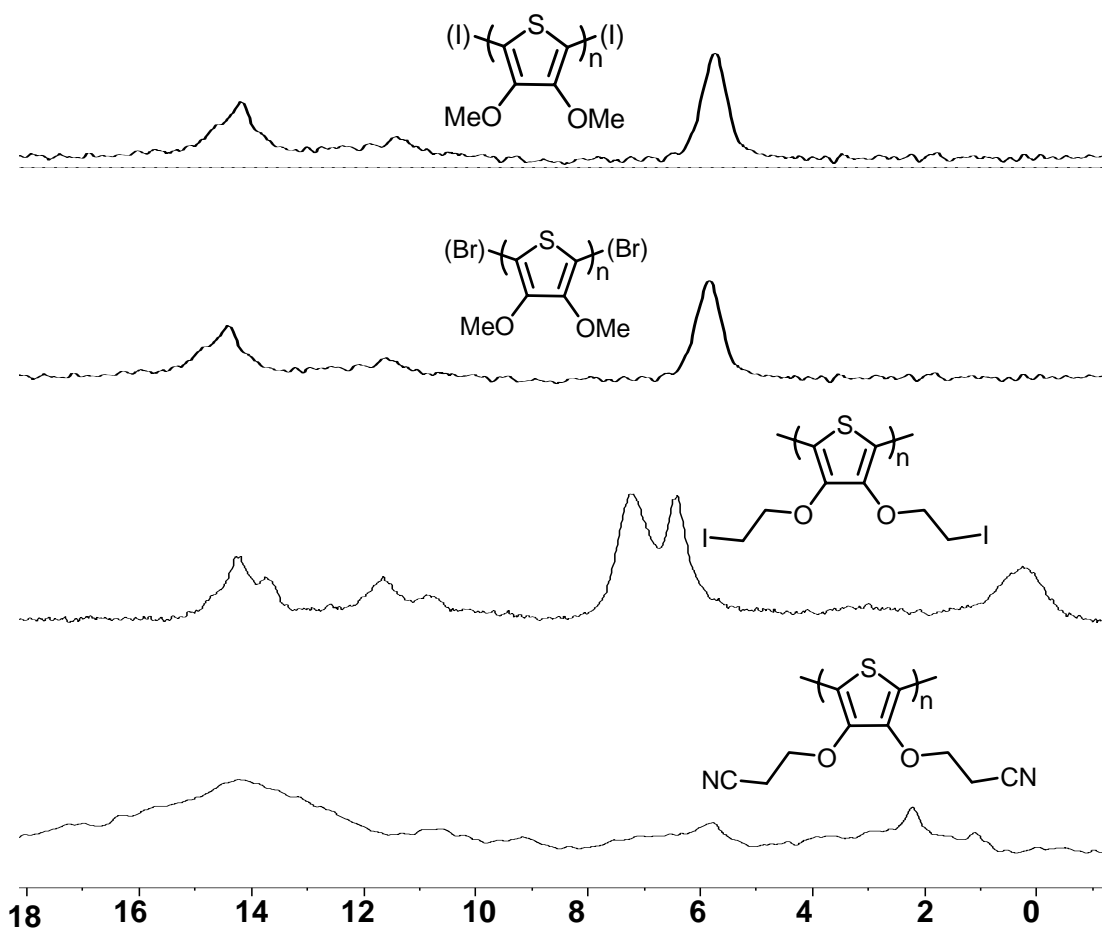


Figure 6.6. Solid state ^{13}C NMR data of natural polymer **5**, **6**, **13** and **14**.

6.3 Conclusion

In conclusion, we have shown that solid-state polymerization of thiophene is not true only for PEDOT derivatives; it is also true for many dihalothiophenes. These new examples of conjugated polymers have been fully characterized by solid-state ^{13}C NMR, FT-IR and XRD. The highly ordered polymers will have impact on device technology.

6.4 Experimental

Instrumentation. The ^1H and ^{13}C NMR spectra were taken with a Varian 300 MHz spectrometer using broadband probe. The ^1H chemical shifts are referenced to the residual proton peaks of CDCl_3 at δ 7.24(vs. TMS). The ^{13}C resonance is referenced to the central peak of CDCl_3 at δ 77.0 (vs. TMS). UV-VIS measurements were made with a Shimadzu UV-2401PC recording spectrophotometer. IR data were collected by a Shimadzu FTIR-8400S infrared spectrophotometer. Compound **1-2** were prepared according to literature procedure.⁵

General Experimental 1; 3,4-Dimethoxythiophene Substitution: In a Schlenk flask 3,4-dimethoxythiophene p-toluenesulfonic acid, and aliphatic alcohol were dissolved in toluene. The mixture was stirred under a flow of nitrogen for 48 h. After the reaction mixture was cooled down to RT, ether was added and organic layer was washed with water. The organic layer was dried over MgSO_4 , filtered and evaporated. The crude product was purified by flash column chromatography or by crystallization.

General Experimental 2; Iodination of 3,4-dialchoxythiophene: In a round bottom flask a solution of 3,4-dialchoxyl-thiophene in DMF stirred in the dark at room temperature. N-iodosuccinimide was added to a solution as portion wise in 2 h. and the mixture was stirred at RT for 48 h. The mixture was extracted with water and diethyl ether. The combined organics were dried over MgSO_4 , filtered, and solvent was removed to give pure product.

General Experimental 3; Solid State Polymerization of Thiophenes: Thiophene monomers were sat at room temperature or heated below their melting points for several days to form black solid. These polymers were no longer soluble in organic solvents.

General Experimental 4; Dedoping Thiophene Polymers: Polymeric material was grounded to fine particles and dried. Material was stirred in 50 % aqueous hydrazine hydrate solution in MeCN overnight at RT, then filtered and washed with MeCN and dried. A dark brown-black color dedoped polymers were formed.

3,4-Bis-(2-iodo-ethoxy)-thiophene 7: Following the general experimental 1 outlined above 3,4-dimethoxythiophene (500.0 mg, 3.46 mmol), p-toluenesulfonic acid (67 mg, 0.56 mmol) and 2-iodoethanol (1.30 g, 7.62 mmol) were reacted. The crude product was purified by flash column chromatography by using CH₂Cl₂ as solvent to give product as colorless solid (91%). IR: ν 3099, 3022, 2933, 2851, 2378, 1986, 1715, 1566, 1498, 1473, 1415.65, 1377, 1362, 1263, 1198, 1175, 1148, 1070, 1005, 986, 946, 889, 876, 831, 750, 663. ¹H NMR (CDCl₃): δ 6.28 (s, 1H), 4.27 (t, 4H), 3.44 (t, 4H). ¹³C NMR (CDCl₃): δ 146.14, 99.74, 71.34, 1.03. Mp. 86-87 °C.

2,5-Diiodo-3,4-bis(2-iodo-ethoxy)-thiophene 9: Following the general experimental 2 outlined above 3,4-bis-(2-iodo-ethoxy)-thiophene 7 (2.00 g 4.72 mmol) and N-iodosuccinimide (2.34 g 10.4 mmol) were reacted to give pure colorless solid (86%). IR: ν 3022, 2966, 2947, 2879, 1722, 1668, 1541, 1470, 1425, 1337, 1167, 1140, 1041, 1014, 983, 910, 750, 704, 625. ¹H NMR (CDCl₃): δ 4.29 (t, 4H), 3.41 (t, 4H). ¹³C NMR (CDCl₃): δ 150.1, 74.3, 65.3, 1.60. Mp. 98 °C.

3,4-Bis-(2-cyano-ethoxy)-thiophene 8: Following the general experimental 1 outlined above 3,4-dimethoxythiophene (3.00 g, 20.78 mmol), p-toluenesulfonic acid (500 mg,

4.17 mmol) and 3-hydroxypropionitrile (4.43 g, 62.36 mmol) were reacted. The crude product was purified by crystallization in ethanol to give product as colorless solid (84%). IR: ν 3121, 2959, 2642, 2403, 2251, 1944, 1738, 1566, 1495, 1462, 1373, 1259, 1211, 1153, 1038, 912, 849, 775. ^1H NMR (CDCl_3): δ 6.35 (s, 2H), 4.22 (t, 4H), 2.85 (t, 4H). ^{13}C NMR (CDCl_3): δ 146.1, 117.2, 100.8, 65.4, 18.8. Mp. 120-121 °C.

2,5-Diiodo-3,4-bis-(2-cyano-ethoxy)-thiophene 10: Following the general experimental 2 outlined above 3,4-bis-(2-cyano-ethoxy)-thiophene **8** (1.60 g, 7.20 mmol) and N-iodosuccinimide (4.05 g, 18.00 mmol) were reacted to give pure colorless solid (96%). IR: ν 3441, 2962, 2253, 1738, 1547, 1475, 1466, 1412, 1383, 0152, 1219, 1165, 1076, 1043, 1026, 833, 712. ^1H NMR (CDCl_3): δ 4.24 (t, 4H), 2.83 (t, 4H). ^{13}C NMR (CDCl_3): δ 150.3, 117.6, 68.6, 65.7, 19.4. Mp. 142-144 °C.

3,4-Bis(2-azido-ethoxy)-thiophene 15: In a 250ml round bottom flask 3,4-bis-(2-iodo-ethoxy)-thiophene **7** (2.00 g, 4.72 mmol) and NaN_3 (1.23 g, 18.88 mmol) was refluxed in acetone for 5 days. The mixture was cooled down and solvent was removed. Mixture was dissolved in 50 mL of CH_2Cl_2 and washed with 3x100 mL water. The organic layer was dried over MgSO_4 , filtered and evaporated to give product as colorless solid (93%). IR: ν 3111, 2962, 2509, 2104, 1944, 1564, 1497, 1373, 1257, 1200, 1051, 1024, 862, 793, 702. ^1H NMR (CDCl_3): δ 6.25 (s, 2H), 4.10 (t, 4H), 3.54 (t, 4H). ^{13}C NMR (CDCl_3): 146.8, 99.1, 69.5, 50.3. Mp. 44-45 °C.

3,4-Bis(2-azido-ethoxy)-2,5-diiodo-thiophene 16: Following the general experimental 2 outlined above 3,4-bis-(2-azido-ethoxy)-thiophene **15** (1.50 g, 5.90 mmol) and N-iodosuccinimide (3.32 g, 14.8 mmol) were reacted to give pure colorless solid (87%). IR: ν 3329, 3111, 2935, 2870, 2525, 2096, 1564, 1495, 1456, 1373, 1346, 1299, 1202, 1153, 1051, 929, 856, 754. ^1H NMR (CDCl_3): δ 3.61 (t, 4H), 4.17 (t, 4H). ^{13}C NMR (CDCl_3): δ 150.8, 72.6, 64.9, 51.1. Mp. 50 °C.

6.5 References

1. a) Groenendaal, L. B.; Jonas, F.; Freitag, D.; Pielartzik, H.; Reynolds, J. R. *Adv. Mater.* **2000**, *12*, 481. b) Jonas, F.; Schrader, L. *Synth. Met.* **1991**, *41-43*, 831. c) Groenendaal, L. B.; Zotti, G.; Aubert, P.-H.; Waybright, S. M.; Reynolds, J. R. *Adv. Mater.* **2003**, *115*, 855.
2. a) Baughman, R. H.; *J. Polym. Sci. Polym. Phys. Ed.* **1974**, *12*, 1511. b) Enkelman, V.; Schleier, G.; Wegner, G. *Phys. Letter* **1977**, *52*, 314.
3. Meng H.; Perepichka D. F.; Wudl F. *Angew. Chem. Int. Ed.* **2003**, *42*, 658-661.
4. a) Spencer H. J.; Berridge R.; Crouch D. J.; Wright S. P.; Giles M.; McCulloch I.; Coles S. J.; Hursthouse M. B.; Skabare P. J.; *J. Mater. Chem.* **2003**, *13*, 2075-2077. b) Meng H.; Perepichka D. F.; Bendikov M.; Wudl F. *J. Am. Chem. Soc.* **2003**, *125*, 15151-15162.
5. Goldoni F., *Thiophene-Based pi-Conjugated Polymers* ISBN.90-386-2891-9.

CHAPTER 7

CONCLUSION

Conjugated polymers are a novel class of semiconductors which has the properties of semiconductors with the processing advantages of polymers. Conjugated polymers have many different applications in the area of light-emitting diodes, thin film transistors, photovoltaic cells, sensors, plastic lasers, and nonlinear optical systems.

Our research is intended towards the design, synthesis and exploration of well-defined conjugated polymers and attempts to provide an answer to the question of how to synthesize better polymeric materials with optimized optic and electronic characteristics. Employing conjugated polymers as our central attention, we have extensively explored the preparation and processing of such materials. Their synthetic adaptability to a broad range of functional groups inspired us to make new classes of conjugates and conjugated polymers. The synthesis of various interesting conjugated polymers and their optical properties were explained along with their future applications in device fabrication.

A series of new novel alkyne bridged trispyrazolylmethane ligands were synthesized and their crystallographic properties were investigated. Sonogashira coupling reactions were used to prepare phenylalkynyl based compounds while oxidative Glaser homocoupling reactions have been used to prepare butadiynyl based compounds. The main architectural feature of the new linked ligands is their overall rigid linear geometry, but with semi-rigid ending groups. The flexibility of these ending groups is

important to future chemistry as they provide solubility and structural adaptivity to metal complexes. This chemistry opens the door for the further exploration into incorporating methyl-substituted pyrazolyls or even other metal systems with the purpose of putting electro- and/or photoactive centers into highly organized coordination network solids.

The post-polymerization functionalization of conjugated polymers is a useful technique in which a specific polymer backbone is post-synthetically altered. These approaches allow introduction of molecular diversity late, in the final step, of the synthetic sequence and are therefore highly efficient compared to the introduction of functional elements during the synthesis of specific monomers. Additionally, post-functionalization schemes allow the introduction of groups that might not be compatible with the polymerization conditions. Fast assembly of libraries of polymers and introduction of different and potentially sensitive functional groups are some of the advantages of post polymerization functionalization.

Click chemistry provided a means to completely functionalize PPEs via a postmodification strategy. While all of these triazole-functionalized polymers aggregate, their absorption spectra are quite insensitive to the aggregation process, which suggests that triazole-functionalized PPEs may find attractive applications in biological sensing schemes.

By click chemistry aromatic diazides and aromatic diynes are coupled to produce a library of 1,2,3-triazoles and new class of conjugated polymers, poly(arylenetriazoline)s. Click chemistry was used as a tool to functionalize and structure surfaces to form organic semiconductors. Nanostructures in soft materials are generated from mixed diazide/dialkyne on thin films with the use of heated atomic force microscope (AFM)

cantilever tips. This technique allows the reversible or irreversible writing of nanostructures in thin films.

Almost any area of high tech materials profits from the generation of nanostructures. This powerful strategy should generate a significant impact in the chemistry and physics of conjugated polymers.

The last part of my research was accidental discovery of solid state polymerize thiophenes. Many different dihalothiophenes are used in solid state polymerization route. Due to their conductivity, these highly ordered, solvent and catalyst free polythiophenes can be used in inexpensive and facile device fabrication. Solid state polymerization via single crystal or powder has great advantages because no further purification is necessary, and the formed polymer has a high degree of molecular order and often shows less defects.

APPENDIX

CRYSTALLOGRAPHIC DATA

Crystallography Data for Chapter 2

A colorless chunk sectioned from a larger crystal of $\text{HC}_2\text{CH}_2\text{OCH}_2\text{C}(\text{pz})_3$ (**2.2**), an irregular colorless block sectioned from a larger crystalline mass of **2.4**, a colorless plate of **2.7**, and a purple plate of **2.9** were each mounted onto the end of thin glass fibers using inert oil. X-ray intensity data covering the full sphere of reciprocal space were measured at 150(1) K (**2.2**, **2.4**, **2.7**) or 100(1) K (**10**) on a Bruker SMART APEX CCD-based diffractometer (Mo $K\alpha$ radiation, $\lambda = 0.71073 \text{ \AA}$).¹ The raw data frames were integrated with SAINT+,¹ which also applied corrections for Lorentz and polarization effects. The final unit cell parameters for **2.2**, **2.4**, **2.7**, and **2.10** are based on the least-squares refinement of 4515, 5607, 6918, and 9926 reflections, respectively, each with $I > 5(\sigma)I$ from the appropriate data set. Analyses of the data showed negligible crystal decay during data collection. Structures were solved by a combination of either direct methods for **2.2**, **2.7**, and **2.9** or Patterson methods² for **2.4**, and subsequent difference Fourier syntheses, and refined by full-matrix least-squares against F , using SHELXTL.³ Except where noted in the refinement of **2.9**, all non-hydrogen atoms were refined with anisotropic displacement parameters while hydrogen atoms were placed in geometrically idealized positions and included as riding atoms. Crystallographic data are collected in Table 2.1 and further details of the structure solutions and refinement are noted for each

below.

Summary of Crystallographic Data for **2.2**, **2.4**, **7** and **2.10**.

	2.2	2.4	2.7	2.10
Empirical formula	C ₁₄ H ₁₄ N ₆ O	C ₃₀ H ₂₉ IN ₁₂ O ₂	C ₆₂ H ₅₈ N ₂₄ O ₄	C ₆₂ H ₆₀ B ₂ Cl ₈ FeN ₂₄ O ₂
Formula weight	282.31	716.55	1203.32	1534.41
Temperature (K)	150(1)	150.0(2)	150.0(2)	100(1) K
Crystal system	Monoclinic	Triclinic	Monoclinic	Triclinic
Space group	Cc	P-1	P2 ₁ /c	P-1
Unit cell dimensions				
<i>a</i> , Å	13.2954(8)	8.7819(6)	8.1473(5)	8.5941(4)
<i>b</i> , Å	12.4529(8)	12.1248(8)	34.148(2)	13.4373(7)
<i>c</i> , Å	8.5445(5)	15.3073(10)	11.3257(7)	16.3188(8)
α , deg	90	96.8400(10)	90	103.9530(10)
β , deg	97.9170(10)	99.5630(10)	109.1850(10)	98.3300(10)
γ , deg	90	105.9950(10)	90	106.9990(10)
<i>V</i> , Å ³	1401.20(15)	1521.48(18)	2976.0(3)	1701.26(15)
<i>Z</i>	4	2	2	1
ρ (calcd.) Mg m ⁻³	1.338	1.564	1.343	1.498
Abs. Coeff., mm ⁻¹	0.091	1.103	0.091	0.600
Final <i>R</i> indices [<i>I</i> > 2 σ (<i>I</i>)]				
R1	0.0294	0.0318	0.0639	0.0728
wR2	0.0625	0.0796	0.1656	0.2133
<i>R</i> indices (all data)				
R1	0.0314	0.0340	0.0815	0.0816
wR2	0.0630	0.0812	0.1752	0.2232

Systematic absences in the intensity data of **2.2** were consistent with the space groups C2/c and Cc; intensity statistics indicated acentricity. The space group Cc was verified by examination of the structure and checked with ADDSYM / PLATON.⁴ Due to the

lack of heavy atoms in the structure, Friedel opposites were merged during data processing and the absolute structure was not determined.

Compound **2.4** crystallizes in the triclinic crystal system. The space group P-1 was assumed and confirmed by the successful solution and refinement of the structure.

Systematic absences in the intensity data from **2.7** determined the space group $P2_1/c$. The molecule resides on a crystallographic inversion center. One of the pyrazolyl rings (N21-C23) is rotationally disordered about the N-C_{methine} bond in equal proportions.

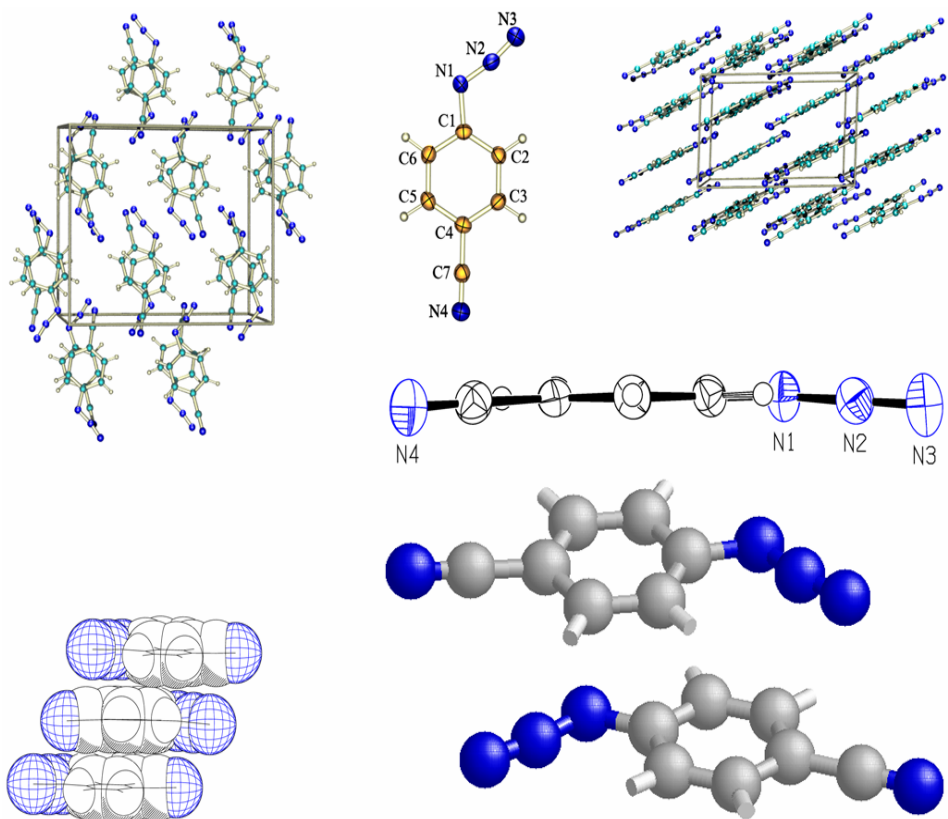
Compound **2.10** crystallizes in the triclinic system. The space group P-1 was assumed and eventually confirmed. Half of the iron cation is located on an inversion center and two CH₂Cl₂ molecules of crystallization could be identified in the asymmetric unit. One CH₂Cl₂ is disordered over several orientations and was accounted for with the SQUEEZE program after several unsuccessful attempts at modeling the disorder. (61 electrons and 208.5 Å³ solvent-accessible volume per unit cell). The contribution of the disordered solvent was subtracted from the structure factors but was included in the final formula weight and calculated density. During the refinement a large residual electron density peak (2.88 e⁻/Å³) persistently appeared near the midpoint of the C77-C78 triple bond, ca. 0.7 Å from each atom. The origin of this peak is unknown, but is responsible for the anisotropy of the displacement ellipsoids of atoms C77 and C78 as well as an unreasonably short (~1Å) C-C bond. To correct for this, the atomic parameters for C77 and C78 were fixed at reasonable U_{ij} values and a C-C bond length of 1.15 Å. This peak as well as the disorder in the crystal is the reason for the low quality of this refinement and the high final residuals.

Crystallographic information for 3.2

Identification code	3.2	
Empirical formula	C ₈ H ₉ N ₃ O ₂	
Formula weight	179.18	
Crystal system	Monoclinic	
Space group	2 ₁ /c	
Crystal color, habit	colorless plate	
Unit cell dimensions	a = 13.0025(15) Å	α = 90°.
	b = 9.5026(11) Å	β = 94.778(2)°.
	c = 13.7953(16) Å	γ = 90°.
Volume	1698.6(3) Å ³	
Z	8	
Density (calculated)	1.401 Mg/m ³	
Absorption coefficient	0.104 mm ⁻¹	
F(000)	752	
Crystal size	0.36 x 0.22 x 0.08 mm ³	
Theta range for data collection	1.57 to 25.03°.	
Index ranges	-15 ≤ h ≤ 15, -10 ≤ k ≤ 11, -16 ≤ l ≤ 16	
Reflections collected	14003	
Independent reflections	3000 [R(int) = 0.0582]	
Completeness to theta = 25.03°	100.0 %	
Absorption correction	None	
Refinement method	Full-matrix least-squares on F ²	
Data / restraints / parameters	3000 / 45 / 253	
Goodness-of-fit on F ²	1.030	
Final R indices [I > 2σ(I)]	R ₁ = 0.0525, wR ₂ = 0.1225	
R indices (all data)	R ₁ = 0.0656, wR ₂ = 0.1300	
Largest diff. peak and hole	0.329 and -0.456 e.Å ⁻³	

Crystallographic Information for 3.3

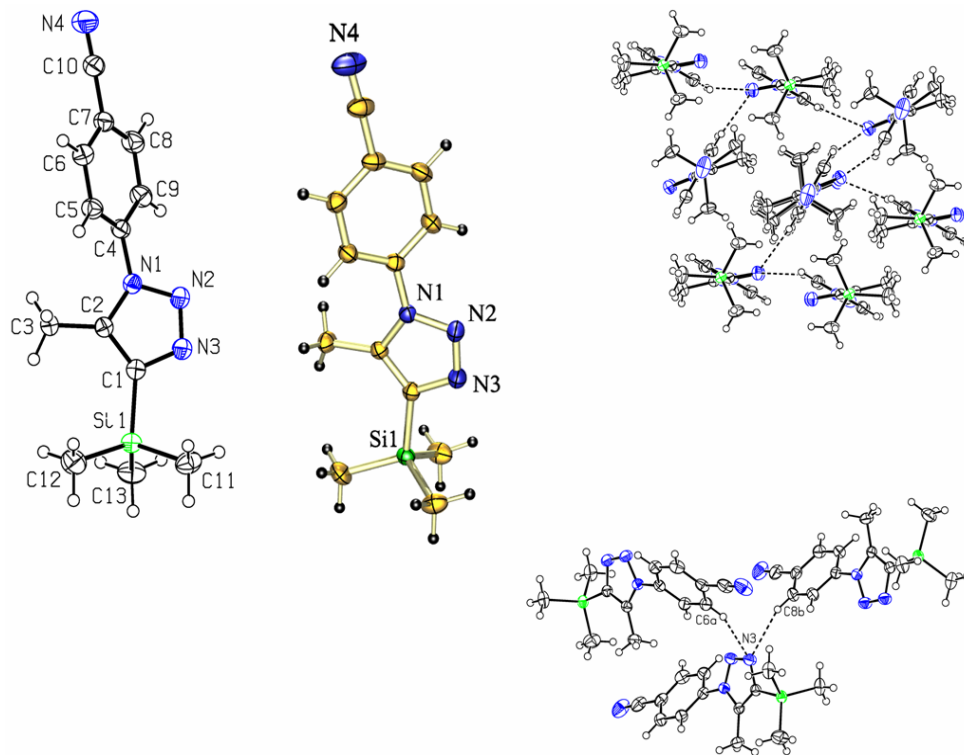
X-Ray Structure Determination, 3.3



Identification code	3.3	
Empirical formula	C7 H4 N4	
Formula weight	144.14	
Temperature	150(2) K	
Wavelength	0.71073 Å	
Crystal system	Monoclinic	
Space group	C2/c	
Unit cell dimensions	a = 7.6716(7) Å	$\alpha = 90^\circ$.
	b = 14.8121(13) Å	$\beta = 92.753(2)^\circ$.
	c = 12.2933(11) Å	$\gamma = 90^\circ$.
Volume	1395.3(2) Å ³	
Z	8	
Density (calculated)	1.372 Mg/m ³	
Absorption coefficient	0.093 mm ⁻¹	
F(000)	592	
Crystal size	0.36 x 0.16 x 0.04 mm ³	
Theta range for data collection	2.75 to 25.02°.	
Index ranges	-9 ≤ h ≤ 9, -17 ≤ k ≤ 17, -14 ≤ l ≤ 14	
Reflections collected	5047	
Independent reflections	1234 [R(int) = 0.0562]	
Completeness to theta = 25.02°	99.9 %	
Absorption correction	None	
Refinement method	Full-matrix least-squares on F ²	
Data / restraints / parameters	1234 / 0 / 116	
Goodness-of-fit on F ²	0.952	
Final R indices [I > 2sigma(I)]	R1 = 0.0387, wR2 = 0.0736	
R indices (all data)	R1 = 0.0572, wR2 = 0.0783	
Largest diff. peak and hole	0.136 and -0.179 e.Å ⁻³	

Crystallographic information for 3.24

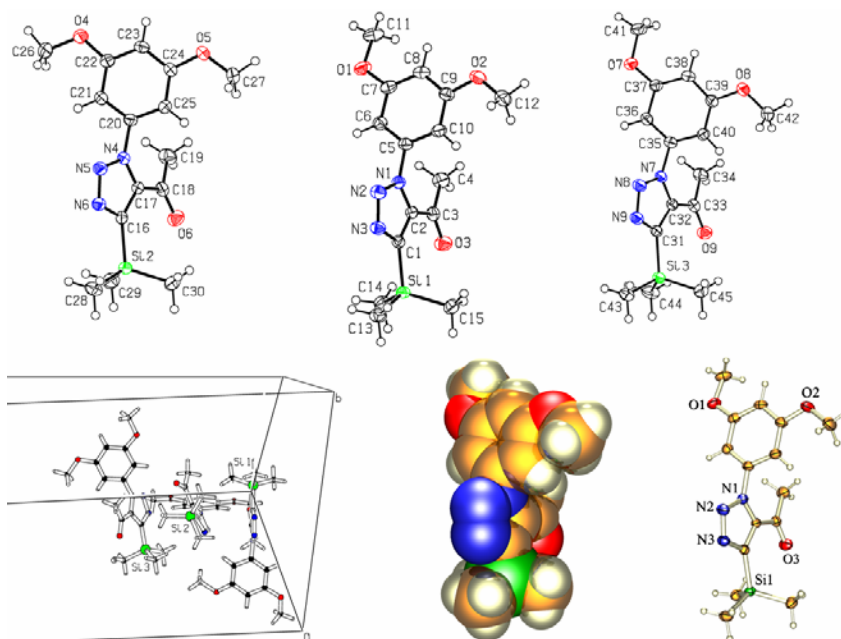
X-Ray Structure Determination, C₁₃H₁₆N₄Si (3.24)



Identification code	3.24	
Empirical formula	C13 H16 N4 Si	
Formula weight	256.39	
Temperature	150(1) K	
Wavelength	0.71073 Å	
Crystal system	Orthorhombic	
Space group	P2 ₁ 2 ₁ 2 ₁	
Unit cell dimensions	a = 9.9546(6) Å	α = 90°.
	b = 14.5997(9) Å	β = 90°.
	c = 9.7103(6) Å	γ = 90°.
Volume	1411.24(15) Å ³	
Z	4	
Density (calculated)	1.207 Mg/m ³	
Absorption coefficient	0.155 mm ⁻¹	
F(000)	544	
Crystal size	0.46 x 0.40 x 0.28 mm ³	
Theta range for data collection	2.48 to 27.67°.	
Index ranges	-12 ≤ h ≤ 13, -19 ≤ k ≤ 17, -12 ≤ l ≤ 12	
Reflections collected	13990	
Independent reflections	1896 [R(int) = 0.0369]	
Completeness to theta = 27.67°	100.0 %	
Absorption correction	None	
Refinement method	Full-matrix least-squares on F ²	
Data / restraints / parameters	1896 / 0 / 167	
Goodness-of-fit on F ²	1.072	
Final R indices [I > 2σ(I)]	R1 = 0.0331, wR2 = 0.0869	
R indices (all data)	R1 = 0.0336, wR2 = 0.0873	
Absolute structure parameter	opposites merged	
Largest diff. peak and hole	0.203 and -0.310 e.Å ⁻³	

Crystallographic information for 3.18

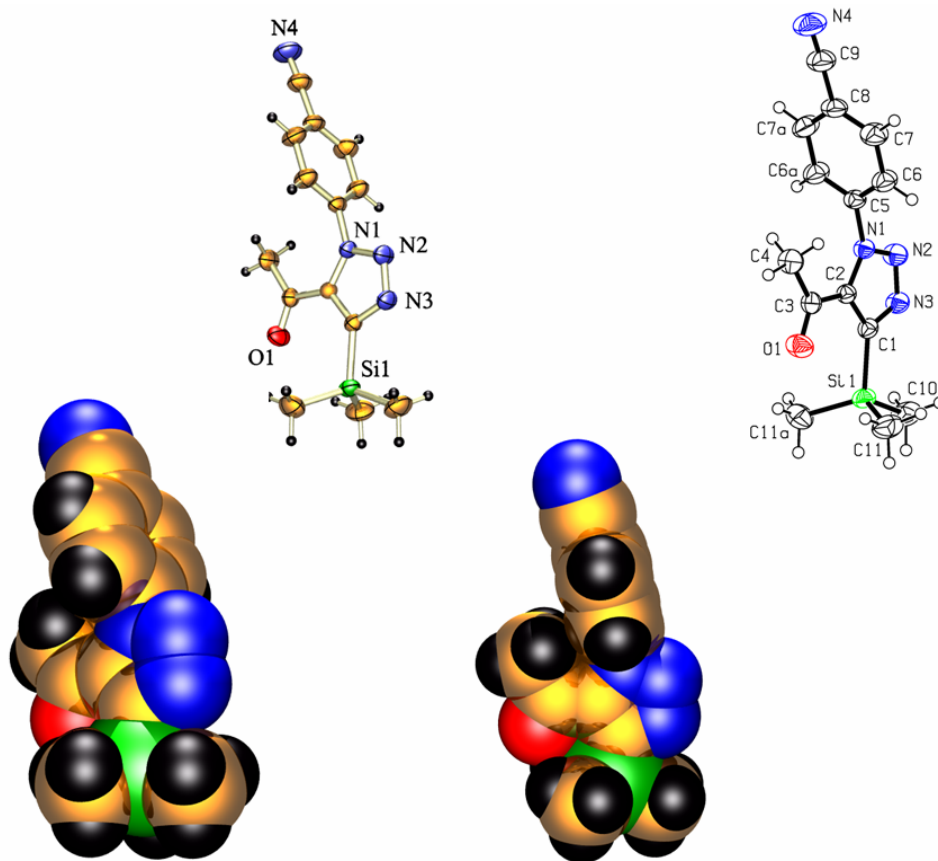
X-Ray Structure Determination, C₁₅H₂₁N₃O₃Si (3.18)



Identification code	3.18	
Empirical formula	C15 H21 N3 O3 Si	
Formula weight	319.44	
Temperature	150(1) K	
Wavelength	0.71073 Å	
Crystal system	Orthorhombic	
Space group	Pbca	
Unit cell dimensions	a = 17.8594(10) Å	$\alpha = 90^\circ$.
	b = 21.5853(12) Å	$\beta = 90^\circ$.
	c = 26.2129(15) Å	$\gamma = 90^\circ$.
Volume	10105.1(10) Å ³	
Z	24	
Density (calculated)	1.260 Mg/m ³	
Absorption coefficient	0.155 mm ⁻¹	
F(000)	4080	
Crystal size	0.48 x 0.42 x 0.22 mm ³	
Theta range for data collection	1.55 to 26.42°.	
Index ranges	-22 ≤ h ≤ 22, -27 ≤ k ≤ 26, -30 ≤ l ≤ 32	
Reflections collected	95261	
Independent reflections	10375 [R(int) = 0.0544]	
Completeness to theta = 26.42°	99.8 %	
Absorption correction	None	
Refinement method	Full-matrix least-squares on F ²	
Data / restraints / parameters	10375 / 0 / 613	
Goodness-of-fit on F ²	1.057	
Final R indices [I > 2sigma(I)]	R1 = 0.0401, wR2 = 0.1106	
R indices (all data)	R1 = 0.0490, wR2 = 0.1155	
Largest diff. peak and hole	0.452 and -0.273 e.Å ⁻³	

Crystallographic information for 3.25

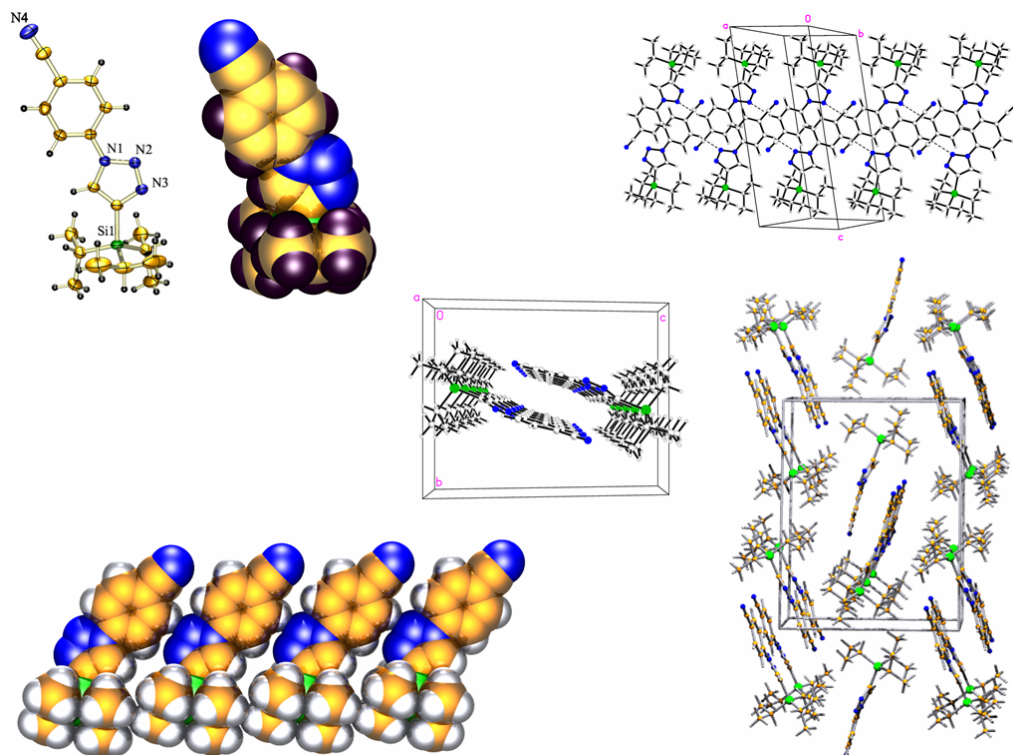
X-Ray Structure Determination, C₁₄H₁₆N₄OSi (3.25)



Identification code	3.25	
Empirical formula	C ₁₄ H ₁₆ N ₄ O Si	
Formula weight	284.40	
Temperature	150(2) K	
Wavelength	0.71073 Å	
Crystal system	Orthorhombic	
Space group	Pnma	
Unit cell dimensions	a = 16.1527(10) Å	α = 90°.
	b = 7.0332(4) Å	β = 90°.
	c = 13.7637(9) Å	γ = 90°.
Volume	1563.63(17) Å ³	
Z	4	
Density (calculated)	1.208 Mg/m ³	
Absorption coefficient	0.151 mm ⁻¹	
F(000)	600	
Crystal size	0.54 x 0.40 x 0.12 mm ³	
Theta range for data collection	1.94 to 25.02°.	
Index ranges	-19 ≤ h ≤ 19, -8 ≤ k ≤ 7, -16 ≤ l ≤ 16	
Reflections collected	12537	
Independent reflections	1509 [R(int) = 0.0761]	
Completeness to theta = 25.02°	100.0 %	
Absorption correction	None	
Refinement method	Full-matrix least-squares on F ²	
Data / restraints / parameters	1509 / 0 / 113	
Goodness-of-fit on F ²	1.165	
Final R indices [I > 2σ(I)]	R ₁ = 0.0501, wR ₂ = 0.1242	
R indices (all data)	R ₁ = 0.0534, wR ₂ = 0.1261	
Largest diff. peak and hole	0.284 and -0.316 e.Å ⁻³	

Crystallographic information for 3.23

X-Ray Structure Determination, $C_{18}H_{26}N_4Si$ (3.23)



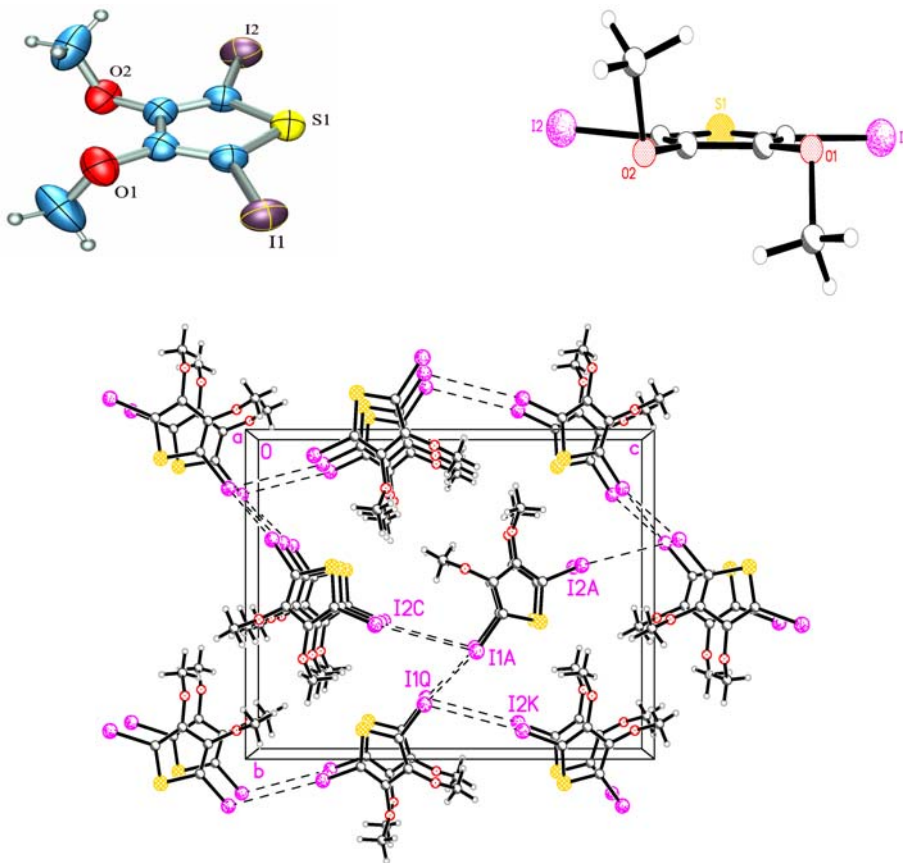
Identification code	3.23	
Empirical formula	C ₁₈ H ₂₆ N ₄ Si	
Formula weight	326.52	
Temperature	150(1) K	
Wavelength	0.71073 Å	
Crystal system	Orthorhombic	
Space group	P2 ₁ /n	
Unit cell dimensions	a = 7.4598(4) Å	α = 90°.
	b = 14.1758(7) Å	β = 99.7570(10)°.
	c = 18.1362(9) Å	γ = 90°.
Volume	1890.14(17) Å ³	
Z	4	
Density (calculated)	1.147 Mg/m ³	
Absorption coefficient	0.129 mm ⁻¹	
F(000)	704	
Crystal size	0.50 x 0.44 x 0.40 mm ³	
Theta range for data collection	1.83 to 25.05°.	
Index ranges	-8 ≤ h ≤ 8, -16 ≤ k ≤ 16, -21 ≤ l ≤ 21	
Reflections collected	13613	
Independent reflections	3334 [R(int) = 0.0421]	
Completeness to theta = 25.05°	100.0 %	
Absorption correction	None	
Refinement method	Full-matrix least-squares on F ²	
Data / restraints / parameters	3334 / 0 / 214	
Goodness-of-fit on F ²	1.055	
Final R indices [I > 2σ(I)]	R1 = 0.0532, wR2 = 0.1464	
R indices (all data)	R1 = 0.0601, wR2 = 0.1515	
Largest diff. peak and hole	0.541 and -0.273 e.Å ⁻³	

Crystallographic information for 6.1

X-Ray Structure Determination, C₆H₆I₂O₂S, (6.1)

A colorless needle was epoxied onto the end of a thin glass fiber. X-ray intensity data covering the full sphere of reciprocal space were measured at 293 K on a Bruker SMART APEX CCD-based diffractometer (Mo K α radiation, $\lambda = 0.71073$ Å).¹ The raw data frames were integrated and corrected for Lp effects with SAINT+.¹ The final unit cell parameters are based on the least-squares refinement of 5788 reflections from the data set with $I > 5\sigma(I)$. Analysis of the data showed negligible crystal decay during data collection. An empirical absorption correction based on the multiple measurement of equivalent reflections was applied with the program SADABS.⁵

Systematic absences in the intensity data were consistent with the space group $P2_12_12_1$. The structure was solved by a combination of direct methods and difference Fourier syntheses, and refined by full-matrix least-squares against F^2 (SHELXTL).⁵ Non-hydrogen atoms were refined with anisotropic displacement parameters; hydrogen atoms were idealized and included as riding atoms. After the final refinement cycle, the absolute structure (Flack) parameter was $-0.03(4)$, indicating the correct absolute structure and the absence of inversion twinning.



Identification code	6.1	
Empirical formula	C ₆ H ₆ I ₂ O ₂ S	
Formula weight	395.97	
Temperature	293(2) K	
Wavelength	0.71073 Å	
Crystal system	Orthorhombic	
Space group	P2 ₁ 2 ₁ 2 ₁	
Unit cell dimensions	a = 4.4145(3) Å	α = 90°.
	b = 13.4356(9) Å	β = 90°.
	c = 17.2262(11) Å	γ = 90°.
Volume	1021.71(12) Å ³	
Z	4	
Density (calculated)	2.574 Mg/m ³	
Absorption coefficient	6.315 mm ⁻¹	
F(000)	720	
Crystal size	0.36 x 0.08 x 0.04 mm ³	
Theta range for data collection	1.92 to 26.38°.	
Index ranges	-5 ≤ h ≤ 5, -16 ≤ k ≤ 16, -21 ≤ l ≤ 21	
Reflections collected	9223	
Independent reflections	2098 [R(int) = 0.0317]	
Completeness to theta = 26.38°	100.0 %	
Absorption correction	Semi-empirical from equivalents	
Max. and min. transmission	1.0000 and 0.5946	
Refinement method	Full-matrix least-squares on F ²	
Data / restraints / parameters	2098 / 0 / 102	
Goodness-of-fit on F ²	1.039	
Final R indices [I > 2σ(I)]	R1 = 0.0264, wR2 = 0.0596	
R indices (all data)	R1 = 0.0285, wR2 = 0.0605	
Absolute structure parameter	-0.03(4)	
Largest diff. peak and hole	0.623 and -0.388 e.Å ⁻³	

References:

1. SMART Version 5.625 and SAINT+ Version 6.02a. Bruker Analytical X-ray Systems, Inc., Madison, Wisconsin, USA, 1998.
2. The DIRDIF99 program system. P.T. Beurskens, G. Beurskens, R. de Gelder, S. Garcia-Granda, R. Israel, R.O. Gould, J. M. M. Smits, Crystallography Laboratory, University of Nijmegen, The Netherlands. **1999**.
3. G.M. Sheldrick, SHELXTL Version 5.1; Bruker Analytical X-ray Systems, Inc., Madison, Wisconsin, USA, 1997.
4. PLATON, A Multipurpose Crystallographic Tool, Utrecht University, Utrecht, The Netherlands, A. L. Spek, **1998**.
5. Sheldrick, G. M. SHELXTL Version 6.1; Bruker Analytical X-ray Systems, Inc., Madison, Wisconsin, USA, 2000.